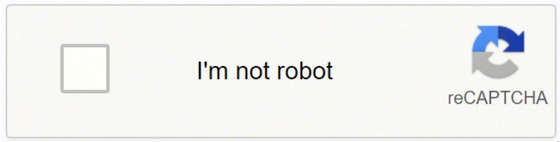

Next

East guidelines blunt abdominal trauma

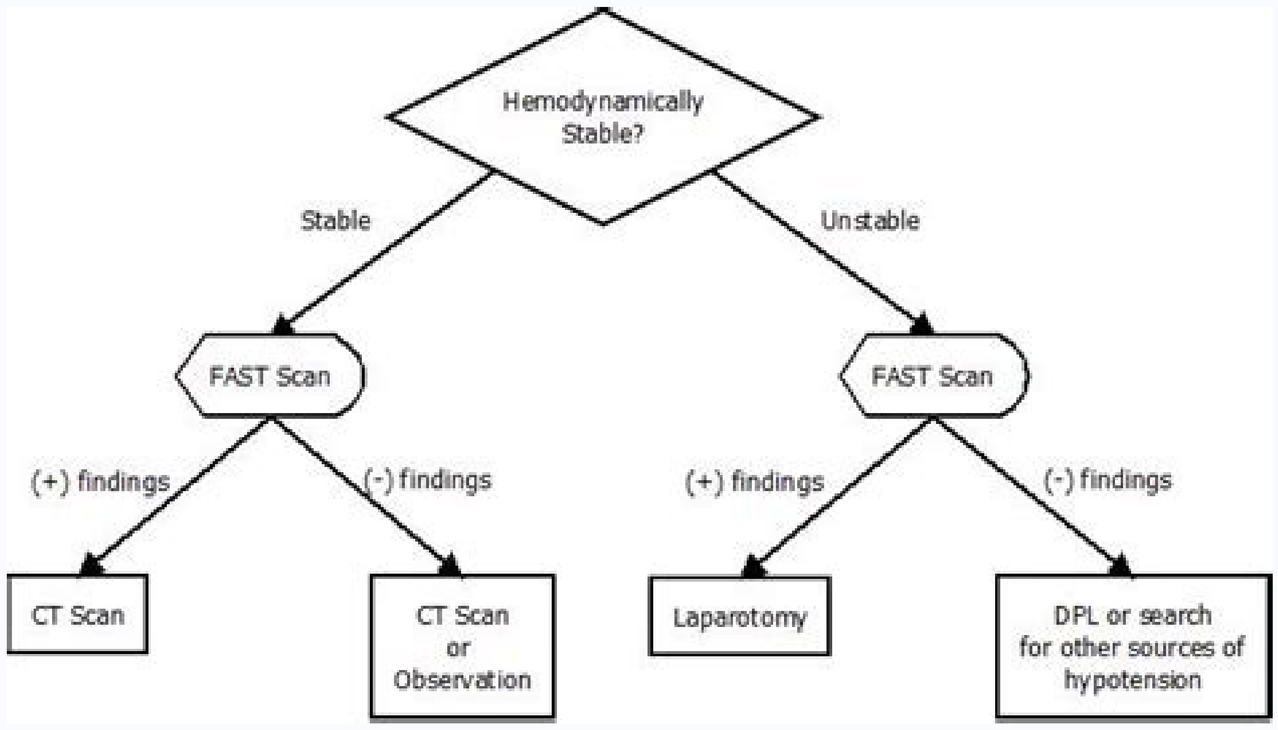

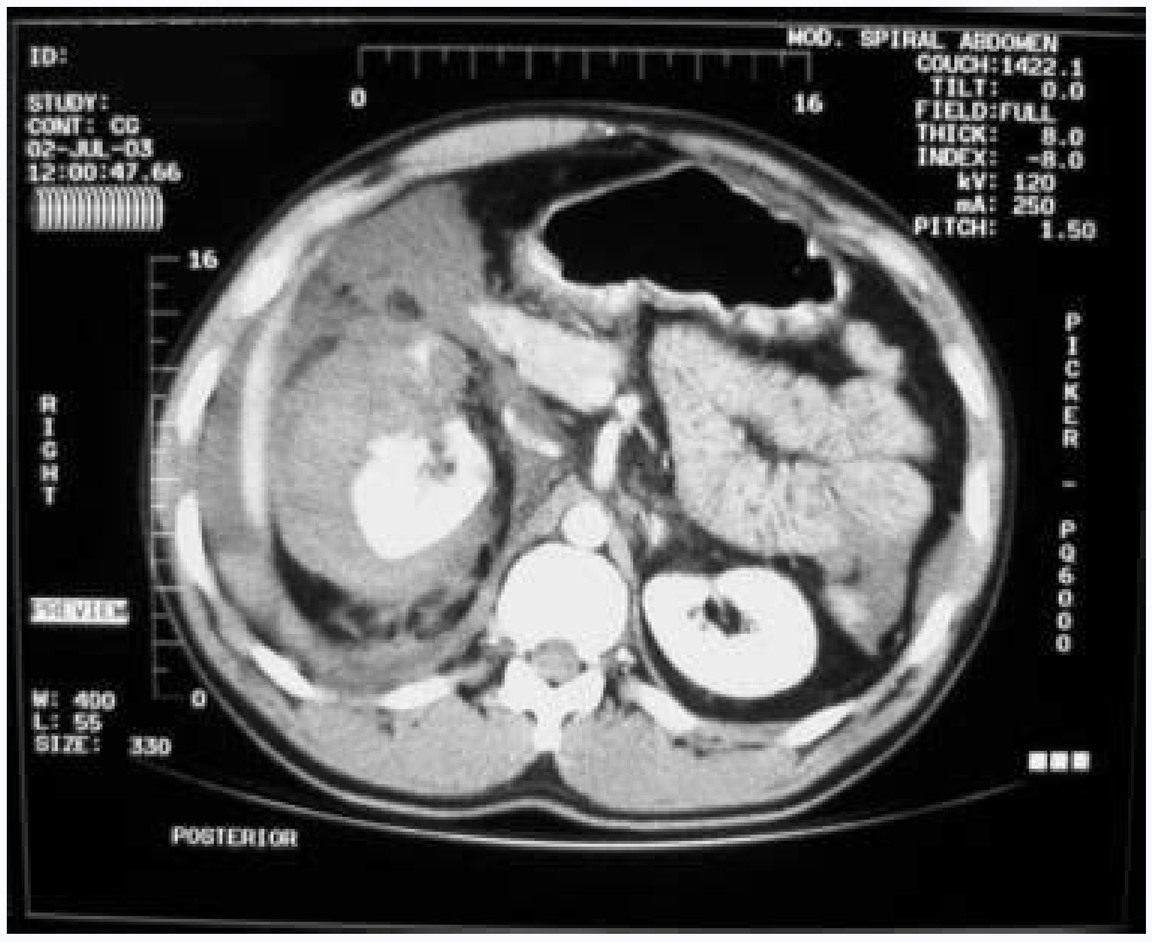

Airway	Maintain airway with cervical spine control.
Breathing	Assess breathing and ventilation. Apply high flow O_2.
Circulation	Assess circulation with haemorrhage control.
Disability	Check neurological status.
Exposure/ Environment	Complete assessment of the patient but prevent hypothermia.

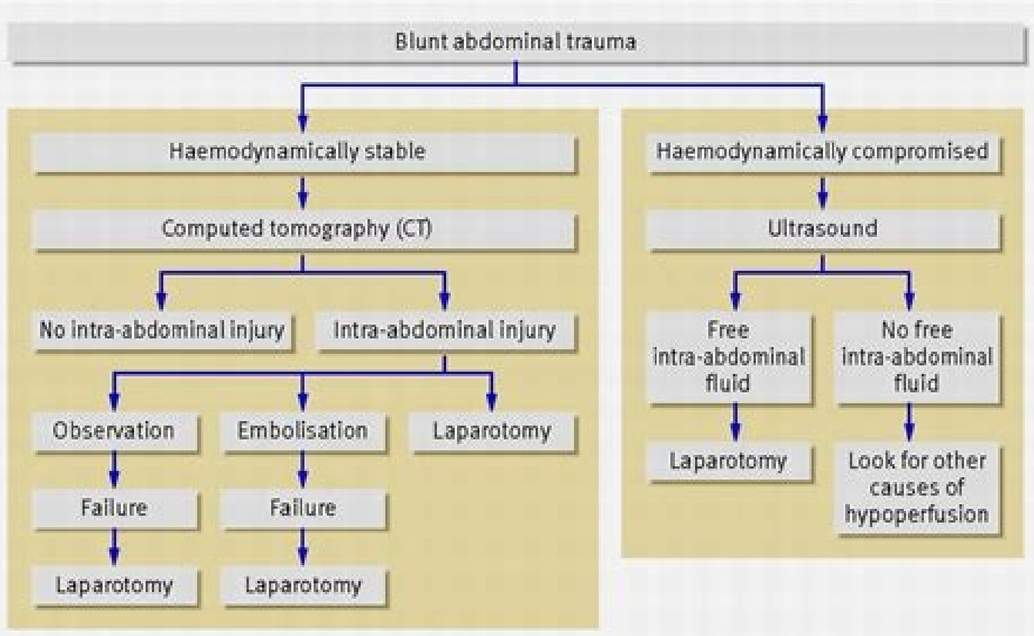

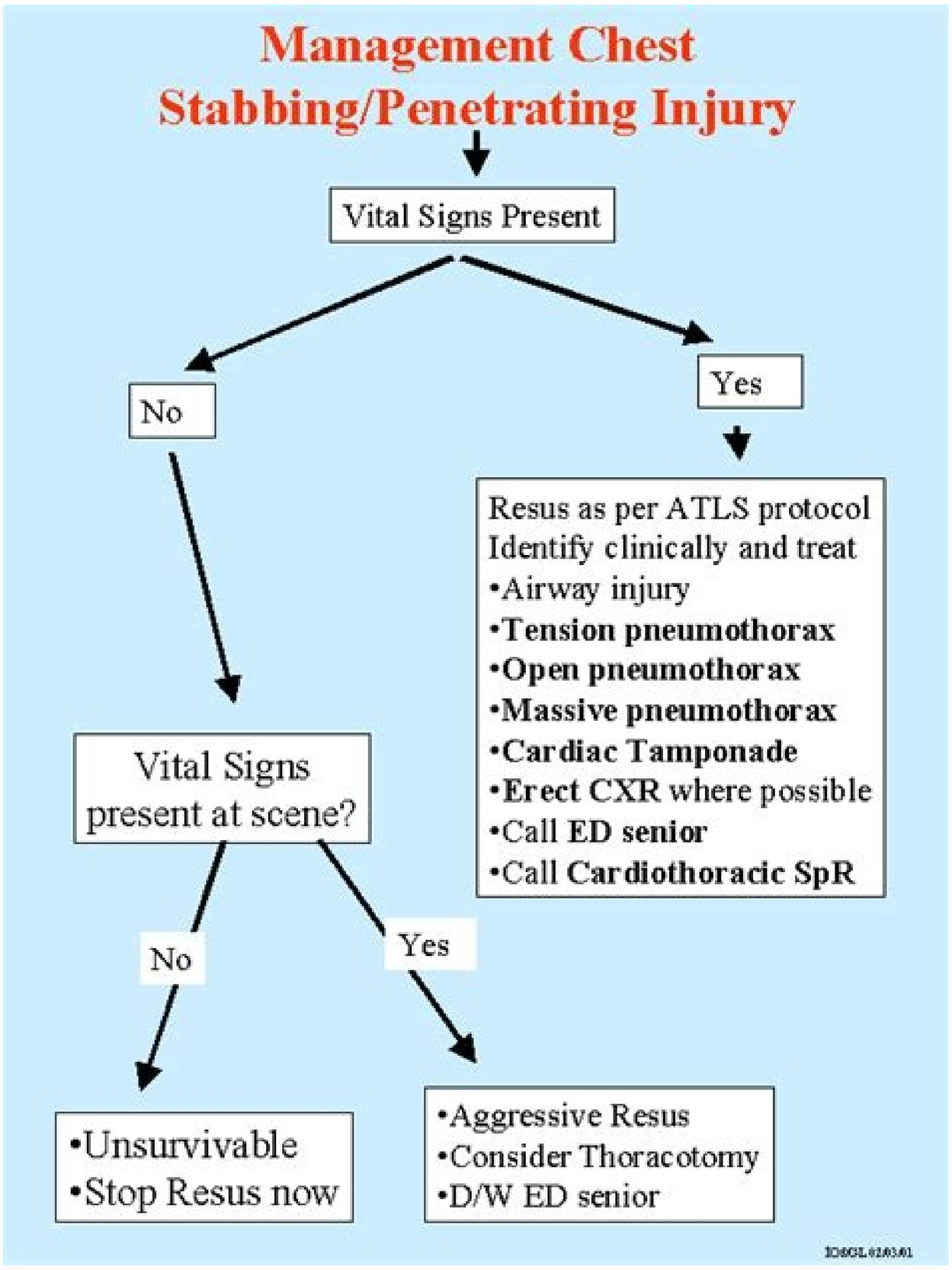

Crossref, Medline, Google Scholar36 Nguyen D, Platon A, Shanmuganathan K, Mirvis SE, Becker CD, Poletti PA. L.C. No relevant conflicts of interest to disclose. Google Scholar26 Hambly NM, McNicholas MM, Phelan N, Hargaden GC, O'Doherty A, Flanagan FL. Crossref, Medline, Google Scholar41 Sengupta S, Lohse CM, Leibovich BCet al.. There were few cases (n = 23) of discordance between the CT findings and the final clinical diagnosis. Medline, Google Scholar34 Daniel J, Holland J, Quigley L, Sprague S, Bhandari M. Crossref, Medline, Google Scholar2 Hock LM, Lynch J, Balaji KC. J Am Coll Cardiol 1997;30(1):76–82. Crossref, Medline, Google Scholar48 Bennett CM, Wolford GL, Miller MB. Crossref, Medline, Google Scholar7 Chiu WC, Cushing BM, Rodriguez Aet al.. Cte is a proportionality constant and hematocrit, Hct, was determined animal by animal, as discussed above in In Vivo MR Experiments.Data analysis was performed (B.L., with 4 years of experience in MR imaging data processing; C.M., with no experience; and G.L. and E.L.B., each with 15 years of experience in MR imaging data processing).Region of interest.—Tumor regions of interest (ROIs) were manually delineated on all T2-weighted images that contained tumor tissue. These critical results were chosen from an established list of more than 20 critical radiology values established by the Quality Committee in the Department of Radiology at our institution. Eur Radiol 2004;14(4):736–742. Iodixanol significantly impaired nitric oxide bioavailability in isolated perfused afferent arterioles when compared with control group. Med Phys 2007;34(4):1364–1371. In our hands, the 9L gliosarcoma tumor was hypoxic and necrotic, both in vivo (MR estimate of sO2) and ex vivo (pimonidazole staining). Percutaneous liver biopsy by prior ultrasound marking versus direct ultrasound guidance: complications and adequacy. The purpose of this study was to evaluate the midterm clinical and angiographic outcomes after PED placement for intracranial aneurysms.This was a prospective multicenter study conducted in accordance to the Declaration of Helsinki and Declaration of Good Clinical Practice and approved by the review boards of all involved centers. Correction for heart rate variability during 3D whole heart MR coronary angiography. Histologic coagulative tumor necrosis as a prognostic indicator of renal cell carcinoma aggressiveness. Crossref, Medline, Google Scholar5 Johnston SC, Dowd CF, Higashida RTet al.. The book is supplemented by several organizational/leadership charts, which greatly supplement the written text.A Practical Guide to Leadership and Management in Academic Radiology clearly fulfills its intended purpose of providing pragmatic information and pearls to those individuals managing or aspiring to manage an academic ra/diology department. In our sample, overall prevalence of pseudotumors per patient was 69% (120 of 174; 95% confidence interval [CI]: 62%, 76%); overall prevalence per hip was 69% (132 of 192; 95% CI: 62%, 75%). Previously, Israel et al (19) studied the relationship between CTDIvol, dose, and patient size (weight) for a clinical population, but by using a different AEC system (smart mA, GE Healthcare, Milwaukee, Wis) with the user-selectable parameter noise index set to 11.5. Their results differed markedly from those of our study. Am J Surg 2007;193(5):641–643; discussion 643. We acquired images at multiple b values (0, 10, 20, 40, 80, 110, 140, 170, 200, 300, 400, 500, 600, 700, 800, and 900 sec/mm2) in three orthogonal directions, averaged four times. Crossref, Medline, Google ScholarPage 20Second-generation metal-on-metal bearings were introduced in the 1990s, and their use quickly increased because of good initial clinical results (1–3). These conditions often require hospitalization and invasive treatment, and diagnostic CT plays an instrumental role in the triage and treatment of these patients. Gadolinium concentration in tissues is not the sole determinant of T1 time; T1 shortening can also be due to the presence of fat, amyloid protein, or iron, for example. Immediate and midterm results following treatment of unruptured intracranial aneurysms with the pipeline embolization device. In general terms, the authors believe that the key factors to a successfully managed academic radiology department are people, money, and space—with quality people and staff, led by the right leaders, being the key ingredient.The 25 chapters are as follows: Introduction, The Search Process and Negotiating for the Chair, Compensation Plan and Incentives, Financial Management, Billing Organization, Joint Ventures and Strategic Support, Capital Budgets, Clinical Services, Turf Issues, Faculty Workload, Building Research, Building a Strong Residency Program, Fellowship Program, Faculty Recruitment and Retention, Faculty Relations and Morale, Departmental Organization, Information Systems, Leadership Development and Succession Planning, Strategic Planning and Scenario Planning, Marketing and Outreach, Fundraising and Alumni Relations, Postgraduate Education, Quality and Safety, Culture, and Conclusions and Summary.This book is well organized, clearly written, and succinct. Patients underwent MR imaging evaluation of the renal masses between October 2008 and June 2010 with a noncommercially available ASL sequence (see below) followed by our standard clinical MR imaging protocol for renal masses.All patients were imaged in the supine position with a commercial 1.5-T unit (Excite TwinSpeed; GE Medical Systems, Waukesha, Wis) by using an eight-channel phased-array surface coil. We observed a significant correlation between peak perfusion and clear cell RCC (r = 0.71, P = .003) (Fig 6), whereas no relationship was found between tumor size and mean perfusion for these tumors (r = 0.03, P = .92).Table 2 ASL Perfusion of Clear Cell RCC according to Histologic Grade and Clinical StageFigure 6: Scatterplot shows correlation between peak tumor perfusion and size of clear cell RCC (r = 0.71, P = .003).The mean and median perfusion values measured from pure noise were 13.1 mL/min/100 g ± 5.3 and 11.9 mL/min/100 g, respectively. Morphologic typing of papillary renal cell carcinoma: comparison of growth kinetics and patient survival in 66 cases. Wechsler Adult Intelligence Scale-III. Ambiguous cases (where more than one enhancing lesion was present at dynamic contrast-enhanced MR imaging or the report was unclear) were reviewed for final consensus by a radiologist specializing in breast imaging and breast MR imaging (H.R., with 3 years of experience) who was blinded to the final results of pathologic examination.DW images were spatially registered by using a nonlinear two-dimensional registration algorithm (CADstream) to correct for patient motion and eddy current–induced image distortion. These associations were found in patients with RR MS and benign MS when analyzed separately, whereas they were not detected in patients with SP MS (Table 3).Conventional MR imaging measures.—In patients with MS, T2 LV was correlated with activity of the left MFG, whereas NBV was inversely correlated with activity of the right precuneus. Normalized brain volume (NBV) was measured by using structural imaging evaluation of normalized atrophy software (SIENAx; (23).A comprehensive methodological description of the functional MR imaging analyses is provided in Appendix E1 (online). Major spatial differences between these two measurements (section thickness, 1 mm for in vivo vs 10 μm for ex vivo tissue deformation, and no staining of normoxic tissue) and difference in nature (MR estimate of sO2 is analogic where pimonidazole is digital [three possible values]), precluding further spatial correlation analysis, however. Crossref, Medline, Google Scholar31 Delahunt B, Eble JN. Gastric outlet obstruction is a common complication of duodenal hematomas, particularly in the early stages after the injury. Am J Surg 2001;182(1):6–9. We believe our study was adequately sensitive because we detected pseudotumors as small as 0.7 cm; our approach may be most applicable in practice because ultrasonography is operator dependent, and most clinical practitioners do not currently have access to more novel sequences. A search of all available literature (from 1950 onward) was undertaken by using both MEDLINE and National Health Service evidence (including Cochrane Library of Systematic Reviews and National Library of Guidelines) to establish relevant literature on the topic and to derive figures for audit standards.Table 1 Audit StandardsIt is considered good practice and it is required that a consent form be completed and contained within the patient record for all cases; this should be accompanied by documented postprocedural instructions (10,11). In situ carcinomas were classified on the basis of nuclear grade and necrosis (17,18), whereas invasive carcinoma was classified on the basis of the Bloom and Richardson grading system modified by Elston and Ellis, all according to the World Health Organization classification system (24). In all subjects, the interval from trigger delay to the next R wave was long enough to acquire at least three TRAPD images. Slope of line regressing SSDE against AP+LAT (which used robust variance estimator) had 95% CI of −0.02 to 0.07 mGy/cm.Figure 2b: Scatterplots show (a) CT scanner output, as indicated by CTDIvol, and (b) SSDE as function of patient size, which is indicated by sum of AP thickness and LAT width (AP+LAT). For SSDE as a function of size, we also used localized smoothing of the regression model by using the SAS procedure for localized estimation.To account for heteroscedasticity (nonconstant variance of the residuals over the observed data range), the robust variance estimator (commonly called a "sandwich estimator," and using the HC0 model) was used to provide heteroscedasticity-consistent estimates of the model parameter standard errors (18).For each model, the slope of the fitted line, along with its standard error (model-based for CTDIvol and robust for SSDE) and 95% confidence interval (CI) for the fit and for single observations, were estimated and graphed. The tests were performed by using statistical software (JMP, version 8.0.2; SAS Institute, Cary, NC). Crossref, Medline, Google Scholar41 Filippi M, Riccitelli G, Mattioli Fet al.. This phenomenon, combined with the iodixanol-induced constriction of afferent arterioles, may contribute to the reduction of renal blood flow observed in contrast medium–induced AKI (29–31).With iodixanol and ioxaglate, afferent arterioles constricted similarly, and also the effect on the angiotensin II response was not different. Link, Google Scholar24 Boss A, Martirosian P, Schraml Cet al.. Haemodynamic and rheological effects of contrast media: the role of viscosity and osmolality. Crossref, Medline, Google Scholar24 Shapiro B, Rufini V, Jarwan Aet al.. General rules for the clinical and pathological study of primary liver cancer. Am Heart J 2009;157(2):361–368. M.L.O. No relevant conflicts of interest to disclose. 1995;80(7):2041–2045. Synovial hypertrophy is also seen (arrowhead).Figure 3c: Images in a 72-year-old asymptomatic woman after metal-on-metal total hip arthroplasty. Crossref, Medline, Google Scholar27 Rocca MA, Gavazzi C, Mezzapesa DMet al.. Coiling of intracranial aneurysms: a systematic review on initial occlusion and reopening and retreatment rates. In the setting of less severe or more diffuse fibrosis, the inversion-recovery cardiac MR technique is unlikely to reveal the presence of diffusely abnormal tissue given the lack of normal myocardium as a reference.Direct measurement of myocardial T1 time ("T1 mapping") may improve on these methodologic problems of LGE cardiac MR in the setting of diffuse retention of gadolinium-based contrast material. Automated detection of radiology reports that document non-routine communication of critical or significant results. (Hematoxylin-eosin stain; original magnification, ×200.) No evidence of carcinoma was detected at excisional biopsy.Figure 3f: Images in 61-year-old woman with personal history of right-breast ductal carcinoma in situ. Helical CT combined with contrast material administered only through the colon for imaging of suspected appendicitis. P.B. No relevant conflicts of interest to disclose. Link, Google ScholarPage 22Cognitive disorders affect up to 60% of patients with multiple sclerosis (MS) (1). The CT scan was also immediately interpreted as positive or negative for the presence of packets by the same radiologist. ROI values obtained from these perfusion images represent blood flow in milliliters per minute per 100 g of tissue (27).Preliminary experience indicates that a small positive perfusion value can be measured even in the absence of perfusion (30). Angiogenic response of locally advanced breast cancer to neoadjuvant chemotherapy evaluated with parametric histogram from dynamic contrast-enhanced MRI. Neuropsychologia 2008;46(12):2888–2895. Crossref, Medline, Google Scholar34 Etienne A, Botnar RM, Van Muiswinkel AM, Boesiger P, Manning WJ, Stuber M. MR pancreatography is a valuable noninvasive method to establish integrity of the main duct (88), but endoscopic retrograde pancreatography remains as the standard of reference and serves as a means for endoscopic therapy (eg, stent placement) in some patients as well.Figure 7a: CT images in a 53-year-old man who was in a motor vehicle collision. Inflammatory pseudotumor associated with femoral nerve palsy following metal-on-metal resurfacing of the hip: a case report. The test is appropriate for comparison of series of repeated measurements with no normal distribution and was performed by using R (20). clinical course, long term follow up, and assessment of prognostic factors. Disease and the brain's dark energy. Crossref, Medline, Google Scholar70 Cohn SM, Arango JI, Myers JGet al.. Stroke 2002;33(4):1146–1151. The donor vein, bronchus, and artery were inserted into the respective recipient structure. Altered functional adaptation to attention and working memory tasks with increasing complexity in relapsing-remitting multiple sclerosis patients. Ventilation/perfusion imaging of the lung using ultra-short echo time (UTE) MRI in an animal model of pulmonary embolism. J Bone Joint Surg Am 2011;93(Suppl 2):118–121. Crossref, Medline, Google Scholar29 Ratziu V, Charlotte F, Heurtier Aet al.. Crossref, Medline, Google Scholar22 Hawkins SA, McDonnell GV. Between D15(T5) and D18(T8), the mean BVf in treated tumors increased with respect to the contralateral value (repeated-measures test, P < .05) (Fig 4c) and became significantly larger than the mean BVf in contralateral striatum (4.0% ± 0.5 [treated tumors] vs 2.5% ± 0.5 [contralateral striatum], P < .01) (Fig 4c).At D9(T−1), for both groups, the mean MR estimate of sO2 values in tumor and in contralateral striatum, respectively, were comparable for the untreated group (72.0% ± 9.9 vs 63.5% ± 8.6) and the treated group (71.7% ± 5.1 vs 67.4% ± 5.0) (Fig 4d). The enhanced images were obtained with the same parameters by using flip angle α. Submillimeter three-dimensional coronary MR angiography with real-time navigator correction: comparison of navigator locations. Rapid assessment of longitudinal relaxation time in materials and tissues with extremely fast signal decay using UTE sequences and the variable flip angle method. Lesion characteristics, including size and location, as well as the BI-RADS assessment and recommendation, were recorded at the time of interpretation. Foci located laterally in the neck and obviously apart from the medial portion were categorized as positive for uptake of LN metastases, while those adjacent to the medial portion were interpreted as equivocal for thyroid bed uptake. Ultimately, the T1 mapping approach could potentially offer advantages over biopsy, in that noninvasive imaging allows sampling of the entire myocardium.The majority of patients in this analysis (72%) did not have pathognomonic findings for a specific cause of cardiomyopathy at biopsy. Crossref, Medline, Google Scholar30 Kelly RE, Wang Z, Alexopoulos GSet al.. Eur Radiol 2007;17(10):2646–2655. Third, there was a variability of the imaging parameters, such as strength of magnetic field, section thickness, and on imaging timing, because this was multicenter study.In conclusion, hyperintense HCCs on hepatobiliary phase images showed significantly higher differentiation grades, less frequent portal vein invasion, and lower recurrence rates than did hypointense HCCs. Moreover, hyperintense HCCs showed significantly lower expression of AFP and PIVKA-II than did hypointense HCCs. Hyperintense HCCs on hepatobiliary phase gadoxetic acid–enhanced MR images may be a particular form of hypervascular HCC with biologically less aggressive features than those of hypointense HCCs.Advances in Knowledge• Hypervascular hepatocellular carcinomas (HCCs) that hyperintensity relative to the surrounding liver on hepatobiliary phase gadoxetic acid–enhanced MR images demonstrate a significantly higher grade of differentiation (P = .028) and rarer portal vein invasion (P = .039) than those of hypointense HCCs.• Hyperintense HCCs on hepatobiliary phase gadoxetic acid–enhanced MR images show significantly lower serum level of α fetoprotein, Lens culinaris agglutinin reactive fraction of α fetoprotein, and protein induced by Vitamin K absence or antagonist-II than hypointense HCCs (P = .003, P = .004, and P = .026, respectively).• Hyperintense HCCs on hepatobiliary phase gadoxetic acid–enhanced MR images similarly show significantly weaker expression of α fetoprotein and protein induced by Vitamin K absence or antagonist-II at immunohistochemical evaluation than did hypointense HCCs (both P < .001).• Hyperintense HCCs on gadoxetic acid–enhanced MR images show a significantly lower recurrence rate than do hypointense HCCs (P = .039).Implication for Patient Care• Hypervascular HCCs that show hyperintensity on hepatobiliary phase gadoxetic acid–enhanced MR images have biologically less aggressive features than do those that show hypointensity.Disclosures of Conflicts of Interest: A.K. No relevant conflicts of interest to disclose. T1 values for individual pixels within the myocardium were determined (E.B.T., R.A.N.) by means of an iterative curve fitting technique and corrected for contrast agent dose, contrast agent relaxivity, postcontrast delay time, heart rate, and renal function by using a previously described method (17,18). Liver biopsy. Med Phys 1999;26(11):2235–2247. Lancet 1988;1(8594):1076–1078. Crossref, Medline, Google Scholar9 Loitfelder M, Fazekas F, Petrovic Ket al.. Crossref, Medline, Google Scholar71 Fang JF, Wong YC, Lin BC, Hsu YP, Chen MF. Crossref, Medline, Google Scholar8 Sengupta A, Page P. Insets in d and e = ROIs. The lesion was classified as ADH on the basis of (f) US-guided core biopsy results, which showed intraductal papilloma and ductal hyperplasia with focal atypia with no evidence of invasive carcinoma. Endovascular placement of flow diversion devices such as the pipeline embolization device (PED) (ev3 Neurovascular, Irvine, Calif) for endoluminal circumferential reconstruction of segmental vascular defects as a treatment for intracranial aneurysms is gaining widespread acceptance (7–10). Improved bulk myocardial motion suppression for navigator-gated coronary magnetic resonance imaging. Crossref, Medline, Google Scholar14 Selvin E, Najjar SS, Cornish TC, Halushka MK. AJNR Am J Neuroradiol 2010;31(6):1139–1147. Thirty-six containers stuffed with cocaine were found at stool analysis.Figure 3b: (a) False-negative abdominal radiograph at admission in a 54-year-old man suspected of conveying drug packets. The test was repeated at the end of the experiment. After all, DCIS is considered to be a heterogeneous disease with varying morphology and behavior, ranging from rather indolent lesions to aggressively growing DCIS with invasive components (15,16). Comparison of the distribution of diagnostic and thyroablative I-131 in the evaluation of differentiated thyroid cancers. Crossref, Medline, Google Scholar6 Knutsson L, Ståhlberg F, Wirestam R. Follow-up with MR angiography is also expected to reduce costs compared with follow-up with intraarterial DSA (5). Mammographic screening and "overdiagnosis". J Am Coll Cardiol 2009;53(18):1708–1715. "Hot" colors (yellow to red) mean increase with respect to air; "cold" colors (light to dark blue) mean strict decrease. Hum Brain Mapp 2009;30(2):625–637. T.P. No relevant conflicts of interest to disclose. Crossref, Medline, Google Scholar4 Luster M, Clarke SE, Dietlein Met al.. 2012;25(1):30–36. = 318&type = PP¤t = true. This might aid the detection of a change in the occlusion grade of the coiled aneurysm at the next follow-up MR angiography, which can facilitate therapeutic decision making during follow-up.We conclude that the comparable therapeutic decisions based on findings of MR angiography and intraarterial DSA, as found in our study, in addition to the high diagnostic performance, safety, and convenience of MR angiography, support the use of MR angiography instead of intraarterial DSA in the follow-up of patients with coiled intracranial aneurysms.Advance in Knowledge• For patients with coil-treated intracranial aneurysms, there is substantial agreement on treatment decisions based on findings of MR angiography and intraarterial digital subtraction angiography with a weighted κ of 0.73 (95% confidence interval: 0.66, 0.80).Implication for Patient Care• MR angiography can be used for therapeutic decision making in the follow-up of patients with coil-treated aneurysms.Disclosures of Conflicts of Interest: J.D.S. No relevant conflicts of interest to disclose. Differences between two groups were tested with a t test for continuous variables and with the Fisher exact test for proportions. An evaluation of the sensitivity of the intravoxel incoherent motion (IVIM) method of blood flow measurement to changes in cerebral blood flow. (b) Axial low-dose CT scan shows a large quantity (>12) of packets within the stomach (arrowheads) and small bowel (arrow), isoattenuated to the surrounding gastric and bowel content. C, Binarized image of combined-network seeding from the MPFC and PCC show a more inclusive connectivity pattern of the DMN.No hemorrhagic brain lesions were detected with conventional imaging, including T2-weighted MR imaging and susceptibility-weighted MR imaging in patients with MTBI. Magn Reson Med 2008;60(6):1488–1497. Magn Reson Med 1990;15(2):287–304. More passes lead to a greater chance of inadequate biopsy (P = .009).Table 12 Needle Parameters and Adequacy of Initial HistologyA funnel plot was used to compare departmental performance in terms of diagnostic accuracy and is shown in the Figure. Crossref, Medline, Google Scholar15 Allen G, McColl R, Barnard H, Ringe WK, Fleckenstein J, Cullum CM. The observed relationships between DMN disruption and neurocognitive dysfunction, as well as clinical symptoms, provide an additional important clue to the pathophysiology underlying PCS after injury.Regarding the normal DMN pattern, previous study findings (43,50), together with the current study results in which seed-based methods were used, demonstrated very different connectivity patterns of the DMN in healthy control subjects when the seed was placed separately in PCC versus MPFC regions. (b) Sagittal reformation shows the collar sign, in which a defect in the diaphragm creates a waistlike constriction of the herniated stomach (arrow).Figure 10b: CT images in a 40-year-old man who was the driver in a high-speed motor vehicle accident. Furthermore, the lack of anatomic landmarks, as well as the possibility of physiologic or other benign uptake of this tracer, may make interpretation of images more difficult. Crossref, Medline, Google Scholar22 Morris TW, Katzberg RW, Fischer HW. Separation of diffusion and perfusion in intravoxel incoherent motion MR imaging. Structural and functional MRI correlates of Stroop control in benign MS. 2008;191(6):1785–1794. Crossref, Medline, Google Scholar9 Chang JD, Lee SS, Hur M, Seo EM, Chung YK, Lee CJ. Currently, the success rate of nonsurgical therapy varies between 80% and 90% (54) Thus, accurate identification of injuries that may necessitate surgical or angiographic intervention is of critical importance (21,55,56). Of particular interest is the application of quantitative T1 mapping techniques in the assessment of such patients with cardiomyopathy and without LGE. Further study related to the use of arterial phase imaging in abdominal trauma on the basis of this work is ongoing, and this area deserves further inquiry.Table 2 Multidetector CT–based Splenic Injury Grading SystemHepatic injuries are common and are associated with important complications. Items are rated on a Likert scale, indicating severity of the symptom, from 0 (none) to 6 (severe). (d) Six containers stuffed with cocaine were found at stool analysis.Figure 3a: (a) False-negative abdominal radiograph at admission in a 54-year-old man suspected of conveying drug packets. Analysis of impairment related functional architecture in MS patients during performance of different attention tasks. Arterial spin labeling MR imaging for characterisation of renal masses in patients with impaired renal function: initial experience. We further sought to determine which particular subtypes exhibit ADCs below a previously proposed diagnostic ADC threshold and comprise the overlap with malignancies reported by previous studies.Our study was approved by our institutional review board and was Health Insurance Portability and Accountability Act compliant. For the few patients in this study who were imaged with their arms by their side, the best effort to measure body dimensions was made if the extremities masked the chest and abdomen boundaries. To correct for the macroscopic inhomogeneities of B0, the multiple GRE 3D sequence was spatially averaged, as described before (23). No significant difference was noted in rate of diagnosis between the sexes for all other specific alternative diagnoses (P = .1015 to >.99).Among patients who received a diagnosis at CT, the rate of diagnosis for appendicitis and alternative diagnoses varied according to both age and sex (Fig 3). No statistical difference (P = .06) was found between the body mass index of subjects with CAD risk factors (mean, 25 ± 5; range, 16–34) and healthy subjects (mean, 22 ± 4; range, 20–30). Medline, Google Scholar5 Rieker CB, Schön R, Köttig P. Our methods provided a global measure of fibrosis and did not correlate T1 measurements to biopsy site. Semin Oncol 2006;33(5):534–543. The principled control of false positives in neuroimaging. Reported cases so far involved the use of a SILK flow diverter (12,13,17,18), but not a PED (7–10); the current study showed that aneurysms treated with the PED are not exempted. Link, Google Scholar68 Yoon W, Jeong YY, Kim JKet al.. Finally, dynamic contrast-enhanced MR imaging and dynamic susceptibility contrast-enhanced imaging are affected by first-pass extravasation of contrast material (8).A fourth method, which is much less popular, called intravoxel incoherent motion (IVIM) imaging, measures perfusion locally and quantitatively (9). J Magn Reson Imaging 2010;32(2):326–333. Eur J Pharmacol 2008;584(1):57–65. A simple risk score for prediction of contrast-induced nephropathy after percutaneous coronary intervention: development and initial validation. Finally, the MR estimate of sO2 appears sensitive to changes induced by an antiangiogenic treatment in a gliosarcoma model (9L gliosarcoma).BVf values observed in the contralateral striatum are comparable to those measured in the contralateral striatum of rats bearing C6 and RG2 (11) or U-87 MG (22) glioma cells. Crossref, Medline, Google Scholar37 Minardi D, Lucarini G, Filosa Aet al.. Kidney Int 2005;68(1):14–22. Approximately 90% of the data were between these values, and the simple linear regression model and smoothed curve were essentially coincident in this range. We recognize that communication with the pseudocapsule may be underestimated because walls may be opposed as a result of supine patient positioning; however, for the purposes of this study, we categorized communication as designated in Figure 1.Figure 1a: Axial T2-weighted MR images in four patients demonstrate pseudotumors (thick arrow) with (a) no communication with the pseudocapsule, (b) possible communication with the pseudocapsule, and (c, d) definite communication with the pseudocapsule. The most common method in clinical use, dynamic susceptibility contrast material–enhanced imaging, is based on the measurement of the first-pass T2* effect of a bolus of paramagnetic exogenous contrast material (gadolinium chelate) (3) and its volume distribution. Magnetic resonance imaging–measured blood flow change after antiangiogenic therapy with PTK787/ZK 222584 correlates with clinical outcome in metastatic renal cell carcinoma. Am J Surg 2008;196(3):389–397. Radiology 2010;255(2):459–466. Skeletal Radiol 2012;41(2):149–155. One author (R.J.v.d.G.) is a consultant for Medis Medical Imaging Systems (Leiden, the Netherlands). Link, Google Scholar5 Lam JS, Shvarts O, Leppert JT, Figlin RA, Belldegrun AS. Invest Radiol 2011;46(10):610–617. This finding suggests that presumed overdiagnosis does not increase with the use of digital mammography in breast cancer screening programs.Advances in Knowledge• The performance of digital mammography in screening is substantially better than that of screen-film mammography with regard to the detection of both ductal carcinoma in situ (DCIS) (detection rates: 0.2 vs 0.1 per 1000 women in initial examinations, 1.1 vs 0.7 per 1000 women in subsequent examinations) and invasive carcinoma (detection rates: 0.8 vs 0.6 per 1000 women in initial examinations, 4.1 vs 3.8 per 1000 women in subsequent examinations).• The improved detection of DCIS with digital mammography is seen throughout the histopathologic grading spectrum, without an increase in the proportion of low-grade DCIS (14.4% with either modality).• Digital mammography seems to add to the detection of high-grade DCIS (58.5% vs 50.5% of DCIS detected with conventional screening).Implication for Patient Care• Digital screening mammography demonstrates advantages in the early detection of breast cancer by increasing the detection of clinically relevant cancers while keeping potential overdiagnosis low.Disclosures of Conflicts of Interest: A.M.J.B. No relevant conflicts of interest to disclose. RadioGraphics 2008;28(4):985–1003. The true incremental gain of adding DW imaging to dynamic contrast-enhanced MR imaging is yet to be studied in a large multicenter trial.Repeated measurements in a consecutive subgroup of lesions demonstrated good intra- and interobserver repeatability. The region of interest of the tumor was determined as the maximum oval or round area at the level of the largest diameter of the tumor, avoiding degeneration area and artifact. These lesions included three cases of usual ductal hyperplasia, one fibroadenoma, and one focal fibrosis. (b) T1-weighted spoiled gradient-echo image obtained during corticomedullary phase after administration of gadopentetate dimeglumine (0.1 mmol per kilogram body weight) shows that tumor exhibits avid enhancement. Renal perfusion in humans: MR imaging with spin tagging of arterial water. Link, Google Scholar35 Pinto A, Niola R, Tortora Get al.. M.S. No relevant conflicts of interest to disclose. Furthermore, analysis of WL enhancement histogram distribution may be able to be used to discriminate ccRCC from pRCC without reliance on the absolute measure of signal intensity change.Therefore, the purpose of our study was to compare histogram analysis of voxel-based WL enhancement to qualitative assessment and ROI-based enhancement analysis in discriminating ccRCC from pRCC.Siemens Medical Solution and Siemens Corporate Research (Princeton, NJ) provided research support in the form of the software (MROncoTreat) used to perform automated registration and semiautomated WL segmentation. This corresponds to a 36% increase in patients' wal thickness compared with that with single-frame dual inversion-recovery imaging (25% increase). J Neurol Neurosurg Psychiatry 2004;75(11):1524–1531. A previous study of 27 patients with incompletely occluded aneurysms showed a substantial interobserver variability in whether and how to additionally treat the aneurysm based on intraarterial DSA findings (10). J Trauma 2008;64(3):666–672. One screening center, however, routinely obtained both views in first as well as subsequent screening examinations. H.S. No relevant conflicts of interest to disclose. The only drawback is the occasional mention of a grading system, such as Pfirrman or Modic, without details of the grades. Neuroimage 2011;55(4):1716–1727. J R Stat Soc Ser D (Statistician) 1998;47(1):183–189. J Am Soc Nephrol 2007;18(11):2912–2920. Crossref, Medline, Google Scholar9 Tatum JL, Kelloff GJ, Gillies RJet al.. Top and middle: Axial view. Two radiologists read and rated the images independently. Assessment of breast lesions with diffusion-weighted MRI: comparing the use of different b values. Hepatocellular carcinoma. More DCIS and invasive ductal carcinomas were detected with digital screening, the latter particularly when associated with microcalcifications. Crossref, Medline, Google Scholar27 Del Turco MR, Mantellini P, Ciatto Set al.. Water proton MR properties of human blood at 1.5 Tesla: magnetic susceptibility, T(1), T(2), T*(2), and non-Lorentzian signal behavior. Immediate clinical outcome of patients harboring unruptured intracranial aneurysms treated by endovascular approach: results of the ATENA study. Crossref, Medline, Google Scholar28 Fischer SE, Wickline SA, Lorenz CH. Changes in resting connectivity during recovery from severe traumatic brain injury. During the follow-up period, 10 of 13 patients (77%; 95% CI: 46%, 93.8%) completely recovered from symptoms of cranial nerve palsy within a median of 3.5 months (range, 1–8.9 months). Pseudotumours associated with metal-on-metal hip resurfacings. Insert in b shows data grouped between 3 and 7 mGy (for SSDE) and 1 and 9 mGy (for CTDIvol) at a better resolution than in the larger version of the same scatterplot.Figure 7b: Comparison between patient and . Results of a prospective trial. Crossref, Medline, Google Scholar65 Andrews-Hanna JR, Reidler JS, Sepulcre J, Poulin R, Buckner RL. Eur J Radiol 2007;63(3):373–378. Intrarenal blood flow in children with normal kidneys and congenital heart disease: changes attributable to angiography. Urology 2008;71(1):47–51. Textbook of traumatic brain injury. Medline, Google Scholar12 Catre MG. Another limitation was the use of a mouse model, because of the differences between human beings and mice in the renal anatomy and physiologic parameters (eg, the greater capability of urine concentration in mice). Immunostaining of pimonidazole was performed on the largest tumor area, according to the manufacturer's instructions, and was followed by erythrosine counterstaining.MR imaging postprocessing.—Processing was performed within a technical computing language and interactive environment (Matlab 7; MathWorks, Natick, Mass) by using homemade software.BVf maps were estimated by using the steady-state approach described by Tropres et al (21) (Fig 1b). Analysis of the Look-Locker T(1) mapping sequence in dynamic contrast uptake studies: simulation and in vivo validation. Although complete aneurysm occlusion rate was high, occlusion occurred at a slow pace, and the reason for this delayed occlusion rate remains unclear. Crossref, Medline, Google Scholar5 Sørum R, Hofvind S, Skaane P, Haldorsen T. Cases 1 and 2 are a healthy subject in whom all images had adequate (good or excellent) scores for quantitative analysis. J Bone Joint Surg Am 2012;94(4):317–325. Crossref, Medline, Google Scholar4 Rutland-Brown W, Langlois JA, Thomas KE, Xi YL. The natural history of low-grade ductal carcinoma in situ of the breast in women treated by biopsy only revealed over 30 years of long-term follow-up. Renal mass core biopsy: accuracy and impact on clinical management. Side-cutting needles (Tru-cut; Baxter Healthcare, Deerfield, Ill) were used most frequently. P.V. No relevant conflicts of interest to disclose. Medline, Google Scholar10 Pedrosa I, Chou MT, Ngo Let al.. Sixteen nonrespondents replied to the postaudit communication regarding lack of participation; their reasons for not responding included no liver biopsies performed in the department (n = 8), contact failure (n = 4), and lack of time or resources (n = 4).Table 2 Responses to Organizational Data Items (Questionnaire A)The primary indication for liver biopsy as recorded on the original request form is summarized in Table 3, together with the number of cases with a known focal lesion for biopsy. Abdominal ultrasound is an unreliable modality for the detection of hemoperitoneum in patients with pelvic fracture. Blunt trauma of the pancreas and biliary tract: a multimodality imaging approach to diagnosis. In addition, a larger difference in wall thickness between healthy subjects and those with CAD was obtained (0.38 mm difference) when three or more frames were used to identify the wall thickness, compared with single-frame calculations (0.31-mm difference). The nine authors who are not employees of Siemens had full control of the data.This Health Insurance Portability and Accountability Act–compliant retrospective single-center study was performed after obtaining a waiver of informed patient consent from our institutional review board. In a third patient, whose aneurysm was treated with Nexus coils (EV3, Irvine, Calif), findings of MR angiography were not interpretable as a result of large coil artifacts. Current status of breast MR imaging. Radiother Oncol 1997;44(2):163–169. Reproducibility of BOLD, perfusion, and CMRO2 measurements with calibrated-BOLD fMRI. ROIs were then copied to the ASL perfusion image obtained at the same level. For patients with AP+LAT less than 72 cm, multiplying CTDIvol by an fsize greater than 1 will cause the variability in CTDIvol to be magnified for SSDE. Crossref, Medline, Google Scholar3 Miao C, Chen S, Macedo Ret al.. A small amount of sterile ophthalmic ointment (Vitamin A Crème, Bausch & Lomb, Steinhausen, Switzerland) was applied to protect the eyes from drying. J Orthop Res 2007;25(10):1325–1332. C.H.M. Financial activities related to the present article: none to disclose. Nichtparametrische analyse longitudinaler daten. Each text-classification algorithm was unique and consisted of more than 50 to many hundreds of rules, depending on the critical result in question.Algorithm accuracy was represented by precision and recall and overall accuracy (F1 score or harmonic mean of precision and recall). Software (SPSS, version 20; SPSS, Chicago, Ill) was used. Clin Orthop Relat Res 1995;(311):54–59. SSDEage was then calculated by using either Equation (1) or (2).The degree to which CTDIvol correlated with SSDE was investigated. Crossref, Medline, Google Scholar30 Volders PGA, Willems IEMG, Cleutjens JPM, Arends JW, Havenith MG, Daemen MJAP. J Forensic Leg Med 2010;17(4):198–202. Diagnosis of aortic transection on CT images is obvious when accompanied by a large hematoma or active extravasation of contrast-enhanced blood. This would not change the interpretation of our study results, because these routine follow-up schedules are irrespective of previous imaging

results. A recent study (15) that applied a similar protocol to ours showed a relatively low alteration rate from whole-body scintigraphy findings to SPECT/CT findings: 33 (22.3%) of 148 patients. The two-sided paired Student t test was used to test for a statistically significant difference between T2* value and spin density between ROIs of the transplanted lung, the ventral and apical normal lung, and the dorsal normal lung. Multidetector scanners offer the possibility to acquire images at multiple phases of enhancement. J Trauma 2007;63(1):97–102. Kobayashi, W.K., T.G., T.Y., S. However, many important questions remain. Curr Pharm Biotechnol 2004;5(6):551–566. Box plots show median and range of ADCs for each subtype in the order of frequency. Crossref, Medline, Google Scholar8 Janjua KJ, Sugrue M, Deane SA. Medline, Google Scholar17 Pedrosa I, Chou MT, Ngo Let al.. Radioactive iodine treatment and external radiotherapy for lung and bone metastases from thyroid carcinoma. Thirty-two of these 52 areas were believed to be positive findings, and 20 were noted as equivocal for distant metastases. The registration was applied to the precontrast and postcontrast acquisition. Crossref, Medline, Google Scholar27 Garcia-Tsao G, Boyer JL. Optimal sensitivity and specificity (0.85 and 0.94, respectively) are obtained at the cutoff point of 4, when a negative result with a level of confidence of 1 is considered a positive result.There was a strong likelihood ratio (>10 or 30 kg/m2). Only five lesions with ADCs above the threshold were given an assessment of BI-RADS category 5 in the MR imaging reports. This radiograph was initially deemed negative by the radiologist on call, with a low degree of confidence (1 of 4) in his diagnosis. Two to seven samples were analyzed for each individual. (c) ASL image shows that tumor has low perfusion levels (mean perfusion = 50.0 mL/min/100 g).Figure 4c: Coronal images in 64-year-old man with papillary RCC (arrow) in lower pole of left kidney. PIVKA-II is an incomplete coagulation factor prothrombin II whose production is related to the absence of vitamin K or the presence of the antagonist of vitamin K, which is the cofactor of γ carboxylase that converts precursor into prothrombin (10). Data were retrieved from our institutional archive of examinations performed between April 1, 2007, and May 13, 2007.Data included were from the first examinations performed each day, with a limit of three examinations per day for each examination type on each scanner. The association among functional MR imaging activity and RTs differed significantly across the various MS phenotypes (Table 3).Table 3 Correlations between Functional MR Activity during the Stroop Incongruent Condition versus Parameters in Healthy Control Subjects and Patients with MSDisease duration.—In patients with MS, disease duration was inversely correlated with activity of the right cerebellum and was directly correlated with activity of the left IFG and right precuneus (Table 3). In patients who received neither a CT nor clinical diagnosis, 56 of 582 (9.6%) were hospitalized, and 13 surgical procedures were performed within 1 year (11 negative appendectomies performed immediately and two unrelated surgical procedures later in the year). Pseudotumors associated with total hip arthroplasty. These samples were digitized by using a commercial high-resolution scanner (ScanScope; Aperio, Vista, Calif). 2011. A prognostic index for ductal carcinoma in situ of the breast. Crossref, Medline, Google Scholar43 Lebret T, Poulain JE, Molinie Vet al.. Magn Reson Med 2011;65(5):1407–1415. For patients with incompletely occluded aneurysms, either additional treatment or further follow-up imaging was advised when the recurrence was considered too small for additional treatment. J.L.M. No relevant conflicts of interest to disclose. Yield and complications in ultrasound-guided biopsy of abdominal lesions: comparison of fine-needle aspiration biopsy and 1.2-mm needle core biopsy using an automated biopsy gun. Magn Reson Med 2004;51(2):353–361. Methodology of brain perfusion imaging. Crossref, Medline, Google Scholar23 Nyman RS, Cappelen-Smith J, Brismar J, von Sinner W, Kagevi I. The data were reviewed retrospectively.Between September 2010 and December 2011, 227 patients presented to a single orthopedic surgeon (J.V.H.) in response to the Depuy Articular Surface Replacement voluntary hip recall in August 2010. Crossref, Medline, Google Scholar25 Gharib AM, Ho VB, Rosing DRet al.. The distribution of image scores over the individual cine frames is summarized in Figure E3 (online). Multisubject fMRI studies and conjunction analyses. (d) Frontal DSA image shows complete obliteration of the aneurysm (arrow) 6 months after treatment.Figure 1c: Cranial nerve palsy in a 55-year-old woman. O.M. Financial activities related to the present article: Received a consulting fee or honorarium and fees for participation in review activities from Bayer Japan. Nonetheless, to our knowledge, this is the first study to show the difference between subjects with CAD risk factors and healthy subjects by using this technique with a 95% success rate.In conclusion, TRAPD imaging of the coronary artery wall improves the success rate of obtaining good- to excellent-quality images and imaging sections orthogonal to the longitudinal axis of the vessel, with artery wall thickness measurements showing a more distinct difference between normal and patient populations.Advances in Knowledge• High-spatial-resolution time-resolved imaging of the coronary artery wall is feasible at 3 T with multiframe dual inversion-recovery imaging by using spiral k-space acquisition and phase-sensitive reconstruction.• Coronary vessel section orthogonality, which is critical for accurate wall thickness measurement, is better achieved with time-resolved imaging than with a single-time-frame approach because of cardiac cycle phase dependence.• Preliminary experience with the time-resolved phase-sensitive dual inversion-recovery (TRAPD) sequence in healthy subjects and subjects with risk factors for coronary artery disease suggests improved ability to distinguish coronary wall thickness between the two groups (1.07 vs 1.46 mm, respectively; 36% increase) compared with that with single-frame dual inversion-recovery imaging (1.24 vs 1.55 mm, respectively; 25% increase).Implications for Patient Care• This time-resolved multiframe technique improves the success rate of obtaining vessel wall images with good to excellent image quality compared with the success rate of conventional single-frame imaging.• Overcoming residual uncompensated cardiac motion in coronary artery wall imaging is feasible without subject-dependent optimization or section tracking.Disclosures of Conflicts of Interest: K.Z.A. No relevant conflicts of interest to disclose. Google Scholar37 Meyers JE, Meyers KR Rey Complex Figure Test and Recognition Trial: Professional manual. Previous studies, outside of traumatic brain injury, have also shown MPFC connectivity changes in patients with anxiety and depression, although the pattern of changes in connectivity appears to be different compared with MTBI (17,62,63). 2000;73(870):627–635. Mult Scler 2011;17(4):411–422. Diffuse bowel wall thickening is usually not a result of direct trauma but more likely related to the hypoperfusion complex (“shock bowel”) (83). Crossref, Medline, Google Scholar10 McAuliffe W, Wycoco V, Rice H, Phatouros C, Singh TJ, Wenderoth J. (b) Protocols for investigation of the effect of iodixanol, L-NAME, and the combination of both on arteriolar diameter (tone) and vasoreactivity to angiotensin II in efferent arterioles. Radiology 2009;251(3):731–742. Crossref, Medline, Google Scholar13 Byrne JV, Beltechi R, Yarnold JA, Birks J, Kamran M. Crossref, Medline, Google Scholar40 Heusner TA, Kuemmel S, Koeninger Aet al.. Crossref, Medline, Google Scholar10 Barbier EL, Lamalle L, Décorps M. However, the resulting comparison between and SSDE for an adult population weighing more than 100 kg may vary from this study with greater adult patient population sampling statistics. Hypoxia and necrosis in rat 9L glioma and Morris 7777 hepatoma tumors: comparative measurements using EF5 binding and the Eppendorf needle electrode. When compared with air inhalation, differences were mostly statistically significant ($P < .05$, Fig 2) for CO_2 inhalation at various concentrations and showed a trend for O_2.Figure 2a: Box and whisker plots (median, 25th and 75th percentiles, minimum, maximum, outliers) compare variations of (a)f, (b)D*, (c)fD*, and (d)D, averaged in ROIs drawn in white matter (WM), gray matter (GM), thalamus (T), and lenticular nucleus (LN), in four to seven volunteers and in both sides of the brain. The hematocrit level of each blood sample was determined by using a blood gas analyzer (ABL 510; Radiometer, Copenhagen, Denmark). All patients experienced a closed head injury with either posttraumatic amnesia of less than 24 hours duration or loss of consciousness of approximately 30 minutes or less, with Glasgow Coma Scale scores between 13 and 15 obtained by the emergency or ambulatory care staff after injury. Crossref, Medline, Google Scholar40 Aubry M, Cantu R, Dvorak Jet al.. Diagnostic performance of multidetector computed tomography for suspected acute appendicitis. Subtypes with the highest mean ADCs were apocrine metaplasia ([2.01 ± 0.38] × 10^{-3} mm2/sec), inflammation ([1.95 ± 0.46] × 10^{-3} mm2/sec), fibroadenoma ([1.94 ± 0.38] × 10^{-3} mm2/sec), and focal fibrosis ([1.84 ± 0.48] × 10^{-3} mm2/sec), while the those with the lowest mean ADCs were lymph nodes ([1.28 ± 0.23] × 10^{-3} mm2/sec), lobular neoplasia ([1.34 ± 0.51] × 10^{-3} mm2/sec), fibromatosis (1.46 × 10^{-3} mm2/sec), and ADH ([1.48 ± 0.36] × 10^{-3} mm2/sec) (Fig 3). World J Radiol 2011;3(6):155–158. Crossref, Medline, Google Scholar30 Barter S, Drinkwater K, Remedios D. Crossref, Medline, Google Scholar21 Appelbaum L, Kane RA, Kruskal JB, Romero J, Sosna J. Accurate and precise diagnosis of local recurrence and metastasis of lymph node (LN) and distant sites is essential for adequate clinical follow-up and management (treatment and monitoring, including watchful waiting) of patients with well-differentiated thyroid carcinoma. G.L.D. No relevant conflicts of interest to disclose. The thinnest wall measurements were mostly obtained from frames 1, 2, and 3 in eight (21%), 10 (26%), and 11 (29%) of the 38 subjects, respectively. Although several well-executed studies of CT performance have included some incidental data on alternative diagnoses detected at CT (16,18,20–25), the primary focus, selection criteria, and relatively small sample sizes of these prior studies preclude an accurate assessment of the true nature and effect of alternative diagnoses. International Classification of Diseases and Related Health Problems. The final cohort included 175 nonmalignant lesions in 162 examinations in 161 women. ICA can help separate the whole-brain signal fluctuations from physiologic noise and automatically capture the entire DMN as a single major component (27). Med Phys 1981;8(4):488–495. Most if not all of these diagnoses could have been made without the use of intravenous contrast material, but that a more focused examination for appendicitis (in terms of coverage) could conceivably have missed at least one of these.Figure 2h: Representative examples of alternative diagnoses made at abdominal multidetector CT in the setting of suspected appendicitis. Kobayashi, T.G., S. Drop-down lists facilitated ease of data entry, while data validation configuration restricted data entry to valid responses. Apparent diffusion coefficient values for discriminating benign and malignant breast MRI lesions: effects of lesion type and size. Inclusion criteria were a cardiac MR examination that included inversion-recovery images obtained after contrast material administration (hereafter, “postcontrast”) permitting T1 mapping and a clinically indicated endomyocardial biopsy adequate for quantitative analysis of collagen as described below. However, based on the observation that not all vascular injuries of the spleen are identified on the combination of portal venous and delayed phase images, some advocate routine acquisition of an additional arterial phase series during the CT examination of the abdomen (20). However, both were fellowship trained in musculoskeletal radiology and had interpreted MR images in the setting of metal prostheses throughout their years of training and in practice.In conclusion, we have found a high prevalence of pseudotumor formation in patients presenting for follow-up of their ASR XL metal-on-metal total hip arthroplasty system. The pathophysiology and management of bowel and mesenteric injuries due to blunt trauma. In general, tumor stages were comparable.Table 3 Histopathologic Characteristics of Detected Cancers at Initial and Subsequent ExaminationsTable 4 Staging Data for Detected Invasive CancersOverall, the histopathologic grade distribution of DCIS did not differ significantly between the two modalities ($P = .105$). The mean ADC of the voxels in the ROI was calculated.Pathology reports were reviewed to determine the diagnosis and histologic subtype of each nonmalignant lesion. Crossref, Medline, Google Scholar4 Young SD, Marshall RS, Hill RP. However, to the best of our knowledge, our data represent the first report regarding ASL MR imaging in the characterization of untreated solid renal masses in humans.Our initial results suggest that ASL imaging has the potential to help in the MR characterization of renal masses by providing a quantification of tumor perfusion. Automated dose modulation is another method used routinely with modern CT scanners to decrease radiation exposure. The afferent arterioles constricted by 7%, which corresponds to a physiologically important increase of the resistance of the blood vessel by about 20%. J Trauma 1998;44(4):599–602; discussion 603. After the last MR imaging session, these animals were euthanized for subsequent ex vivo experiments. The final clinical diagnosis, as determined by the treating clinician, was recorded for each patient and compared with the initial diagnosis at CT. The majority of patients with cranial nerve palsy became asymptomatic after PED treatment. All the patients were receiving treatment with immunomodulatory (38 patients; 22 were receiving interferon beta and 16 were receiving glatiramer acetate) or immunosuppressive (19 patients) drugs for at least 6 months. Financial activities not related to the present article: institution received payment from Philips HealthCare for CT stroke imaging workshops. To assess peak tumor perfusion, an additional ROI of approximately 1 cm2 was placed within the region of the tumor that demonstrated the highest signal intensity with visual assessment of the perfusion image. J Trauma 2005;58(3):492–498. Measures of the amount of ecologic association between species. Three-dimensional high-resolution fast spin-echo coronary magnetic resonance angiography. Radiology 2008;249(2):524–533. PS-DIR relaxes the constraints related to blood signal nulling time and the period of minimal myocardial motion and thus enables black-blood imaging to be less sensitive to imaging time parameters. Crossref, Medline, Google Scholar27 Schalla S, Bekkers SC, Dennert Ret al.. For 47 of these patients, both diagnostic biopsy specimens and postcontrast cardiac MR images were available. Angiographic findings were reviewed independently and anonymously by two reviewers. Device diameter was at least equivalent to that of the proximal parent artery. Our study enabled us to partially confirm that finding. Crossref, Medline, Google Scholar78 Mirvis SE, Gens DR, Shanmuganathan K. Blind biopsies are still performed (nine [11%] of 80 departments); however, radiographer training to perform image-guided biopsy is still unusual (four [5%] of 85 departments). Although peak enhancement in each solid organ occurs at slightly different points in time, the portal venous phase offers a good compromise to maximize detection of parenchymal injuries. F.B. Financial activities related to the present article: none to disclose. A SPECT image, on the other hand, is a tomographic image that reduces summation artifacts and more clearly defines the spatial (ie, depth) localization of hot spots. We did establish the identity of respondents in terms of (a) teaching or district general hospital and (b) region of the United Kingdom in an attempt to evaluate potential selection bias between respondents and nonrespondents. 2008;35(10):1941–1959. Indeed, tumor size and necrosis, both at histopathologic examination (41) and MR imaging (10), have been associated with a higher histologic grade in clear cell RCC. We suspected that these atypical hypervascular HCCs that show hyperintensity on hepatobiliary phase images (hyperintense HCC) might reflect a distinct subtype of HCC with a particular molecular background and biologic features.The main tumor marker of HCCs is α-fetoprotein (AFP), especially the Lens culinaris agglutinin reactive fraction (L-3). BMC Urol 2008;8:3. Link, Google Scholar3 Saslow D, Boetes C, Burke Wet al.. J Am Coll Cardiol 2004;44(7):1393–1399. Neutralizing IL-17 prevents obliterative bronchiolitis in murine orthotopic lung transplantation. Crossref, Medline, Google Scholar2 Friedman JA, Nichols DA, Meyer FBet al.. Curative endovascular reconstruction of cerebral aneurysms with the pipeline embolization device: the Buenos Aires experience. Crossref, Medline, Google Scholar12 Guo Y, Cai YQ, Cai ZLet al.. These findings suggest that these procedures may be underused in high-risk patients and that this may to some extent relate to lack of access.Most studies on the safety and accuracy of liver biopsy have looked at patients with diffuse liver disease rather than those with focal lesions. Revised Guide for the Care and Use of Laboratory Animals available. Crossref, Medline, Google Scholar50 Piechnik SK, Chiarelli PA, Jezzard P. Crossref, Medline, Google Scholar33 Turner R, Le Bihan D, Maier J, Vavrek R, Hedges LK, Pekar J. Additionally, traditional calculations were found to be accurate predictors of SSDE for patients weighing 36 kg or less (in the case of) and for patients weighing 100–140 kg (in the case of); SSDE calculations are required for patients weighing between 36 and 100 kg and for those weighing more than 140 kg.Advances in Knowledge• The combination of lateral and anteroposterior measurements taken from the CT radiograph, when used to select conversion factors for the calculation of size-specific dose estimates (SSDE), leads to less calculated SSDE variability within anatomic sites compared with either measurement used individually.• No SSDE correction was required for patients of varying size who weighed 36 kg or less when volumetric CT dose index (CTDI) (CTDIvol) was measured by using a 16-cm-diameter CTDI phantom.• No SSDE correction was required for patients of varying size who weighed approximately 100–140 kg when CTDIvol was measured by using a 32-cm-diameter CTDI phantom.• CTDIvol values for patients of varying size and weight between 36 and 100 kg or greater than 140 kg required SSDE correction to more accurately estimate patient absorbed dose.Implication for Patient Care• The use of SSDE will provide a better predictor for pediatric patient absorbed dose than current implementations of CTDIvol using traditional 32-cm-diameter CTDI phantoms; for pediatric patient weight categories of 36 kg or less, a 16-cm-diameter CTDI phantom would be a better choice for CTDIvol calculations.Disclosures of Conflicts of Interest: S.L.B. No relevant conflicts of interest to disclose. It is unclear whether prior authors used primarily T2-weighted sequences for this determination, but if so they may have underestimated the number of cases with increased wall thickness. Images underwent the same blind procedures used for the original data sets, including analysis and wall thickness measurements. I-131 uptake in bilateral ovarian endometrial cysts. Differences in age between healthy subjects and those with CAD risk factors and between male and female patients were analyzed by using the unpaired Student t test.Scout images and coronary MR angiographic images of the right coronary artery were obtained similar to previously described methods (25,26).For coronary vessel wall imaging, a single-section TRAPD data set was acquired with segmented k-space spiral acquisition with spectral-spatial water-selective excitation (27) and use of a 32-channel phased-array cardiac receiver coil and vector electrocardiographic triggering (28). 1H MR spectroscopy and diffusion-weighted imaging of the breast: are they useful tools for characterizing breast lesions before biopsy? Pathophysiology of contrast-induced nephropathy. Stroke 2010;41(1):110–115. Crossref, Medline, Google Scholar42 Carl M, Koch K, Du J. Statistically, we were able to show that as the number of passes increased, so did the chance of an inadequate biopsy result. The median dose of aspirin was 100 mg (range, 80–300 mg). In the case that a lesion was not hyperintense at DW imaging, the ROI was drawn at the corresponding location and size as reflected at dynamic contrast-enhanced MR imaging with respect to other anatomic details. Voxelwise PPI analysis was first conducted at an individual level. Crossref, Medline, Google Scholar4 Golfieri R, Renzulli M, Lucidi V, Corcioni B, Trevisani F, Bolondi L. J Med Screen 2001;8(3):149–151. This work was performed by an experienced investigator (Z.Z.L.). Crossref, Medline, Google Scholar37 Rocca MA, Valsasina P, Absinta Met al.. Coronal reformation image reveals extraperitoneal bladder injury with extraluminal contrast material leaking from the bladder into the extraperitoneal space inferior to the bladder (arrow).Given that the trauma population often involves young, otherwise healthy patients, it is important to balance the risk of radiation exposure with the benefits of an examination that helps answer all the clinically important questions. Crossref, Medline, Google Scholar82 Malhotra AK, Fabian TC, Katsis SB, Gavant ML, Croce MA. Accessed January 12, 2012. Studies that used various generations of CT scanners report a sensitivity that varies between 70% and 95% and a specificity that varies between 92% and 100% for the diagnosis of bowel and mesenteric injuries (25,78–81).Table 4 Sensitivity and Specificity of Various CT Signs of Bowel InjuryFigure 6a: Axial contrast-enhanced CT images in a 35-year-old man, a pedestrian struck by a car, show (a) focal thickening of right colon (white arrows) with associated mesenteric hematoma (black arrow), (b) a moderate amount of hyperattenuation (measured attenuation, 30 HU) in the pelvis (arrow), and (c) pneumoperitoneum (arrow). Artifacts and pitfalls in diffusion MRI. AJR Am J Roentgenol 2007;188(2):540–546. Data were from 545 adult patients who underwent CT scans of torso. All participants provided written informed consent. (c) Immunohistochemical expression of PIVKA-II was significantly lower in hyperintense HCCs (0.59 ± 0.61) than that in hypointense HCCs (1.93 ± 1.10) ($P < .001$, κ = 0.81).Figure 4b: Bar graphs show immunohistochemical expression of AFP and PIVKA-II. We did not correlate perfusion with tumor grade in papillary RCC because of the characteristic very low perfusion levels for these tumors and the fact that papillary RCC has been relatively recently classified into two different subvariants (types 1 and 2) that have distinct biologic behavior and prognosis independent of their Fuhrman grade (40).We observed a statistically significant relationship between maximum tumor perfusion and increasing tumor size for the clear cell RCC subtype ($r = 0.71$, $P = .003$). Crossref, Medline, Google Scholar35 Perry NM, Patani N, Milner SEet al.. Crossref, Medline, Google Scholar3 Durante C, Haddy N, Baudin Eet al.. Financial activities not related to the present article: institution has patent pending related to IVIM. Although echo-planar techniques allow for fast imaging, the need for acquisitions with multiple b values extends acquisition time and makes the technique very motion-sensitive if the curve is fitted on a voxel-by-voxel basis. High-resolution 3D coronary vessel wall imaging with near 100% respiratory efficiency using epicardial fat tracking: reproducibility and comparison with standard methods. Washington, DC: American Psychiatric Publishing, 2011. Serum AFP levels were measured by using chemiluminescent enzyme immunoassay (Lumipulse presto; Fujirebio, Tokyo, Japan). Notable exceptions would include adnexal evaluation in women and acute cholecystitis. AJR Am J Roentgenol 2009;192(1):3–10. The interpretation of 131I scans in the evaluation of thyroid cancer, with an emphasis on false positive findings. A total of 332 consented to participate. Appendicitis near its centenary. At pathologic evaluation, the lesion was proved to be ccRCC.Figure 4b Findings in a 58-year-old woman with an enhancing lesion in the lower pole of the right kidney (arrow), which on review of (a) precontrast and (b) postcontrast T1-weighted fat-saturated gradient-echo VIBE MR images was diagnosed as pRCC by all three radiologists, owing to low-level homogeneous contrast enhancement at corticomedullary phase. CM, no LGE = cardiomyopathy without visually evident LGE, CM, +LGE = cardiomyopathy with visually evident LGE.The diagnostic performance of myocardial T1 time to detect mild (>5%) degrees of histologic fibrosis, expressed as an area under the curve (AUC), was 0.84 (95% CI: 0.70, 0.93; $P < .0001$) with a cutoff T1 time of 383 msec (Fig 4). (d) Six containers stuffed with cocaine were found at stool analysis.Figure 2b: (a) False-negative abdominal radiograph at admission in a 26-year-old man suspected of conveying drug packets. Crossref, Medline, Google Scholar3 Kwee TC, Kwee RM. Further protocol parameters of the very short sequence were TR, 8 msec; matrix, 128 × 128 × 128; field of view, 45 × 45 × 45 mm; spatial resolution, 0.35 × 0.35 × 0.35 mm; flip angle, 18.9 degrees; number of acquisitions, one; acquisition time, 6 minutes and 50 seconds. Box plots represent medians and ranges of ADCs. Benign and high-risk lesions (including ADH and LCIS) were analyzed for our study, and ADCs of all malignant (n = 31) breast lesions from a prior study (20) are shown for comparison. Defining the clinical course of multiple sclerosis: results of an international survey. However, because we found the results to be quite similar whether including or excluding the data from this pilot study, we felt reassured that the missing values represent a random sample and do not compromise the validity of our study. However, we do not know whether this process also occurs in patients with other MS clinical phenotypes and whether the release of cerebellar recruitment and the mobilization of prefrontal areas is a shared phenomenon among the various clinical phenotypes of the disease.Researchers in several other previous studies have shown that the cerebellum (particularly the posterior lobules) is involved in cognitive processes, including attention, language, visuospatial skills, and working memory (10–12). Organ injury scaling: spleen and liver (1994 revision). 1979;20(2):92–97. Crossref, Medline, Google ScholarPage 18Medical radiation exposure to the public has been reported to have increased over the past 10–15 years and now accounts for nearly 50% of the total collective dose (person-Sieverts) to the U.S. population, where nearly half of all medical radiation to patients comes from computed tomography (CT) (1). D.C.A. Financial activities related to the present article: none to disclose. Appendicitis can be a difficult diagnosis on the basis of clinical grounds alone, with one large study of more than 20 000 adults reporting a 20% negative appendectomy rate in the era before computed tomography (CT) (2). With the improvement in packet manufacturing, it would not be surprising if a majority of intracorporeal containers became undetectable at abdominal radiography in a short time. Such outliers can corrupt the mean estimates derived from the ROI analysis. The management of isolated duodenal hematomas is conservative (90,91).Surgical management of duodenal lacerations hinges on the extent and severity of the duodenal injury, as well as the involvement of the adjacent vasculature, biliary tree, and pancreas (10,90,91). Link, Google Scholar32 Jørgensen KJ, Keen JD, Gøtzsche PC. Average values for each group are shown for each ROI and each time for BVf (c) and MR estimate of sO_2 (d). Magn Reson Med 2009;61(5):1040–1048. Assessment of a new trauma workflow concept implementing a sliding CT scanner in the trauma room: the effect on workup times. Mean patient age was 39.2 years ± 17.2 (standard deviation) (age range, 18–93 years). quantitative blood oxygen level-dependent analysis in brain tumor. Lesional studies have demonstrated that the right cerebellum is mainly involved in executive and attentional functions (13,14). Radiology 2009;251(2):398–407. Contrast material–enhanced CT scans in eight different symptomatic patients with clinical concern for appendicitis show (a) right-sided omental infarction in 42-year-old woman, (b) epiploic appendagitis in 41-year-old woman, (c) cecal diverticulitis in 51-year-old woman, (d) right-sided colonic ischemia in 58-year-old man, (e) Meckel diverticulitis in 33-year-old man, (f) acute cholecystitis in 65-year-old woman, (g) pelvic inflammatory disease with tubo-ovarian abscess in 28-year-old woman, and (h) spontaneous rectus sheath hematoma in 54-year-old woman. The use of coronal and sagittal reformations led to the description of two additional variants of the collar sign: the hump sign, in which a rounded portion of the superior liver herniates through the diaphragmatic rent and the band sign, in which the torn free edge of the diaphragm causes a linear indentation in the herniated liver edge (42,43). Radiation risk in perspective. Ex vivo necrotic, hypoxic, and normoxic pixel values were set to one (necrotic), two (hypoxic), or three (normoxia) according to their staining (no cells, brown staining, and no staining, respectively).Figure 2b: Spatial correlation between MR estimate of sO_2 map (MR_SO2) and pimonidazole staining. Data were acquired by using prospective navigator gating and correction (29). Melamed, A.P.K.; statistical analysis, H.C., J.S.B., A.P.K.; and manuscript editing, H.C., A.B.R., S.K., A.A.A., S.D.R., J. In our study, the follow-up period averaged 727 days, which might not have been sufficient to demonstrate a significant difference.Several prior reports have suggested that transcription factor hepatocyte nuclear factors control both OATP8 and AFP expression (9,12,13,17). The treated group received a daily oral administration of sorafenib between D10(T0) and D18(T8). Packets consisted exclusively of large fingerlike containers that weighed 7–25 g each. Breast Cancer Res Treat 2009;115(1):181–183. Once a person has been suspected of carrying intracorporeal drug containers, he or she is usually referred to a medical center to undergo a radiologic examination. BVf in the treated tumors decreased down to the value measured in the healthy brain tissue. In all series, the last 15 seconds of each interval was used for statistical analysis of steady-state responses. Hybrid ICA-seed-based methods for fMRI functional connectivity assessment: a feasibility study. The radiologist on call rated this radiograph as positive, with very high confidence (4 of 4) in his diagnosis. D.A.B. No relevant conflicts of interest to disclose.We gratefully acknowledge the contributions of Charles Steenbergen, MD, PhD, for his expertise in cardiovascular pathology. Crossref, Medline, Google Scholar13 Roberts TP, Mikulis D. a 10-year study. Part 2–44: Particular requirements for the safety of x-ray equipment for computed tomography. 2004;31(10):1435–1442. MR angiography in the follow-up of intracranial aneurysms treated with Guglielmi detachable coils: systematic review and meta-analysis. The term fibrocystic change encompasses a heterogeneous group of histologic findings (44), and in our study this term was used only when a specific subtype was not evident at histologic examination.We further evaluated many other subtypes that proved to be false-positive findings at dynamic contrast-enhanced MR imaging—subtypes that have not been commonly reported in prior DW imaging studies. Our findings suggest that clinical symptoms do not correlate with presence or size of pseudotumor formation, although bone marrow edema and high-grade abductor tendon tears at MR imaging are correlated with patient pain. McMenamy, and S.K., with 2–11 years of experience in the interpretation of abdominal MR images), who were blinded to the pathologic findings, independently evaluated pre- and postcontrast acquisitions including subtraction data sets (23). (c) Serum level of PIVKA-II was in normal range (10 cm), which may relate to necrosis.We found certain significant variables relating to the chance of an inadequate initial biopsy insufficient for diagnosis, including presence of a focal lesion and increasing number of biopsy passes. A P value less than .05 was considered to indicate a statistically significant difference. CTDIvol values were recorded from the “Dose Report” (Fig 1a) archived with each patient’s CT examination.Figure 1a: (a) Dose report lists CTDIvol, DLP, and CTDI phantom diameter (where Body 32 =) for a 5-year-old girl. Perlewitz No relevant conflicts of interest to disclose. In the treated group, however, tumor MR estimate of sO_2 values became significantly lower than in the contralateral striatum as soon as D13(T3) (58.5% ± 4.6 vs 70.8% ± 4.7, respectively; $P < .001$) (Fig 4d) and remained low at D15(T5) (54.8% ± 4.5 vs 70.3% ± 4.2, respectively; $P < .001$) (Fig 4d). The cohort of seven volunteers was small, and the study was performed at a single center. Crossref, Medline, Google Scholar51 Le Bihan D, Turner R. Other relationships: none to disclose.Advances in Knowledge• In 57 patients with multiple sclerosis (MS), higher cerebellar recruitment is associated with better behavioral performance, while higher precuneus recruitment is related to worse behavioral performance ($P < .001$).• In MS, cognitive-related cerebellar activity decreases with longer disease duration ($P < .001$).• With increasing task demand, abnormal functional interactions between cerebellar and prefrontal areas occur in MS patients.• In MS patients, T2 lesion volume was correlated with activity of the left middle frontal gyrus, whereas normalized brain volume was inversely correlated with activity of the right precuneus ($P < .001$).Author contributions: Guarantors of integrity of entire study, M.C.B., M.F.; study concepts/study design or data acquisition or data analysis/interpretation, all authors; manuscript drafting or manuscript revision for important intellectual content, all authors; approval of final version of submitted manuscript, all authors; literature research, M.A.R., M.C.B., B.C., M.F.; clinical studies, M.C.B., B.C., M.F.; experimental studies, M.A.R., M.C.B., M.F.; statistical analysis, M.A.R., M.C.B., P.V., M.F.; and manuscript editing, M.A.R., M.C.B., P.V., B.C., G.C., M.F.Supported in part by a grant from Fondazione Italiana Sclerosi Multipla (grant FISM/2008/R/13).References1 Rao SM. This is consistent with the observations reported by Jenkins et al (14) using in vivo (Eppendorf needle electrode) and ex vivo (2-nitroimidazole EF5) techniques in the 9L gliosarcoma model. The intraclass correlation coefficient for absolute agreement was calculated to assess intraobserver, interobserver, and interexamination agreement. Neuroimage 1995;2(1):45–53. Crossref, Medline, Google Scholar30 Le Bihan D, Moonen CT, van Zijl PC, Pekar J, DesPres D. Quantification of cerebral arterial blood volume and cerebral blood flow using MRI with modulation of tissue and vessel (MOTIVE) signals. Radiology 1990;177(2):407–414. This may explain the improved delineation of the vessel wall and the larger resolved arterial wall thickening (from 25% to 36%) in subjects with CAD risk factors relative to healthy subjects. Radiology 2007;244(2):356–378. J Trauma 2001;50(2):195–200. There was a significant correlation between mean whole tumor perfusion at ASL imaging and mean whole tumor contrast enhancement at the corticomedullary phase ($r = 0.54$, $P = .002$) and nephrogenic phase ($r = 0.56$, $P = .001$). The preparation of arterioles took less than 1 hour in most cases. It was thought to be beyond the scope of this audit to examine specifically the number of portal tracts, and the presence of a histologic report with a diagnosis was considered consistent with adequacy for the purposes of the audit. This study did include a small subset of patients who underwent unenhanced CT, which could potentially skew the results because some alternative diagnoses are not as readily identified at unenhanced CT, but these cases represented less than 8% of our total. As suggested by findings in previous studies in disabled patients (8,9,27,28), this latter finding is likely to reflect an exhaustion of the capacity of overrecruiting brain areas with disease progression. For the subgroups of patients imaged at either 1.5 or 3.0 T, the agreement between intraarterial DSA- and MR angiography–based advice was also substantial (weighted κ = 0.64; 95% CI: 0.47, 0.81 for 1.5 T and weighted κ = 0.75; 95% CI: 0.67, 0.84 for 3.0 T). Signed informed consent was obtained. Link, Google Scholar13 van Randen A, Laméris W, van Es HWet al.. AJR Am J Roentgenol 2007;189(4):860–866. Crossref, Medline, Google Scholar32 Chenevert TL, Pipe JG, Williams DM, Brunberg JA. However, it has been shown that the diagnostic performance of quantitative breast DW imaging is not affected by the choice of different b values or the use of multiple versus two b values (53,54). Numbers for breakfast: summary of hip arthroplasty outcomes from the National Joint Registry for England and Wales 8th Annual Report (2011). Among the 90 patients who received a specific alternative diagnosis at CT but did not receive a final clinical diagnosis, the most common CT diagnoses included benign adnexal mass (n = 32); gastroenteritis, colitis, or adenitis (n = 22); constipation (n = 16); inflammatory bowel disease (n = 6); and pelvic congestion syndrome (n = 3). Heterogeneity of intraductal carcinoma of the breast. (b) Graph shows fraction of pixels within the tumor and with an MR estimate of sO_2 less than 40% (necroticohypoxic fraction) as function of the necroticohypoxic tumoral fraction estimated ex vivo for the untreated group. The hypointense HCCs showed higher positive rates for fibrous capsule invasion and hepatic vein invasion, although the differences did not reach statistical significance ($P = .81$ and .21, respectively). Circ Cardiovasc Imaging 2012;5(1):78–85. Medline, Google Scholar76 Killeen KL, Shanmuganathan K, Poletti PA, Cooper C, Mirvis SE. MAGMA 2010;23(1):1–21. Of 14 lesions classified as having ADCs greater than 1.81 × 10^{-3} mm2/sec by SP1, one lesion (focal fibrosis) was reclassified having an ADC below the threshold at the SP2 analysis. Therefore, larger-scaled studies are required to confirm our results.In conclusion, ASL MR imaging enables unenhanced perfusion measurements of untreated renal masses. Traditional MR imaging features of oncocytoma may be indistinguishable from those of chromophobe RCC (42). The CTDIvol is generally defined for two diameters of polymethylmethacrylate (PMMA) phantoms representing the head (16 cm in diameter, yielding) and body (32 cm in diameter, yielding); some manufacturers use the 16-cm “head” phantom to measure CTDIvol for the pediatric body.CTDIvol and DLP metrics are sensitive to changes in scanning parameters (eg, tube current, tube voltage, bowtie filter selection, and scan length) and therefore are useful metrics with which to compare relative patient dose to diagnostic reference levels (eg, those published by the American College of Radiology) (6,7). The role of diffusion-weighted imaging and the apparent diffusion coefficient (ADC) values for breast tumors. For this AEC system, the user specifies two parameters. (a) Axial dynamic contrast-enhanced initial postcontrast subtraction MR image shows 13-mm lobular heterogeneously enhancing mass (arrow) in the subareolar region of the left breast, 16 mm from the nipple. Thirty-eight departments submitted 50 cases, with the remainder submitting fewer cases (range, six to 49 cases). In some cases, departments were within individual hospitals; in others, the patient cohort was drawn from more than one hospital within an organization containing multiple centers. doi: 10.1186/s13017-020-00302-7. J Magn Reson Imaging 2003;17(5):538–544. They were derived from evaluation of relevant available literature (1–8). Crossref, Medline, Google Scholar24 Schmidt AJ, Kee ST, Sze DYet al.. Thinner image reconstructions and multiplanar reconstructions were reviewed at the discretion of the interpreting radiologist on a case-by-case basis.Results of each CT examination were prospectively interpreted by a board-certified staff radiologist (range of experience from 5 to more than 20 years) within the abdominal imaging section. Circ Res 2004;94(12):1533–1542. Lancet 2001;357(9254):463–467. The agreement between SSDEsize and SSDEage for patients between 13 and 18 years was within 16% (16.2/19.2) but demonstrated a maximum difference of 28% (20.0/27.9). Serious response bias does not appear evident from these comparisons.In conclusion, this study provides data in a large number of image-guided and image-assisted biopsies of focal and diffuse liver lesions and gives an indication of current United Kingdom radiologic practice. 2009;50(1):18–23. Note large degree of hemoperitoneum related to this grade V splenic injury. Crossref, Medline, Google Scholar2 Ferns SP, Sprengers ME, van Rooij WJet al.. AJNR Am J Neuroradiol 2000;21(7):1184–1189. Anthony et al reported that approximately 9.6% of all reports may have critical findings, but that study had a broad definition and included many more potential values (more than 30), such as lung nodules, renal masses, fractures, all types of pneumothoraces, and intracranial hemorrhage, which occur far more frequently than some of the critical values identified in this study (13). Presence and type of symptoms (pain or mechanical) were recorded at the time of patient contact by an orthopedic surgeon (J.R.V.H.).MR imaging of the pelvis and hips was performed with a 1.5-T clinical superconducting imager (Signa; GE Medical Systems, Milwaukee, Wis) by using an eight-channel flexible coil. Six patients were excluded from our study because they had a massive thyroid remnant that was detected as an obvious mass with CT. Crossref, Medline, Google Scholar16 D’Urso PI, Lanzino G, Cloft HJ, Kallmes DF. Because of the depiction of lung parenchyma, the pneumothorax was only visible in very short TE sequences. (b) Immunohistochemical expression of AFP was significantly lower in hyperintense HCCs (0.36 ± 0.47) than that in hypointense HCCs (1.34 ± 1.11) ($P < .001$, κ = 0.78). We hypothesized that there are abnormal neuronal activations of DMN subregions in the resting brain in patients with MTBI, which can be detected with advanced ICA techniques.To validate our findings, we used three different strategies of ICA, which included a template-based ICA method (29), a hybrid ICA seed-based method (30), and a group ICA method (31) in patients with MTBI compared with healthy individuals. Slope of line regressing CTDIvol against AP+LAT had 95% CI of 0.31 to 0.37 mGy/cm. In the iodixanol group, the response to angiotensin II in afferent arterioles was increased significantly, compared with the control group ($P = .03$).DAF-FM fluorescence increased over 20 minutes in the control situation (Fig 5). Evaluation of a transcutaneous carbon dioxide monitor (“TOSCA”) in adult patients in routine respiratory practice. Combination of signals from array coils using image-based estimation of coil sensitivity profiles. Link, Google Scholar26 Stuber M, Botnar RM, Danias PG, Kissinger KV, Manning WJ. Y.C.W. No relevant conflicts of interest to disclose. E.B.T. No relevant conflicts of interest to disclose. J Bone Joint Surg Am 2011;93(23):2164–2171. Transjugular biopsy was recorded as a separate entity, with the majority of these procedures (65 of 68 [96%]) undertaken as nonfocal biopsies for diffuse liver disease. In the 14 patients with cranial nerve palsy, mRS score was 1 (n = 10) or 2 (n = 4). Mean ages at operation were 66 years (range, 36–89 years) for the asymptomatic group, 63 years (range, 39–83 years) for the pain symptoms group, and 62 years (range, 68–81 years) for the mechanical symptoms group. Differences in occlusion grading on intraarterial DSAs and MR angiograms can also be explained by, to some extent, the subjective discrimination between neck remnant and residual aneurysm. Crossref, Medline, Google Scholar8 Lakhani P, Langlotz CP. Furthermore, the sensitivity dropped to 0.25 (two of eight) when packets were both isoattenuated and small in quantity (≤12). Because a whole-body scintigraphic image is an image obtained in the anterior and posterior projections, it is difficult to identify the precise site of uptake for some patients. This is, in part, because uncertainties in available data make it difficult to estimate the risk associated with effective doses or organ doses below 100 mSv (22–24). An image-based approach to understanding the physics of MR artifacts. In fact, the injured pancreas may appear normal on CT images, particularly in the first 12 hours after a trauma injury (85). Crossref, Medline, Google Scholar9 Horiguchi J, Fukuda H, Yamamoto Het al.. Vascular emergencies in liver trauma. Researchers utilized prior clinical radiology reports to identify lesions at DW imaging and were blinded to the results of pathologic examination (nonmalignant subtype). Nat Rev Neurol 2010;6(1):15–28. The intratumoral ROI was placed within the region of the tumor that demonstrated most avid contrast enhancement during the corticomedullary phase. Impairment of movement-associated brain deactivation in multiple sclerosis: further evidence for a functional pathology of interhemispheric neuronal inhibition. Evaluation of a quantitative blood oxygenation level-dependent (qBOLD) approach to map local blood oxygen saturation. Effects of intravoxel incoherent motions (IVIM) in steady-state free precession (SSFP) imaging: application to diffusion imaging. Treatment with L-NAME also significantly enhanced the angiotensin II response of afferent arterioles perfused with iodixanol (median, 42.5% [25th and 75th percentiles, 31.7% and 50.6%, respectively] vs 74.9% [25th and 75th percentiles, 67.0% and 88.3%, respectively]; $P = .03$) (Fig 8). Crossref, Medline, Google Scholar6 Blumenfeld AJ, Guru K, Fuchs GJ, Kim IIL. Crossref, Medline, Google Scholar51 Yu J, Fulcher AS, Wang DBet al.. (b) Image obtained in corticomedullary phase after administration of contrast material shows homogeneous tumor enhancement. The first is the effective tube current–time product (effective mAs) required to achieve the desired level of image quality for the specific diagnostic task in a reference patient (adults who weigh 70-80 kg). Clin Cancer Res 2008;14(17):5548–5554. Finally, the number of patients investigated in this study is relatively small, resulting in a limited number of masses in each non–clear cell RCC subtype and in the oncocytoma group. Curr Opin Psychiatry 2010;23(3):267–272. We suspect that the molecular regulatory mechanism of OATP8 expression may have some common channels with those of AFP or PIVKA-II expression.In addition, hyperintense HCCs on hepatobiliary phase images showed a significantly lower recurrence rate than did hypointense HCCs. The patients with hyperintense HCCs showed longer survival than those with hypointense HCCs, but the difference was not statistically significant. Crossref, Medline, Google Scholar56 Fitzek C, Mentzel HJ, Fitzek S, Sauner D, Kaiser WA, Reichenbach JR. Is SPECT/CT with a hybrid camera useful to improve scintigraphic imaging interpretation? Diagnostic performance of ADC for non-mass-like breast lesions on MR imaging. In the remaining patients, endomyocardial biopsy demonstrated findings consistent with chronic, borderline, or resolving myocarditis (six patients). South Med J 2009;102(5):470–475. On the other hand, we were able to exclude—in all but one graft—false-positive signals of the transplanted lung, such as atelectasis, because the lung had been almost fully expanded throughout the images. Financial activities not related to the present article: author is a consultant for Medis Medical Imaging Systems. Financial activities not related to the present article: institution has a grant or grant pending from Matakina Technology and Riverain Medical; institution received money for patent (planned, pending, or issued) from Mevis Medical Solutions; has stock in Matakina Technology. D.L. Financial activities related to the present article: none to disclose. Fitting variables were S0, T2*, and N. Solid renal cortical tumors: differentiation with CT. Dynamic contrast-enhanced-MRI of tumor hypoxia. Published 2008. There was no difference in specificity between the two methods ($P = .62$). Furthermore, at the time when our study was performed, stents were rarely used to treat aneurysms. Financial activities not related to the present article: received consultancy fees from Bayer Pharma and payment for lectures including service on speakers bureaus from Bayer Pharma, Guerbet, Bayer Vital, and Bracco Imaging Deutschland; institution received grants or has grants pending from Bayer Pharma. Because of the strong differences between the T2* relaxation time of well-ventilated lung parenchyma (0.5–1.0 msec), soft tissue (approximately 10–100 msec) and blood (several seconds), the best image quality could be achieved for log-transformed T2* maps, which still provided sufficient sensitivity for the detection of tissue alterations in transverse relaxation.Figure 4: Very short TE images (left) in transverse (top row) and coronal (bottom row) orientation acquired with TE = 50 µsec. Therefore, the enhanced depiction of microcalcifications on digital images has most likely added to its higher detection performance. Partial volume effects with cerebrospinal fluid may have been variable during the experiment.Nevertheless, quantification of cerebral blood perfusion with current methods, such as dynamic susceptibility contrast-enhanced and dynamic contrast-enhanced MR imaging and arterial spin labeling, remains a major challenge for many reasons (5–8). Radioactive foci located from the neck down and outside both lung fields were categorized as positive for uptake in distant metastasis when they clearly were not physiologic accumulation in the stomach or intestines.SPECT/CT findings were next described with the anatomic localization of 131I uptake. To this end, the purposes of this study were to determine the prevalence of abnormalities at magnetic resonance (MR) imaging after metal-on-metal total hip arthroplasty and to determine whether presence of symptoms correlates with MR imaging findings.The institutional review board approved this Health Insurance Portability and Accountability Act–compliant study and waived informed consent. This observation suggests that abdominal radiography cannot be relied on to detect packets when the radiologist is not confident in his or her interpretation; in the current series, this corresponds to 31% (104 of 330) of our study group. However, although reports have been mixed, the application of such a CT-based scheme established according to the AAST liver injury scale has limitations in the ability to guide subsequent management decisions or predict complications related to liver injuries, similar to imaging of splenic trauma (65,70). Crossref, Medline, Google Scholar12 Berlin L. Crossref, Medline, Google Scholar94 Shanmuganathan K, Mirvis SE, Amoroso M. Original values were converted to by dividing the value by 2, and, conversely, original values were converted to by multiplying the value by 2.The data sets in this study were summarized by using descriptive statistical analysis. The AUC is 0.84 (95% CI: 0.70, 0.93; $P < .0001$).Exclusion of three patients with cardiac amyloidosis at biopsy did not meaningfully alter the overall correlation between percent fibrosis and T1 ($r = -0.52$; $P < .01$) or AUC (5% fibrosis, 0.83; 95% CI: 0.68, 0.92; $P < .0001$).The results of quantitative LV structure and function analysis are summarized in Table 2. Radiology 2010;256(3):817–826. (c) Delayed phase image demonstrates further enlargement of areas of hemorrhage (arrows). Crossref, Medline, Google Scholar20 Lyng H, Sundfør K, Rofstad EK. A major stroke was defined as any stroke that resulted in severe disability, with modified Rankin Scale (mRS) score of 4 or 5. This offset results from noise in the difference ASL images in combination with magnitude imaging. Imaging in appendicitis: a review with special emphasis on the treatment of women. This interval was long enough to acquire four and five frames in 37 (97%) and 28 (73%) of the 38 subjects, respectively. Link, Google Scholar24 Wernecke J. The free end of the arteriole is aspirated into a pipette, visible on the left hand side. J Econom 1985;29(3):305–325. Magn Reson Med 2005;54(2):333–342. This well-thought-out text is coauthored by Ronald L. * = Data were available from January 1 to April 13, 2011.During the entire study period, documentation of communication was highest in acute scrotal torsion (70.59%) and ectopic pregnancy (65.43%). C.R. No relevant conflicts of interest to disclose. Magnetization transfer contrast imaging in bovine and human cortical bone applying an ultrashort echo time sequence at 3 Tesla. Evaluation of bowel and mesenteric blunt trauma with multidetector CT. Not surprisingly, traumatic adrenal hemorrhage is usually accompanied by injuries in other upper abdominal organs, especially the liver. A cocaine body packer with normal abdominal plain radiograms: value of drug detection in urine and contrast study of the bowel. Crossref, Medline, Google Scholar13 Gøtzsche PC, Nielsen M. Anterior and posterior images were acquired at a speed of 10 cm/min with high-energy parallel-hole collimators, a 256 × 1024 matrix, and a 364-keV photopeak with 15% windows. J Gastroenterol 2009;44(7):793–798. This most often occurs in older patients, as was the case in our study. Google Scholar43 Le Bihan D, Turner R, MacFall JR. Crossref, Medline, Google Scholar33 Smith A. Financial activities not related to the present article: received payment for development of educational presentations from MCM Education. Y.L.C. No relevant conflicts of interest to disclose. Furthermore, inaccurate RCC subtyping may occur in 12%–14% of renal biopsies and tumor grade has been shown to be unreliable (6).Magnetic resonance (MR) imaging has emerged as a pivotal imaging technique in the characterization of renal lesions (7,8). J Neurol Neurosurg Psychiatry 2007;78(11):1231–1238. High-grade abductor tendon tear was seen in five asymptomatic patients, 13 patients with pain, and three patients with mechanical symptoms. Thus, a total of eight rats per group were imaged at each time.Figure 1a: (a) Diagram shows experimental protocol. Google Scholar22 American Association of Physicists in Medicine. Analysis was performed by using MedCalc v 12.1.1 (MedCalc Software, Mariakerke, Belgium).A description of the study population is provided in Table 1. Crossref, Medline, Google Scholar3 Malnick S, Melzer E. Advances in functional and structural MR image analysis and implementation as FSL. 2, Abdominal radiograph deemed negative (level of confidence, 3). This corresponded to a decrease of turbulent flow in the cerebrospinal fluid, which we assumed was due to an increase in brain volume in the constant skull volume and a consecutive decrease in cerebrospinal fluid volume. Remediation of “working attention” in mild traumatic brain injury. 5, Abdominal radiograph deemed positive (level of confidence, 1). Rats were then randomized and stratified to two groups (n = 24 per group) with similar average tumor volume. Crossref, Medline, Google Scholar6 Persson PB, Hansell P, Liss P. Abdominal injuries without hemoperitoneum: a potential limitation of focused abdominal sonography for trauma (FAST). Moreover, the additional cost of unenhanced CT often precludes systematic use of the test in this setting. Crossref, Medline, Google Scholar14 Weston AR, Jackson TJ, Blamey S. Interestingly, longer RTs in patients with benign MS and longer disease duration in patients with all MS phenotypes were both associated with an increased activation of the right precuneus, a well-known area of the default mode network (34), which has been demonstrated to be altered in patients with MS (35–37). In both sequences, signal intensity of the lung was similar to the noise level for both the normal and transplanted lung, respectively. We have been unable to confidently distinguish between an anatomic trochanteric bursa and other collections; thus, we defined pseudotumor as any soft-tissue collection that was cystic or solid in nature, without exclusion due to size or location. J Magn Reson Imaging 2000;11(2):208–214. The variables investigated with the clinical questionnaire were as follows: characteristics of the individual biopsy (focal lesion present at imaging), size of focal lesion biopsied (measured in centimeters), imaging modality, operator grade, type of anesthesia used, biopsy needle gauge, number of passes at biopsy, and type of biopsy needle. Quantitative measurement of tissue perfusion and diffusion in vivo. Twenty-two patients had no visual evidence of LGE and 25 had visually evident LGE. Eur J Nucl Med Mol Imaging 2010;37(6):1077–1086. The natural length of arterioles varies. Marrow edema surrounding the femoral component was considered present if there was intramedullary hyperintense signal at fluid-sensitive sequences with iso- or hypointense signal at T1-weighted sequences relative to surrounding marrow (Fig 4). Crossref, Medline, Google Scholar4 Ernster VL, Ballard-Barbash R, Barlow WEet al.. Crossref, Medline, Google Scholar13 Chowdhury S, Choueiri TK. CT findings correlate well with the AAST classification. Crossref, Medline, Google Scholar2 Dinneen SF, Valimaki MJ, Bergstralh EJ, Goellner JR, Gorman CA, Hay ID. Patients with adequately occluded aneurysms would be discharged from further follow-up imaging.The MR angiograms were assessed similarly to intraarterial DSA images by another rater from a group of five senior interventional neuroradiologists (G.A.P.d.K., C.B.L.M.M., M.E.S.S., J.C.B., or P.A.B.; mean experience, 10 years; range, 6–15 years; median, 10 years), who was unaware of the parallel intraarterial DSA results. Foci whose location could not be differentiated between the mediastinum and lung were categorized as equivocal for LN metastasis. Possible explanations include our much larger sample size compared with the prior study and our use of both T1 and fluid-sensitive sequences in our determination of wall thickness. Accuracy of enhancement parameters in discriminating ccRCC may be overestimated in our study since cutoff values were generated and evaluated on the same data set.In conclusion, our study has shown that histogram analysis of WL enhancement as well as histogram distribution parameters kurtosis and skewness can be used to discriminate ccRCC from pRCC with high accuracy and high interreader agreement.Advances in Knowledge• Analysis of voxel-based whole-lesion enhancement histogram parameters can be used to discriminate between clear cell and papillary subtypes of renal cell cancers; the whole-lesion parameter of third quartile enhancement had the highest accuracy (area under the curve [AUC], 0.98) with sensitivity of 96% and specificity of 90%.• Whole-lesion enhancement histogram distribution parameters kurtosis and skewness can be used to discriminate clear cell from papillary renal cell cancer with high accuracy (AUC, 0.954 and 0.938, respectively), without reliance on the absolute measure of signal intensity change.Implication for Patient Care• Ability to noninvasively discriminate clear cell from papillary renal cell cancer with analysis of whole-lesion enhancement histogram parameters can potentially affect patient management, as these two subtypes have different prognoses and respond differently to available chemotherapy in advanced disease.Disclosures of Conflicts of Interest: H.C. No relevant conflicts of interest to disclose. This ROI was copied to the precontrast acquisition. Size was determined by summing AP and LAT dimensions at the midline (AP+LAT), measured from transverse CT images at the mid-liver level. The second user-specified parameter for the AEC system is the strength with which the tube current was adjusted as a function of patient size: weak, average, or strong (5,6). We confirmed that the majority of patients underwent biopsy as outpatients; however, 1520 (45%) of 3372 biopsies were performed in inpatients, with 3238 (96%) of 3378 biopsies performed with local anesthesia. Average age was 65.0 years ± 10.3 (range, 34–83) (age of men 64.5 years ± 10.5 [range, 34–83 years]; women, 67.4 years ± 9.5 [43–83 years]). Although on a molecular and histologic level inflammatory mediators may degrade the material properties of tendon and bone, we think this is not evident with current imaging modalities and that these findings should be separated from an MR classification of metal-on-metal disease.One limitation of our study is the cross-sectional nature, with analysis at a single time point. Am Surg 2009;75(2):133–139. Our results suggest that even more subtle degrees of diffuse fibrosis may be identified by means of cardiac MR T1 mapping in a diverse population with cardiomyopathy.Different causes of myocardial injury can result in different patterns, distributions, and degree of myocardial fibrosis, ranging from distinct segmental and replacement fibrosis after coronary occlusion to diffuse interstitial fibrosis in the settings of dilated cardiomyopathy or severe valvular disease (19). Magn Reson Med 2008;60(3):604–615. Radiology 2010;256(3):799–805. According to use of the Anderson MR grading scale for metal-on-metal hip replacements, total agreement was present in 120 of 192 cases. The less specific (but more sensitive) CT signs of bowel trauma include unequivocal focal wall thickening (Fig 6), abnormal bowel wall enhancement, ill-defined increased attenuation (stranding) of the mesentery, and free intraperitoneal fluid (Fig 6). 5340596-1EN (rev 5). I highly recommend this book to neuroradiology fellows in training and practicing radiologists and spine surgeons.Reviewed by Jonelle Petscavage, MD, MPHPage 3A Practical Guide to Leadership and Management in Academic Radiology is a well-written book intended to provide useful and practical information primarily to chairpersons of academic radiology departments. For large-size aneurysms harboring partial thrombosis, the approach of endoluminal coil placement had been challenged, and surgical excision or parent artery occlusion had been advocated, because these aneurysms are likely extraluminal disorders involving subacute or chronic dissections, repeated intramural hematomas, proliferating vasa vasorum, and triggering of inflammatory mechanisms, such that subarachnoid hemorrhage from the aneurysms originates from the periphery of their walls instead of the lumen of their sacs or necks (19). The prior training was 5–6 years of general radiology for the fellows and 3–5 years for the residents, including at least 6 months of conventional radiology and 2 years of body CT. Crossref, Medline, Google Scholar11 The Royal College of Radiologists. W.J.v.R. No relevant conflicts of interest to disclose. Other relationships: none to disclose. Frequencies contributing to functional connectivity in the cerebral cortex in “resting-state” data. Among patients receiving a specific nonappendiceal CT diagnosis, 204 of 496 (41.1%) were hospitalized an average of 5.7 days ± 6.8, and 109 of 496 (22.0%) underwent surgical or image-guided intervention. Invest Radiol 2010;45(3):133–141. Traumatic retroperitoneal injuries: review of multidetector CT findings. Crossref, Medline, Google Scholar92 Sivit CJ, Taylor GA, Bulas DI, Kushner DC, Potter BM, Eichelberger MR. The total number of DMN voxels in the healthy control group with PCC seed (n = 16 877) had only a 41.2% (DICE coefficient) overlap with MPFC seed (n = 20 152). Differences in radiological patterns, tumour characteristics and diagnostic precision between digital mammography and screen-film mammography in four breast cancer screening programmes in Spain. No indirect or direct financial support was provided by an industry. Crossref, Medline, Google Scholar25 Mayer AR, Mannell MV, Ling J, Gasparovic C, Yeo RA. All P values are two sided. In 67 cases, the biopsy included within the audit was the result of a previous nondiagnostic biopsy; the results of the initial nondiagnostic biopsy were not included in the audit. The spiral readout consisted of 20 interleaves per frame with a flat flip angle of 45°, an acquisition window of 20 msec, a repetition time of one RR interval, an echo time of 2.1 msec, and a spatial resolution of 0.69 × 0.69 × 8.0 mm (field of view, 200 × 200 × 8; matrix, 288 × 288). One PED was placed in 145 aneurysms (81.5%; 145 of 178; 95% CI: 74.8%, 86.7%), two in 32 aneurysms (18%; 32 of 178; 95% CI: 12.8%, 24.6%), and four in one aneurysm (0.5%; one of 178; 95% CI: 0%, 3.6%). Crossref, Medline, Google Scholar7 Adey GS, Pedrosa I, Rofsky NM, Sanda MG, DeWolf WC. These persons made decisions to include or exclude samples on the basis of mutual agreement.Data were presented as medians (with 25th and 75th percentiles) in the text. Involvement of the pancreatic duct is an important source of morbidity and increased mortality from complications such as infected pseudocyst, abscess, fistulae, or sepsis (84–86). All patients received a total dose of 0.2 mmol/kg gadolinium chelate. Mice were then orotracheally intubated with a 20-gauge intravenous catheter (BD Insyte, Becton Dickinson S.A., Madrid, Spain) and the tube was connected to a ventilator (UNO Micro Ventilator UMV-03, Zevenaar, Netherlands). Radiat Med 2008;26(1):15–20. Crossref, Medline, Google Scholar19 Evans AJ, Pinder SE, Ellis IO, Wilson AR. Characterization of aneurysm remnants after endovascular treatment: contrast-enhanced MR angiography versus catheter digital subtraction angiography. The smoothed curve was within the 95% CI for the mean of the linear regression model throughout the entire range of observed values. The mean peak perfusion of oncocytoma was significantly higher than that of papillary RCC ($P < .001$), chromophobe RCC ($P = .02$), and unclassified RCC ($P = .03$). (b, c) SPECT/CT fusion images clearly demonstrate the physiologic and benign uptake in the left submandibular gland (b) and subcutaneous soft tissue inflammation (c).Figure 2b: Papillary carcinoma in a 52-year-old woman 6 days after administration of 3.85 GBq 131I sodium iodide. The impact of motion artifacts on the reproducibility of repeated coronary artery calcium measurements. The first image frame had adequate quality in only 29 (76%) of the 38 subjects. Crossref, Medline, Google ScholarPage 7The presence of myocardial fibrosis in the failing heart is associated with a wide range of adverse outcomes including ventricular arrhythmia, decompensated heart failure, and death (1–3). J Ultrasound Med 2000;19(8):537–541. Blunt splenic injury in adults: Multi-institutional Study of the Eastern Association for the Surgery of Trauma. Radiology 2008;249(3):891–899. Melamed. This discrepancy might be attributed to our relatively small sample size, the differences in imaging techniques, and the grading of only the clear cell RCC subtype in our cohort; in the study by Palmowski et al (12), tumor perfusion was correlated with tumor grade for all histologic subtypes. Google Scholar4 ACR Committee on Drugs and Contrast Media. Outpatient liver biopsy: how safe is it? The trouble with CTD100. Radiol Clin North Am 2012;50(1):1–14. Rotterdam, the Netherlands: Department of Public Health, Erasmus University, 2011. Radiat Res 2009;172(6):653–665. Roentgenographical detection of cocaine smuggling in the alimentary tract. The result suggests that the toxicity of contrast media is more important for the observed effect than the different physicochemical properties of contrast media with in vitro conditions.In contrast to afferent arterioles, efferent arteriolar tone was not significantly affected by iodixanol, and the angiotensin II sensitivity of efferent arterioles was not changed after perfusion with iodixanol. Techniques, safety and accuracy of sampling of renal tumors by fine needle aspiration and core biopsy. In: Feliciano DV, Moore EE, Mattox KL, eds. Structural basis of end-stage failure in ischemic cardiomyopathy in humans. J.S.B. No relevant conflicts of interest to disclose. A careful analysis of the attenuation of the hemorrhagic fluid helps identify the source of bleeding. (d) Oblique DSA image shows complete obliteration of the two aneurysms and preservation of the perforating arteries 3 months after treatment.In our series of PED treatment for unruptured intracranial aneurysms or recurrent aneurysms after a previous treatment, high rates of complete aneurysm occlusion and preservation of the parent artery were achieved. Ann ICRP 2007;37(1):1–79, iii. A comparison of national findings against these standards was expressed in terms of counts and percentages. Altered brain activation during cognitive control in patients with moderate to severe traumatic brain injury. Blind biopsies were not included in the audit analysis, and numbers of blind biopsies were not requested; this figure only relates to the number of hospitals and departments in which blind biopsy is known to be performed by either radiologists or clinicians. Crossref, Medline, Google Scholar37 Ikeda DM, Hylton NM, Kuhl CKet al.. Kaplan-Meier analysis with Log-rank test, logistic regression, and Cox regression were performed for the evaluation of clinical outcome and recurrence. Stroke 2003;34(6):1398–1403. Surgically important bowel and/or mesenteric injury in blunt trauma: accuracy of multidetector CT for evaluation. Investigations of human material are extremely difficult because of restrictions in the availability of nonpathologic kidney tissue. Stent-assisted coiling of intracranial aneurysms: clinical and angiographic results in 216 consecutive aneurysms. Although the recovery of the longitudinal magnetization of the labeled spins is potentially influenced by the T1 of the perfused tissue, this assumption has likely minimal effect in the calculation of tumor perfusion because viable, perfused tumor tissues characteristically have a longer T1, not much shorter than that of blood. Crossref, Medline, Google Scholar52 Jin G, An N, Jacobs MA, Li K. With this ambition, population-based breast cancer screening was initiated in the Netherlands in 1989. The specific signs of bowel injury include transection of the wall with focal discontinuity, extraluminal oral contrast material (on the rare occasions when it is administered), pneumoperitoneum (Fig 6), and pneumoretroperitoneum. Forty-two consecutive patients (34 men, eight women; mean age ± standard deviation, 60.1 years ± 11.3) scheduled to undergo presurgical MR imaging evaluation of suspected renal masses agreed to participate in this study. Twenty-two fellows or senior residents read the results of abdominal radiography and low-dose CT during the study period. Oral contrast is not necessary in the evaluation of blunt abdominal trauma by computed tomography. Images are in neurologic convention. In patients with MTBI, there was a significantly different distribution pattern of DMN connectivity (Fig 2, B) when compared with that of healthy control subjects. Pancreatic injuries may be classified as contusion, laceration, or transection. Crossref, Medline, Google Scholar5 Richter F, Kasabian NG, Irwin RJ, Watson RA, Lang EK. Results were false-positive if initial biopsy yielded a malignant result but there was evidence of a subsequent amended benign histologic diagnosis. Constant dose in all patient sizes is neither predicted nor demanded from the fundamental principles of x-ray attenuation and Poisson statistics, which underlie the relationships between the amount of x-rays required to form an image and the statistical variations of CT numbers observed in the image. Ann Surg 1952;136(2):239–242. Management decisions in cases of acute splenic injury are based on patient demographics (especially age) and clinical signs and symptoms and often rely on the splenic injury grade as determined on the basis of CT results. Novel real-time R-wave detection algorithm based on the vectorcardiogram for accurate gated magnetic resonance acquisitions. J Comput Assist Tomogr 2005;29(5):644–649. K.H.F. No relevant conflicts of interest to disclose.Author ContributionsAuthor contributions: Guarantors of integrity of entire study, S.C.H.Y., Y.L.C., J.W.Y.H., Y.C.W.; study concepts/study design or data acquisition or data analysis/interpretation, all authors; manuscript drafting or manuscript revision for important intellectual content, all authors; manuscript final version approval, all authors; literature research, S.C.H.Y., S.S.L., R.L., H.K.M.C., G.K.C.W., Y.C.W., K.Y.P.; clinical studies, S.C.H.Y., C.K.K., P.W.C., K.Y.C., S.S.L., W.M.L., K.M.L., R.L., H.K.M.C., Y.L.C.,

C.M.C., G.K.C.W., J.W.Y.H., Y.C.W., C.B.T., W.L.P., K.Y.P., K.H.F.; statistical analysis, S.C.H.Y., R.L., Y.C.W., C.B.T., K.H.F.; and manuscript editing, S.C.H.Y., C.K.K., P.W.C., K.Y.C., W.M.L., Y.L.C., G.K.C.W., Y.C.W., K.Y.P., A.K.S.W., K.H.F.From the 2011 RSNA Annual Meeting.References1 Molyneux A, Kerr R, Stratton Iet al.. Liver cirrhosis: intravoxel incoherent motion MR imaging—pilot study. These studies support the notion that DMN cannot be considered a homogeneous entity but instead comprises several nodes that serve different, highly complex cognitive functions that are independent but are maintained in a dynamic equilibrium (65). Int J Radiat Biol 2006;82(10):699–757. Circulation 2000;102(5):506–510. Packets were located in the bowel or rectum (n = 51) or vagina (n = 2 [eight packets of drugs in one suspect and one packet of banknotes in the other]). The WL enhancement parameters of mean, median, and third quartile enhancement were all significantly higher in ccRCC compared with pRCC (P < .001), and the histogram parameter third quartile enhancement had the highest accuracy in discriminating ccRCC from pRCC, which was higher than qualitative assessment by the radiologists.Interestingly, histogram distribution parameters kurtosis and skewness were significantly lower in ccRCC. Recent improvements in ASL MR imaging techniques (eg, pulsed continuous labeling and background suppression strategies) have enabled consistent measurements of renal perfusion; there is good correlation between ASL perfusion measurements and total renal blood flow as measured with phase-contrast MR imaging, and the test-retest repeatability of ASL MR imaging for renal perfusion is 7% (27). Default network connectivity reflects the level of consciousness in non-communicative brain-damaged patients. Crossref, Medline, Google Scholar13 Keyzer C, Tack D, de Maertelaer V, Bohy P, Gevenois PA, Van Gansbeke D. The notion that an abnormal recruitment of regions located in the frontal lobes might be associated with poor cognitive performance in patients with MS is in agreement with the results of several previous studies (31–33). Crossref, Medline, Google Scholar23 Velmahos GC, Toutouzas K, Radin Ret al.. This information may be unknown to a less-experienced imager.Ultimately, this is a well-written text with an online version that addresses the commonly imaged patient with a postoperative spine. Then, labeling was performed in an axial plane 8–10 cm upstream from the center of the target lesion in the upper abdominal aorta for 1500 msec followed by a 1500-msec postlabeling delay. AJR Am J Roentgenol 1997;168(2):405–409. Furthermore, the analysis of the other disease clinical phenotypes showed that the same alteration also in patients with SP MS, whereas those with benign MS, in contrast to patients with RR MS, have a relative sparing of such a connection, as reflected by the increased interaction between the right cerebellum and regions mainly located in the right ventrolateral prefrontal cortex, which play a central role in attentional control (40). Financial activities not related to the present article: is a consultant for Philips, GE Healthcare, and Bayer; institution has grants or grants pending with GE Healthcare; has received, and institution has received, payment from GE Healthcare for development of educational presentations. Therefore, our study does not provide information on calculating the performance of the ADC threshold in terms of sensitivity and specificity, which would require also measuring ADCs for all malignant lesions over the same time period. A SSDE conversion factor may be determined for a particular patient from one of five proposed calculation methodologies. Similar to what exists for liver and spleen, an AAST grading system is applied to classify the severity of renal trauma (Table 5) and takes into account the size and location of renal lacerations and hematomas (97). This may relate to necrotic lesions, where increased numbers of passes are made in an attempt to obtain a diagnostic sample. CVIR Endovasc. Trail Making Test: Manual for Administration and Scoring. Further work is necessary to validate these findings in prospective trials.Advances in Knowledge• Forty-six percent of nonmalignant breast lesions assessed as false-positive findings at dynamic contrast-enhanced MR imaging had apparent diffusion coefficients (ADCs) higher than a previously determined diagnostic threshold (1.81 × 10−3 mm2/sec).• Fibroadenomas were the most common false-positive finding at dynamic contrast-enhanced MR imaging (17%) and typically demonstrated high mean ADCs ([1.94 ± 0.38] × 10−3 mm2/sec).• High-risk lesions were the most common nonmalignant lesion types with mean ADCs below the threshold ([1.46 ± 0.39] × 10−3 mm2/sec) and accounted for 23% of the overlap with malignant lesions.Implications for Patient Care• Our findings show promise for using diffusion-weighted imaging to reduce the number of avoidable false-positive findings at breast dynamic contrast-enhanced MR imaging; improving the specificity of breast MR imaging would reduce the number of avoidable biopsies and associated morbidity for the patient.• Assessing ADC along with dynamic contrast-enhanced MR imaging features can contribute to improved radiologic-pathologic concordance for particular nonmalignant lesion subtypes sampled for biopsy.Disclosures of Conflicts of Interest: S.P. No relevant conflicts of interest to disclose. The mean ADCs of benign and high-risk subtypes were compared with those of malignant lesions (all 31 malignant lesions reported in our prior study—15 invasive ductal carcinomas, five invasive lobular carcinomas, and 11 cases of ductal carcinoma in situ [20]) by using the Kruskal-Wallis test and post-hoc pairwise comparisons (Wilcoxon rank-sum tests). The lack of a specific diagnosis at CT generally portends a benign clinical course. This effect was induced by the highest dose of sorafenib reported in the literature (20–100 mg/kg [17,18,28]) to obtain a proof of principle that the MR estimate of sO2 measurement can be used to detect the effect of an antiangiogenic agent. The randomized trials of breast cancer screening: what have we learned? As such, this represents the largest biopsy series from our review of the literature looking at modern image-guided or image-assisted biopsy practice in the diagnosis of both focal and nonfocal liver disease. B.E. No relevant conflicts of interest to disclose. Crossref, Medline, Google Scholar28 Hooton TM, Stamm WE. Rapid deceleration generates shear forces that create movement of adjacent structures in opposite directions, causing tears at the points of fixation, such as vascular pedicles and mesenteric attachments. There was a tendency of intensified follow-up imaging after MR angiography compared with intraarterial DSA.Discrepant policy advices based on intraarterial DSA and MR angiographic findings were partly the result of differences in aneurysm occlusion grades. Circulation 2010;122(2):138–144. Helical computed tomography of bowel and mesenteric injuries. Small renal masses: assessment of lesion characterization and vascularity on dynamic contrast-enhanced MR imaging with fat suppression. In the case of intraperitoneal injuries, the contrast material flows outside of the bladder lumen to outline peritoneal structures, such as the bowel and mesentery. There were significant differences in the findings between whole-body scintigraphy and SPECT/CT (P < .0001).Figure 2a: Papillary carcinoma in a 52-year-old woman 6 days after administration of 3.85 GBq 131I sodium iodide. Crossref, Medline, Google Scholar19 Schindera ST, Nelson RC, Toth TLet al.. The histologic profile of these cancers, however, did not differ between the two screening modalities.Consistent with our previous work (10) as well as with other studies evaluating screening programs (8,26,27), we found recall rates to be higher with digital mammography. We also observed a trend toward a reduction of the IVIM perfusion parameters when the patient inhaled pure O2 compared with air (P = .11 for f; P = .09 for D*; P = .38 for fD*).Table 2 IVIM Perfusion Parameters in Full Brain with Inhalation of Four Different GasesFigure 1a: (a–c) Graphs show mean ± standard deviation of percentage of variation of average brain (a)f, (b)D*, and (c)fD* as a function of pure O2, 5% CO2, and 8% CO2 inhalation compared with inhalation of air for a 27-year-old male volunteer. Retroperitoneal hematomas may occur secondary to injuries to major vessels, solid organs, hollow viscera, and/or the skeleton. In the iodixanol and L-NAME groups, the fluorescence was reduced similarly and significantly, compared with the control group (P = .009 and P = .049, respectively).Both L-NAME (81.5% of basal diameter [25th and 75th percentiles, 63.8% and 96.1%, respectively]; P < .0001) and L-NAME plus iodixanol (56.4% of basal diameter [25th and 75th percentiles, 38.5% and 80.4%, respectively], P < .0001) significantly reduced the median afferent arteriolar diameters within 20 minutes (Fig 7). J Trauma 1995;39(2):331–333. Large variations in vascular response to hypercapnia between and within participants, both in amplitude and in spatial distribution (which may not be simply attributed to measurement errors) were observed in several studies (46–50). Magn Reson Med 1991;17(1):197–212. Applying this alternate ADC threshold in the present study would have increased the number of lesions with ADCs above the threshold to 110 (63%), potentially sparing additional biopsies. J Magn Reson Imaging 2008;28(5):1108–1115. Treatment started at D10 (D10[T0]). Crossref, Medline, Google Scholar35 Pandit H, Vlychou M, Whitwell Det al.. Crossref, Medline, Google Scholar26 Woodhams R, Matsunaga K, Iwabuchi Ket al.. Crossref, Medline, Google ScholarPage 8Appendicitis remains the most common indication for emergent abdominal surgery, with more than 250 000 cases per year in the United States (1). The degree to which the individual SSDE measurements (AP and lateral) compared with the combination of the individual measurements (sum and effective diameter) was analyzed by using coefficient of variation analysis. J Trauma 2005;59(1):49–53; discussion 53–55. Flow-diverter stent for the endovascular treatment of intracranial aneurysms: a prospective study in 29 patients with 34 aneurysms. Kurtosis had the highest interreader agreement, with a κ coefficient of 1.0.The WL parameter of third quartile enhancement had significantly higher sensitivity and accuracy for diagnosing ccRCC when compared with qualitative assessment (P < .05) (Figs 4, 5). (e) Axial T2-weighted MR images show ROIs drawn to avoid as much cerebrospinal fluid as possible.Figure 2c: Box and whisker plots (median, 25th and 75th percentiles, minimum, maximum, outliers) compare variations of (a)f, (b)D*, (c)fD*, and (d)D, averaged in ROIs drawn in white matter (WM), gray matter (GM), thalamus (T), and lenticular nucleus (LN), in four to seven volunteers and in both sides of the brain. Google Scholar10 Berlin L. Link, Google Scholar16 Gatehouse PD, Keegan J, Yang GZ, Mohiaddin RH, Firmin DN. This algorithm could be used to identify many thousands of different stylistic and phrase variations potentially used by radiologists in documenting such communications.The text-classification algorithms for the eight critical values were applied to the database of 9.3 million reports, and the number and frequency of critical results were determined according to year. J Cereb Blood Flow Metab 2002;22(3):335–341. 4th ed. Average diameters of the proximal and distal parent artery measured 3.7 mm ± 0.6 (range, 2.5–5.3 mm) and 3.4 mm ± 0.6 (range, 2.5–4.9 mm), respectively.Table 1 Aneurysm CharacteristicsThe procedure was successfully accomplished in all aneurysms. Diffusion-weighted magnetic resonance imaging of breast lesions: first experiences at 3 T. J Am Coll Cardiol 2006;48(10):1977–1985. Des-gamma-carboxyprothrombin: clinical effectiveness and biochemical importance. Rupture may occur as early as 2–48 days or as late as 5 months (13,17). A Levene test was used to test the homogeneity of variance for ASL perfusion among different groups, and homogeneity of variances was assumed for P > .05 (mean tumor perfusion with ASL [P = .06] and peak perfusion with ASL [P = .1]). AJNR Am J Neuroradiol 2007;28(3):497–500. Crossref, Medline, Google Scholar29 Potter HG, Nestor BJ, Sofka CM, Ho ST, Peters LE, Salvati EA. Crossref, Medline, Google Scholar22 Ustun A, Desai M, Abd-Elmoniem KZ, Schar M, Stuber M. Eur Radiol 2007;17(1):81–86. Pathophysiology of renal tissue damage by iodinated contrast media. One area of uptake that was believed to be positive for pelvic or femoral bone metastasis at whole-body scintigraphy was shown to be the uptake in a region of soft tissue inflammation in the right buttock at SPECT/CT (Fig 2). The PS-DIR sequence is modified in this work to acquire several successive cine phases or frames, as shown in Figure 1, B. However, for reasons of statistical consistency, intragroup comparisons between tumor and contralateral tissues were performed by using the contralateral values of each rat in each group (Fig 4c, 4d). The number of phases acquired, beyond the routine portal venous phase, should be carefully selected. Crossref, Medline, Google Scholar25 Mohammed MA. Our report is the first to our knowledge to confirm the association between short T1 time and increased fibrosis in a population with a broad range of cardiomyopathies, reflective of the spectrum of disease seen in patients referred for endomyocardial biopsy. Strategies for CT radiation dose optimization. Similar to what was found in other studies, the sensitivity of digital mammography was higher than that of screen-film mammography (8–10,26). A default mode of brain function: a brief history of an evolving idea. Crossref, Medline, Google Scholar13 Christen T, Lemasson B, Pannetier Net al.. (b) Axial and (c) sagittal multiplanar reformatted low-dose CT images show a small quantity (≤12) of packets within the rectum, hyperattenuated to the surrounding bowel content (arrows). In pairwise comparisons, only ADH and fibroadenoma demonstrated significant differences in ADC after sequential Holm-Bonferroni corrections (P = .0003, corrected α = .00047).Figure 2: Graph shows ADCs of nonmalignant breast lesions. Crossref, Medline, Google Scholar25 Zannad F, Alla F, Dousset B, Perez A, Pitt B. Thinner sections of all series in the various planes would lead to image overload, with patient data sets composed of thousands of images in the typical multiphasic acquisition of multiple regions of the body. Crossref, Medline, Google Scholar58 Liu X, Zhou L, Peng W, Qian M. Management of hemobilia and persistent biliary fistula after blunt liver trauma. Diffusion-weighted imaging in breast lesion evaluation. All transplants were performed by W.J., who had 8 years of extensive microsurgical experience, including approximately 600 rat and 400 mouse lung transplants.Donor procedure.—The induction of anesthesia for donor mice was initiated in a sealed cage with inflow isoflurane (Attane; Minrad I, Buffalo, NY), followed by premedication with 0.2 mg/kg of body weight of pentobarbital (Nembutal; Abbott Laboratories, North Chicago, Ill). Crossref, Medline, Google Scholar6 Willekens I, Buls N, Lahoutte Tet al.. Traumatic arthritis of the hip after dislocation and acetabular fractures: treatment by mold arthroplasty—an end-result study using a new method of result evaluation. A validation of the post concussion symptom scale in the assessment of complex concussion using cognitive testing and functional MRI. Curr Opin Neurol 2011;24(3):244–249. Magn Reson Med 1992;27(1):171–178. Radiology 1996;201(3):705–710. Crossref, Medline, Google Scholar7 Malviya A, Holland JP. Crossref, Medline, Google Scholar16 Morelli JN, Runge VM, Ai Fet al.. This cut point leads to a positive predictive value of 74% (45 of 61) and a negative predictive value of 97% (261 of 269).Figure 4: Receiver operating characteristic curve shows the sensitivity and specificity of interpretation of abdominal radiographs for the presence of intracorporeal packets, with regard to the radiologist’s level of confidence in the interpretation. (a) Hyperintense signal surrounds the femoral stem on coronal short inversion time inversion-recovery MR image, which is isointense to surrounding marrow on (b) coronal T1-weighted MR image, consistent with marrow edema (arrow).Figure 4b: Images in a 75-year-old man with pain after metal-on-metal total hip arthroplasty. AJNR Am J Neuroradiol 2011;32(3):566–569. Histologic diagnosis of ccRCC was made in 55 cases, and pRCC was diagnosed in 19.On precontrast T1-weighted images, 37 tumors were isointense; 12 were hyperintense; 14 lesions were heterogeneous with some hyperintense foci; and 11 were hypointense to the renal cortex.Sensitivity, specificity, and accuracy summed for three readers was 84.2% (139 of 165), 91.2% (52 of 57), and 86.0% (191 of 222), respectively (Table 1).Table 1 Discrimination of ccRCC from pRCC at Qualitative Assessment of Enhancement by Three ReadersThe mean κ coefficient over the three reader pairs was 0.70 (range: 0.65–0.74). A study by Rao and colleagues (8) supported the cost effectiveness of routine CT in cases of suspected appendicitis by demonstrating a \$447 per-patient reduction of in-hospital cost attributable to the prevention of negative appendectomies and associated hospitalizations. The number of department identifiers (d) is less than 85 due to departments with identical volumes of cases reporting the same level of diagnostic accuracy.In this retrospective study, we collected data from almost 3500 liver biopsies performed in 41.4% of United Kingdom radiology departments that participated in the audit (87 of 210 departments), with 1225 cases involving focal lesions. Eighty patients (43%) were female, and 106 (57%) were male. Can J Surg 1995;38(2):117–122. Diagnostic accuracy of mammography, clinical examination, US, and MR imaging in preoperative assessment of breast cancer. Diffusion weighted imaging in breast MRI: comparison of two different pulse sequences. Radiology 1999;213(2):321–339. Vessel tracking: prospective adjustment of section-selective MR angiographic locations for improved coronary artery visualization over the cardiac cycle. The latter effect is caused by tissue-air interfaces in the lung resulting in microscopic magnetic field inhomogeneities. Crossref, Medline, Google Scholar19 Niewiarowski S, Gogbashian A, Afaq A, Kantor R, Win Z. A total of 26 patients with MTBI (recruited from a university-affiliated level 1 trauma center and a university hospital) and 21 healthy control subjects were identified and recruited from a large database in our center of several ongoing neuroimaging projects. In patients without LGE, fibrosis ranged from 1.5% of myocardial volume to a maximum of 19.1% (median, 6.5%; interquartile range: 3.0–9.0) at endomyocardial biopsy. Accuracy of nonfocused helical CT for the diagnosis of acute appendicitis: a 5-year review. Crossref, Medline, Google Scholar18 Gui C, Miao Y, Thompson Let al.. Clin Exp Pharmacol Physiol 2011;38(5):292–299. Data for both whole tumor and maximum enhancement were recorded as percentage enhancement, which was calculated as follows: (postcontrast signal intensity - precontrast signal intensity)/precontrast signal intensity.Standard of reference.—Results of the histopathologic analysis served as the standard of reference. Crossref, Medline, Google Scholar20 Noguchi T, Yoshiura T, Hiwatashi Aet al.. J Comput Assist Tomogr 1997;21(2):246–250. Financial activities not related to the present article: has received a grant from Philips Medical Systems. Crossref, Medline, Google Scholar17 Passamonti L, Novellino F, Cerasa Aet al.. 3, Abdominal radiograph deemed negative (level of confidence, 2). Crossref, Medline, Google Scholar16 Choo L, Zekry A, Freiman J. Management of blunt injuries to the spleen. Over the past 3 decades, the CTDI value has been modified from its original definition to account for advances in CT technology. This approach facilitates the detection of small gas collections. J Magn Reson Imaging 2011;34(3):557–562. The VIBE sequence was performed prior to and three times after administration of an intravenously administered gadolinium chelate (gadopentetate dimeglumine, Magnevist; Bayer Healthcare Pharmaceuticals, Wayne, NJ). 6th ed. Mesenteric injuries can be an isolated finding on CT images, and these findings include peritoneal active extravasation of contrast-enhanced blood, mesenteric rent with internal hernia, beading or abrupt termination of the mesenteric vessels, and mesenteric hematoma (80). The transcription of the OATP8 gene is also regulated by the nuclear factor (steroid and xenobiotics receptor or pregnane xenobiotics receptor) (18). Care was taken to avoid regions of high T2 within a lesion, such as cyst, hematoma, or necrosis, by verifying the ROI against the T2-weighted b = 0 sec/mm2 image. The variation between SSDE conversion methodologies was shown to be independent from patient weight and age. This scale is used to assess the severity of 19 symptoms, such as dizziness, balance problems, headache, and sensitivity to light, which are associated with PCS, mild cognitive impairment, or both. Future implementations of SSDE may provide a prospective use for CT technique adjustment. Second, the difference between patients and control subjects with a seed-based method did not reach statistical significance, which raises cautions for the interpretation of our ICA-based findings, despite the fact that the patterns based on the two methods are similar by means of visual inspection. Then, brains were sliced at −20°C by using a cryostat (10-μm-thick sections) by one author (B.L. and R.S., with 4 and 7 years of experience in histologic analysis, respectively).Tumor hypoxia was determined by using a kit (Hypoxyprobe-1 kit; Chemicon International). On the basis of both intraarterial DSA and MR angiographic findings, additional coil placement was recommended because of incomplete occlusion with both imaging modalities.Follow-up imaging was suggested for 37 of the 310 patients (12%) after intraarterial DSA and for 49 patients (16%) after MR angiography (difference: 4%; 95% CI: 20.6%, 8.4%). Medline, Google Scholar3 Vallee JN, Aymard A, Vicaut E, Reis M, Merland JJ. Although diffusion imaging has proved to be largely useful in a wide variety of clinical applications (11–14) as well as in more advanced applications such as diffusion tensor imaging and tractography (15–17), the measurement of perfusion by using IVIM is not common because of its low signal-to-noise ratio (18), with blood volume in the brain estimated to be in the low single-digit percentage range (19,20).Recently, promising perfusion measurements with IVIM have been achieved in humans in multiple organs (21–28). Radiol Clin North Am 1983;21(3):461–475. High-risk lesions were those yielding ADH, ALH, or LCIS. No relevant conflicts of interest to disclose. The quality reference effective mAs values were either 240 or 250 for the studied examinations. Diagnosis and management of blunt pancreatic ductal injury in the era of high-resolution computed axial tomography. In male patients, the question is often raised regarding the clinical importance of free fluid alone and whether laparotomy (or laparoscopy) should be recommended. To comply with privacy regulations, all women signed a general informed consent form permitting the use of data for evaluation and scientific research. Nonclotted blood (typical attenuation of 30–45 HU) tends to flow freely between contiguous peritoneal recesses, following gravity, and may eventually fill the cavity completely. Tables 9–11 show diagnostic performance more specifically according to focal lesion size and needle parameters (gauge, number of passes, and needle type); they also show diagnostic performance for metastases and hepatocellular carcinoma as separate entities. Causes of pneumoperitoneum without bowel trauma include intraperitoneal rupture of the urinary bladder with an indwelling Foley catheter, massive pneumothorax, barotrauma, benign pneumoperitoneum (eg, as observed in some patients with systemic sclerosis) and the occasional diagnostic peritoneal lavage. The measurement of observer agreement for categorical data. This finding, termed the dependent viscera sign, is present if the upper third of the liver, the stomach, or bowel loops are found on CT images to abut the posterior ribs (104) (Fig 10). II. Our results, like those presented by Christen et al (27), show that MR estimate of sO2 and BVf measurements give distinct information about tumor biology. For this study, we excluded 27 patients because of loss to follow-up and 26 patients because of failure to complete MR imaging (refusal, contraindication such as pacemaker, or inability to tolerate the duration of the examination). Linear regression analysis was performed by using the Pearson correlation coefficient. Google Scholar5 Sendeski MM. After washout of DAF-FM, pressure in the pressure head was set back to 100 mm Hg, and the perfusate was exchanged either to a vehicle solution or to a solution containing iodixanol. Data summed across the readers demonstrated sensitivity of 90.9% (100 of 110), specificity of 84.2% (32 of 38), and accuracy of 89.2% (132 of 148) for diagnosis of ccRCC with an ROI enhancement cutoff value greater than 95.There was good agreement between the two readers for discriminating ccRCC from pRCC, with a κ coefficient of 0.83.Segmentation was semiautomated, requiring on average 80 seconds (range, 40–220 seconds) of user interaction per lesion.ccRCC had significantly higher (P < .001) mean, median, and third quartile enhancement on corticomedullary phase images when compared with pRCC (Table 2). E.L.B. No relevant conflicts of interest to disclose.Author ContributionsAuthor contributions: Guarantors of integrity of entire study, B.L., R.S., A.B., G.L.D., C.R., E.L.B.; study concepts/study design or data acquisition or data analysis/interpretation, all authors; manuscript drafting or manuscript revision for important intellectual content, all authors; approval of final version of submitted manuscript, all authors; literature research, B.L., T.C., R.S., C.R., E.L.B.; experimental studies, B.L., T.C., R.S., C.M., A.B., G.L.D., E.L.B.; statistical analysis, B.L., R.S.; and manuscript editing, B.L., T.C., R.S., C.R., E.L.B.References1 Gallez B, Baudelet C, Jordan BF. FAIR true-FISP perfusion imaging of the kidneys. The images and illustrations are of high quality. In contradistinction to a contained vascular injury in which the initially identified contrast material blush is seen to wash out on subsequent delayed phase images, the hyperattenuation of active hemorrhage persists and grows larger with time on a delayed phase study. This was confirmed by our findings, with the majority of papillomas and all lymph nodes in our study exhibiting ADCs below the ADC threshold. Google Scholar3 de Koning HJ, Draisma G, Fracheboud J, de Bruijn A. From October 2005 through June 2006, these studies were performed with a 2.2-mm section thickness, a 350 × 350 matrix, and five postcontrast acquisitions centered at 90, 180, 270, 360, and 450 seconds. The screening interval (range, 18–36 months) was comparable for the digital mammography and screen-film mammography groups, with means of 24.9 and 24.3 months, respectively (P < .001).A total of 15 238 women in the screen-film mammography group and 3658 women in the digital mammography group were recalled. Perforator infarction after placement of a pipeline flow-diverting stent for an unruptured A1 aneurysm. Myocardial fibrosis was calculated as a percentage of total tissue in endomyocardial biopsy samples.Figure 3: Myocardial T1 time according to disease category. Crossref, Medline, Google Scholar15 Seo H, Lee KH, Kim HJet al.. Crossref, Medline, Google Scholar8 Jahnke C, Nehrke K, Paetsch Iet al.. Crossref, Medline, Google Scholar13 Tozaki M, Fukuma E. Clin Radiol 2002;57(9):807–814. V.U.V. Financial activities related to the present article: none to disclose. Crossref, Medline, Google Scholar41 Koch KM, Lorbiecki JE, Hinks RS, King KF. MDCT for suspected acute appendicitis in adults: impact of oral and IV contrast media at standard-dose and simulated low-dose techniques. Menopausal status was not available for the study cohort at the time of our analyses. A.B.R. Financial activities related to the present article: employee of Siemens. P.J.P. Financial activities related to the present article: none to disclose. Am J Cardiol 2006;98(6A):14K–20K. 2004;25(12):1177–1182. At the time of the study, patients with coils who were independent in daily activities were generally followed up with intraarterial DSA twice in the first 2 years after the treatment.Eligible patients were invited for additional MR angiography on the same day as their regular follow-up intraarterial DSA was performed. Radiol Med (Torino) 2010;115(4):648–667. H.W. No relevant conflicts of interest to disclose. Crossref, Medline, Google Scholar16 Keyzer C, Cullus P, Tack D, De Maertelaer V, Bohy P, Gevenois PA. False-positive abdominal radiography in a body packer resulting from intraabdominal calcifications. The static T1 value before enhancement (T1pre) was calculated as follows:where TR is repetition time and SIA and SIB represent the signal intensity in flip angle α and β, respectively. Traumatic disruption of the pancreatic duct: diagnosis with MR pancreatography. Crossref, Google Scholar28 Sheir KZ, El-Azab M, Mosbah A, El-Baz M, Shaaban AA. AJR Am J Roentgenol 1996;166(5):1035–1039. Morphological and immunochemical studies of rat glial tumors and clonal strains propagated in culture. World J Gastroenterol 2007;13(40):5336–5342. Alternatively, if the decision to perform a CT examination of the chest and abdomen has been made, these bedside radiographs can be replaced with the corresponding digital scout images.Persistent clinical findings of occult ongoing hemorrhage indicate the chest, abdomen, and/or pelvis as the likely source(s). Blunt splenic injuries: nonsurgical treatment with CT, arteriography, and transcatheter arterial embolization of the splenic artery. Overall, there was a significant difference between the whole-body scintigraphic and SPECT/CT findings (P < .0001).Figure 1a: Papillary carcinoma in a 58-year-old man 6 days after administration of 4.52 GBq 131I sodium iodide. Research in radiation therapy has focused on overcoming the effects of hypoxia that limit radiation therapy efficiency (6). This orthogonality is crucial for obtaining an accurate measurement of wall thickness. J Am Soc Nephrol 2001;12(6):1122–1127. Histologic type and grade of the tumors were recorded. In 334 (10%) of 3368 cases in our study, a completed consent form was absent, with no postprocedural instructions available in 775 (23%) of 3325 biopsies. Crossref, Medline, Google Scholar3 Carroll LJ, Cassidy JD, Peloso PMet al.. A default mode of brain function. Finally, the readers in this study were relatively inexperienced in number of years of practice. J Clin Invest 1948;27(4):484–492. Radiology 2009;251(1):50–57. Crossref, Medline, Google Scholar51 Johnson MK, Raye CL, Mitchell KJ, Touryan SR, Greene EJ, Nolen-Hoeksema S. Acta Radiol 2011;52(5):575–580. J Natl Cancer Inst 2002;94(20):1546–1554. Thus, the fundamental role of the trauma radiologist in this management algorithm cannot be overemphasized. CA Cancer J Clin 2007;57(1):43–66. Top and bottom of boxes = 25th and 75th percentiles, line in box = median.Similarly, histogram distribution parameter skewness was significantly lower in ccRCC compared with pRCC (0.55 ± 0.62 vs 2.07 ± 0.85; P < .0001) (Table 2 and Fig 3). Magnetic resonance (MR) angiography is increasingly used as a noninvasive alternative to the standard follow-up with intraarterial digital subtraction angiography (DSA) in patients with coiled aneurysms (3). Complete occlusion was defined as complete aneurysm obliteration including the neck or class 1 by using the Montreal scale (6). Crossref, Medline, Google Scholar22 Luciani A, Vignaud A, Cavet Met al.. Details on PS-DIR lumen signal restoration can be found in Appendix E1 (online). In 2007, over 180 000 people died of trauma (1), and abdominal injuries contributed to a large number of these deaths. All other diagnoses of malignancies could be termed overdiagnosis, which is the diagnosis of cancer that, if left undetected and therefore untreated, would never have surfaced clinically in a person’s lifetime.Overdiagnosis is an inevitable side effect of every screening program. A correlation between ASL signal intensity changes and both histologically derived microvascular area in meningiomas and tumor grade in brain tumors has been shown (20,21). Crossref, Medline, Google Scholar9 Kuhl CK. N Engl J Med 1998;338(3):141–146. AJR Am J Roentgenol 2003;180(2):505–512. These changes in DMN pattern were consistent with the single-subject ICA results by means of visual inspection.In patients with MTBI, there was a significant correlation after Bonferroni correction between decreased DMN in the posterior regions with the Trail Making Test B (Pearson correlation coefficient, r = 0.60; corrected, P = .02) (Fig 5, A), which is a measure of executive functioning to assess mental flexibility—specifically, the ability to shift rapidly between cognitive sets. Semin Nucl Med. Patient dosimetry for x rays used in medical imaging. Besides its safety, MR angiography is performed in an outpatient setting and creates less discomfort for patients than does intraarterial DSA. Four lymph nodes that were included in our study were described as suspicious masses at MR imaging and subsequent US. Crossref, Medline, Google Scholar59 Yuen S, Yamada K, Goto M, Nishida K, Takahata A, Nishimura T. Crossref, Medline, Google Scholar25 Stuhlfaut JW, Soto JA, Lucey BCet al.. (c) ASL image shows marked perfusion of entire mass (mean perfusion = 309.6 mL/min/100 g).There were no differences in mean and peak perfusion on the basis of tumor grade (ie, low-grade clear cell RCC vs high-grade clear cell RCC) or stage (ie, pT1 tumors vs pT3 tumors) (Table 2). (c) Histogram of WL enhancement demonstrates a flat peak consistent with low kurtosis value of −0.5 and low skewness value of 0.12.Figure 1b Findings in a 38-year-old man with renal lesion (arrow) in the right kidney shown to be ccRCC at pathologic evaluation. Axial and coronal T1-weighed (repetition time msec/echo time msec, 690/12; echo train length, six), axial T2-weighted (3675/98; echo train length, 22), and coronal short inversion time inversion-recovery (repetition time msec/echo time msec/inversion time msec; 3275/30/200; echo train length, 32) images were acquired. Including either type of tissue would change the CTDIvol value of the scan because the reported CTDIvol value is averaged throughout the entire scan length. Y.T. No relevant conflicts of interest to disclose. Crossref, Medline, Google Scholar34 Sanders ME, Schuyler PA, Dupont WD, Page DL. Specifically, all readers were made aware that ccRCC enhances heterogeneously and avidly (Fig 1), such that a lesion with a portion of the tumor that demonstrates contrast enhancement similar to or higher than the renal cortex in the corticomedullary phase is diagnostic of ccRCC. Interstitial collagen is increased in the non-infarcted human myocardium after myocardial infarction. Radiology 1994;190(1):31–35. As a result, for smaller-sized patients, converting to SSDE appeared to increase rather than decrease variability compared with CTDIvol. Guidelines for radioiodine therapy of differentiated thyroid cancer. Thus, 34 patients (28 men, six women; mean age, 60.4 years ± 11.7) represent our final study group. AJR Am J Roentgenol 2011;196(1):210–217. Furthermore, the potential of ASL MR imaging for assessing differences in baseline perfusion of distinct RCC xenograft cell lines in a mouse model and monitoring perfusion changes in response to an antiangiogenic therapy have been demonstrated (23). This was difficult to control for, since most patients with CAD are usually older. More than one sample is helpful, especially when hepatic involvement by diffuse disease is likely to be patchy. Arch Surg 1998;133(4):373–376. The mean scanner output as indicated by CTDIvol was 18.1 mGy ± 3.7 and the mean SSDE was 21.8 mGy ± 3.4. There were 13 patients with an fsize of approximately 1.00 (range, 0.995–1.004). Figure 2, C, shows comparison results between the two groups (two-sample t test, P < .01), demonstrating significantly increased connectivity primarily in the anterior MPFC region (Table 1) and decreased connectivity primarily in the posterior medial PCC and parietal regions (Table 2) within the DMN in patients with MTBI. Kidney Int 2004;65(2):589–596. No special preparation of the animals for the experiment was needed except the adaptation and housing conditions.Syngeneic transplantation was performed in six C57BL/6 to C57BL/6 mice as described previously (15). The ICA model is a powerful tool for the extraction of imaging patterns of synchronized neural activity from resting-state functional MR imaging time series. Higher radioactive iodine activity and a longer interval between radioactive iodine administration and imaging acquisition on posttherapy scans would result in an increased target-to-background ratio (17,18). RadioGraphics 1996;16(4):943–948. By application of such contrast materials, a more precise differentiation could potentially be made.Another future possibility for further differentiating edema from cell influx in engrafted organs with increased opacity lies in the labeling of immune cells with superparamagnetic iron-oxide particles. Metastatic non–clear cell renal cell carcinoma: current therapeutic options. R.A.N. No relevant conflicts of interest to disclose. Crossref, Medline, Google Scholar8 Skaane P, Hofvind S, Skjennald A. Crossref, Google Scholar26 Grady L. Thirty-six containers stuffed with cocaine were found at stool analysis.A brief report that indicated the presence or absence of packets at both abdominal radiography and low-dose CT was given to the police or border guard authorities.Low-dose CT was considered the reference standard. Crossref, Medline, Google Scholar42 Belli P, Costantini M, Bufi E, Magistrelli A, La Torre G, Bonomo L. CT findings are similar to those for injuries involving other segments of the gastrointestinal tract and include focal wall discontinuity, wall thickening, periduodenal fluid, and extraluminal gas in the retroperitoneum (89). In the test injection method (1.5 mL of Primovist + 8 mL saline flush), arterial-phase timing was determined as the peak time of the abdominal aorta plus 10 seconds minus half of imaging time. Imaging was performed by two radiologists (C.F. and P.H., with 1 year and 7 years of experience in radiology, respectively). The threshold for each metric was chosen by a receiver operating characteristic analysis which identified the threshold that maximized accuracy for discriminating ccRCC from pRCC.All reported P values were two sided, and a statistically significant difference was defined at P < .05. Injuries to the diaphragm have the potential for important morbidity and mortality related to immediate or delayed herniation (and secondary ischemia) of abdominal organs into the thorax (42). Generally, for all patients, the most effective method for determining SSDE is direct measurement of patient dimensions with electronic calipers from the CT radiograph. Trauma. However, to maximize the diagnostic potential of the examination and, at the same time, minimize risks, CT protocols need to be tailored to match the need of each individual patient. Current use of CT in the evaluation and management of injured patients. Emerg Radiol 2007;13(6):313–318. 1996;37(4):598–605. Cost-effectiveness of magnetic resonance angiography versus intra-arterial digital subtraction angiography to follow-up patients with coiled intracranial aneurysms. Link, Google Scholar28 Kim S, Yazici YD, Calzada Get al.. Magn Reson Med 2009;61(2):381–390. Finally, our chest radiologists participate in daily intensive care unit rounds with other physicians and have an opportunity to directly verbally communicate such malpositions. Evaluation of a low-dose CT protocol with oral contrast for assessment of acute appendicitis. Similarly, they can be run periodically throughout the day to ensure that all results get communicated. In the first step, the curve was fitted for a b value greater than 200 sec/mm2 for the single parameter, D. The stomach abuts the posterior ribs in the left hemothorax—the dependent viscera sign. The subset of patients in this study without LGE included individuals with collagen fractions as high as 19%. Link, Google Scholar14 Macedo R, Chen S, Lai Set al.. A.A.A. No relevant conflicts of interest to disclose. Previous authors have studied imaging findings in patients after metal-on-metal arthroplasty, but they used a much smaller sample size (8,12–14,32), evaluated only symptomatic patients (14,32) or those undergoing revision (15), or combined analysis of multiple metal-on-metal implant systems, including a variety of resurfacing arthroplasty systems (11–13,33). W.K. Financial activities related to the present article: none to disclose. In addition, the mean MR estimate of sO2 of treated tumors becomes significantly lower than that of untreated tumors (P < .001). (b) Photomicrograph of hematoxylin and eosin stained slide shows moderately differentiated HCC with trabecular proliferation pattern. The impact of digital mammography on screening a young cohort of women for breast cancer in an urban specialist breast unit. Delayed CT images are necessary to determine the integrity of the collecting system (see Multidetector CT Technique) and allow detection of leakage of opacified urine into the perinephric space (Fig 9). Magn Reson Med Sci 2005;4(1):35–42. In fact, a whole-body CT angiogram (circle of Willis to symphysis pubis or beyond) is possible and has been advocated for patients with severe polytrauma (36,37).Figure 1a: Axial CT images in a 25-year-old man who fell from a second floor. Radiology 2004;233(3):689–694. National conference on dose reduction in CT, with an emphasis on pediatric patients. (c) Immunohistochemical expression of PIVKA-II was significantly lower in hyperintense HCCs (0.59 ± 0.61) than that in hypointense HCCs (1.93 ± 1.10) (P < .001, κ = 0.81).Figure 4c: Bar graphs show immunohistochemical expression of AFP and PIVKA-II. Radiologist B had a significantly lower documentation of communication rates for all three critical test values compared with other radiologists in the Thoracic Imaging Division, Hospital of the University of Pennsylvania (P < .001).Text mining is the application of information-retrieval techniques to automated discovery of useful or interesting knowledge from unstructured text (9). However, the value of abdominal radiography to screen for intracorporeal containers has not, to our knowledge, been prospectively evaluated in a large series of suspects with computed tomography (CT) as the reference standard. Three lung and eight bone metastases were identified at SPECT/CT in three and four patients, respectively (each of two of four bone metastasis patients had three 131I uptake areas). The effect of susceptibility of gadolinium contrast media on diffusion-weighted imaging and the apparent diffusion coefficient. Neuroimage 2010;51(4):1378–1383. Crossref, Medline, Google ScholarPage 6Coronary artery wall assessment with MR imaging has great potential as a radiation-free method in the assessment of coronary artery disease (CAD) and in the evaluation of coronary artery wall remodeling that precedes lumen narrowing (1–3). J Hepatol 1990;11(3):344–348. However, L-NAME alone induced no significant change in afferent arteriolar response to angiotensin II (P = .19).Figure 7: Graphs show afferent arteriolar diameters perfused with vehicle solution or treated with iodixanol, L-NAME (n = 13), and L-NAME plus iodixanol (n = 9). Acta Radiol 1997;38(6):961–964. In this study, we have presented data for only eight critical results algorithms, which represent a minority of critical values (we have a list of more than 25 established in our department). Hum Brain Mapp 2004;22(3):165–178. Radiology 2002;224(3):695–700. DW imaging was not performed during the MR imaging examinations for 50 (20%) of 253 lesions because of time constraints related to scheduling and/or patient discomfort that caused termination of the MR imaging examination prior to DW imaging (acquired at the end of the examination). Eur Urol 2011;59(1):135–141. It is also worth noting that US guidance rather than assistance was most commonly used to sample diffuse and focal liver disease. The lesion (arrow) is hyperintense on (d) axial DW image and has a low ADC (mean, 1.06 × 10−3 mm2/sec) on (e) an ADC map. Microperfusion-induced elevation of ADC is suppressed after contrast in breast carcinoma. Incremental value of 131I SPECT/CT in the management of patients with differentiated thyroid carcinoma. Relatively low sensitivity or specificity has been reported for individual symptoms and signs in patients clinically suspected of having appendicitis, including nausea (sensitivity of 67.5%, specificity of 38.9%), anorexia (sensitivity of 61.0%, specificity of 59.3%), fever (sensitivity of 17.9%, specificity of 72.2%), chills (sensitivity of 6.9%, specificity of 96.3%), right lower quadrant pain (sensitivity of 95.9%, specificity of 3.7%), rebound tenderness (sensitivity of 69.5%, specificity of 38.9%), and guarding (sensitivity of 47.6%, specificity of 63.0%) (3). The 131I uptake in the right paratracheal node is masked by the intense uptake in the thyroid bed in whole-body scintigraphic image, but the (c) SPECT/CT fusion image clearly shows 131I uptake in the iodine-avid right superior paratracheal LN just superior to the thyroid bed.Fifty-two areas of uptake were found and categorized as distant metastases on whole-body scintigraphic images. Endomyocardial biopsy plays a role in diagnosing patients with unexplained cardiomyopathy. B, MPFC-seed–based template shows predominant MPFC connectivity with PCC nodes detected (corrected, P < .05; cluster size, K ≥ 20). Radiology reports. Injury 2002;33(4):295–302. Case 3 also shows a situation in which only the first two frames had acceptable quality. The number of data available per day and that available per group are presented in Table 2. Interstitial fibrosis in the dilated non-ischaemic myocardium. BJU Int 2008;101(11):1343–1345. Does arterial spin-labeling MR imaging–measured tumor perfusion correlate with renal cell cancer response to antiangiogenic therapy in a mouse model? Crossref, Medline, Google Scholar25 Kurth CD, Levy WJ, McCann J. The CTDIvol data compared with both SSDE calculations were averaged as a function of patient age.Figure 5b: (a) Graph shows comparison of calculated effective patient diameters for patients with ICRU 74 data (11). Functional and molecular mapping of uncoupling between vascular permeability and loss of vascular maturation in ovarian carcinoma xenografts: the role of stroma cells in tumor angiogenesis. In patients with a diaphragmatic injury, the herniated viscera adopt an abnormal dependent position along the posterior chest wall. Technical reference manual, Lightspeed VCT. At pimonidazole staining and on the corresponding MR estimate of sO2 map, three areas were delineated: the necrotic, the hypoxic, and the normoxic areas. Int J Cardiol 2012;158(2):186–192. RT differed among the study groups (analysis of variance, P < .0001). The study sample was described. A P value of less than .05 was considered to indicate a significant difference.In 78 patients, there were 120 foci in the thyroid bed that were seen at both whole-body scintigraphy and SPECT/CT as being in the thyroid bed. Crossref, Medline, Google Scholar2 Lehman CD, Isaacs C, Schnall MDet al.. Photomicrographs of histologic specimens from transplanted lungs showed ischemia reperfusion injury, including the accumulation and infiltration of innate immune cells and alveolar edema. The results of the a priori–defined between-group comparisons are shown in Table 2. Medline, Google Scholar11 Miyaaki H, Nakashima O, Kurogi M, Eguchi K, Kojiro M. (c) At immunohistochemical evaluation (magnification, ×200), tumor shows no expression of OATP8, but (d) intense expression of both AFP (brown color) and (e) PIVKA-II (brown color).Figure 1c: HCC in a 65-year-old man shows hypointensity on hepatobiliary phase gadoxetic acid–enhanced MR images (serum AFP level, 13 700 ng/mL [13 700 μg/L]; AFP-L3, 48.7%; and PIVKA-II, 7924 mAU/mL). Dissociating medial frontal and posterior cingulate activity during self-reflection. Second, we only assessed HCC lesions that were hypervascular in the arterial phase, and therefore our results cannot be applied to a general screening population with benign disease, hypovascular HCC on arterial-phase images, or other malignancies. On the conventional T2-weighted image (upper left image), MR imaging signal intensity is visible neither in normal lung (arrowheads) nor in the transplanted lung (arrow). Magn Reson Med 2006;55(5):1065–1074. The use of plugging as part of the biopsy technique was part of the audit. Crossref, Medline, Google Scholar10 Inagaki Y, Tang W, Xu Het al.. B, Situation 20 minutes later. There was no clinical consequence (Table 3). The site of hemorrhage was unrelated to the treated aneurysm or PED in the right carotid siphon. Diffusion-weighted imaging improves the diagnostic accuracy of conventional 3.0-T breast MR imaging. For female patients, the age range was 17–73 years, and the mean age was 51 years ± 14. Computed tomography is inaccurate in estimating the severity of adult splenic injury. In 704 of 1571 (44.8%) patients, a specific diagnosis was not made on the basis of the CT examination (Fig 1, Table 1).Table 1 Diagnoses in Patients with Discordant CT and Clinical ResultsFigure 1: Flow diagram of study cohort. Receiver operating characteristic and logistic regression analyses were conducted to assess the ability of the imaging measures, alone or in combination, to be used to discriminate between papillary and clear-cell cancer subtypes. Periprocedural death or major stroke occurred in three centers, at a rate of 9% (three of 33), 7% (one of 15), and 3% (one of 32), respectively. Characterization of the human OATP-C (SLC21A6) gene promoter and regulation of liver-specific OATP genes by hepatocyte nuclear factor 1 alpha. In addition, among patients in whom CT suggested a specific diagnosis but who did not receive a final clinical diagnosis, the vast majority of entities suggested at CT were of a relatively benign, self-limiting nature, with benign adnexal mass; gastroenteritis, colitis, or adenitis; and constipation accounting for nearly 80% (70 of 90) of these cases. The values from measurements performed in healthy tissue are also consistent with values measured by using other techniques (26), indicating that the proposed MR approach to map local sO2 is accurate. Coronary vessel wall evaluation by magnetic resonance imaging in the multi-ethnic study of atherosclerosis: determinants of image quality. The pertinent fields included the radiology report text, study date and time, interpreting radiologist or radiologists, modality, examination type, examination description, ordering provider, location, and accession number.For this study, we used previously validated rule-based algorithms for identifying radiology reports containing certain critical results, which were developed by using heuristic approaches and were refined after multiple iterations. The contiguous scanning protocols had separate CTDIvol values calculated when the noise index, in conjunction with automatic exposure control, changed with the anatomic region scanned. Neurosci Lett 2010;478(3):165–170. Risk of recurrent subarachnoid haemorrhage, death, or dependence and standardised mortality ratios after clipping or coiling of an intracranial aneurysm in the International Subarachnoid Aneurysm Trial (ISAT): long-term follow-up. Thereafter, they were coregistered and normalized to the Montreal Neurologic Institute (MNI) 152-brain template (2 × 2 × 2 mm). The median diameters of efferent arterioles were not significantly affected by iodixanol (88.1% [25th and 75th percentiles, 75.2% and 96.5%, respectively] vs 97.5% [25th and 75th percentiles, 90.8% and 99.9%, respectively], P = .21) (Fig 3).Figure 3: Graphs show afferent arteriolar (AA) and efferent arteriolar (EA) diameters for perfusion with vehicle solution (afferent arteriolar control group, n = 20; efferent arteriolar control group, n = 16) and with iodixanol (afferent arteriolar iodixanol group, n = 18; efferent arteriolar iodixanol group, n = 22). The slightly lower agreement between intraarterial DSA and MR angiography at 1.5 T was predominantly explained by more frequent recommendation of follow-up imaging after MR angiography at 1.5 T than at 3.0 T.The observers recommended additional treatment based on both intraarterial DSA and MR angiographic findings for 34 of the 310 patients (11%) (Fig 1). Moreover, none of the patients who needed additional treatment based on intraarterial DSA findings would be discharged from extended follow-up after MR angiography. Pancreaticoduodenectomy is reserved for patients with severe combined duodenal and pancreatic head injuries (10).CT findings provide a general overview of the hemodynamic status of the traumatized patient and help detect persistent hypovolemia after initial resuscitation with administration of crystalloid fluids. Test-retest analysis with functional MR of the activated area in the human visual cortex. The retrospective, cross-sectional nature of this analysis precludes assessment of test-retest reproducibility and measurement calibration. A region of interest of the same size as the tumors was placed on the adjacent liver parenchyma, avoiding the large vessels.Hypointense HCC was defined as showing lower SI than that of the surrounding liver (tumor SI/background SI < 1.0) (Fig 1a), and hyperintense HCC as showing equal or higher SI (tumor SI/background SI ≥ 1.0) (Fig 2a).Figure 1a: HCC in a 65-year-old man shows hypointensity on hepatobiliary phase gadoxetic acid–enhanced MR images (serum AFP level, 13 700 ng/mL [13 700 μg/L]; AFP-L3, 48.7%; and PIVKA-II, 7924 mAU/mL). Remarkably, preliminary data suggest that the functional MR imaging paradigm we proposed might be useful even to monitor therapy effectiveness (41). Crossref, Medline, Google Scholar54 Yount R, Raschke KA, Biru Met al.. Brain 2003;126(pt 12):2750–2760. Most of these metastatic LNs were located close to the thyroid bed, and the accumulations in the LNs were masked by intense thyroid bed uptake at whole-body scintigraphy (Fig 1). The mRS score had gradually improved in 10 of 13 patients with cranial nerve palsy and in two patients with residual disability due to previous subarachnoid hemorrhage.Cranial nerve palsy involving the third, fourth, or sixth nerve occurred in 14 patients before the PED procedure. Diagnosis and classification of pancreatic and duodenal injuries in emergency radiology. (b, c) SPECT/CT fusion images clearly demonstrate the physiologic and benign uptake in the left submandibular gland (b) and subcutaneous soft tissue inflammation (c).Figure 2c: Papillary carcinoma in a 52-year-old woman 6 days after administration of 3.85 GBq 131I sodium iodide. Thus, it was associated with pain (P = .0484) but not mechanical (P = .4217) symptoms.In our sample, five pseudotumors demonstrated solid-appearing components with very low signal intensity on all pulse sequences, three of which were in asymptomatic patients (Fig 5). Thus, a small or moderate pneumothorax, as well as a stable or decreasing large pneumothorax, was also not included. Crossref, Medline, Google Scholar5 Silver JM, McAllister TW, Yudofsky SC. Link, Google Scholar29 Chalela JA, Alsop DC, Gonzalez-Atavales JB, Maldjian JA, Kasner SE, Detre JA. Thus, every effort should be made to decrease the radiation delivered while not compromising the diagnostic capability of the CT study.Several techniques may be used to accomplish this task (40). DW imaging misregistration issues can potentially be avoided in future studies by performing DW imaging earlier during the MR imaging examination, improving patient comfort to reduce motion, and employing alternative pulse sequences or postprocessing techniques to reduce eddy current distortions (45–47). The data are presented as absolute diameters (micrometers) and relative values (ie, percentage of the initial diameter).Figure 2: A, B, Video microscopic images of a mouse afferent arteriole. Anatomic regions scanned with a contiguous protocol were separately categorized for SSDE calculations—that is, chest-abdomen-pelvis scans were analyzed for SSDEs of the chest, abdomen, and pelvis separately. Financial activities not related to the present article: institution received money for consultancy from Philips ICT Research; received payment for lectures including service on speakers bureaus from Philips ICT Research. Financial activities not related to the present article: institution received money for consultancy from Intuitive; receives money for expert testimony; is a surgical proctor for Intuitive Surgery. In three (2.0%) of 147 patients, the therapeutic strategy would have been changed after review of the SPECT/CT findings. These included algorithms for malpositioned endotracheal and enteric tubes, acute pulmonary embolism, and tension or new/large increasing pneumothorax (Fig 3). Diagnosis of acute appendicitis with sliding slab ray-sum interpretation of low-dose unenhanced CT and standard-dose i.v. contrast-enhanced CT scans. Crossref, Medline, Google Scholar14 Volpe A, Kachura JR, Geddie WRet al.. Crossref, Medline, Google Scholar49 Leontiev O, Buxton RB. To evaluate inter- and intraobserver agreement, ADC measurements were repeated for a consecutive subset of 30 nonmalignant lesions. Complementary roles of diagnostic peritoneal lavage and computed tomography in the evaluation of blunt abdominal trauma. In many such centers, state-of-the-art CT scanners have been installed in the vicinity of the emergency or trauma room. Although dose is a concern, we think that the wide array of alternative diagnoses detected during this study—as well as the downstream ramifications of these diagnoses—provide support for a nonfocused protocol. The significance levels of the multiple post-hoc tests were adjusted by using sequential Holm-Bonferroni corrections in multiple comparisons (the corrected α is given in parentheses for each comparison). One patient had findings consistent with hypertrophic cardiomyopathy. Munich, Germany: R Oldenbourg Verlag, 1999. Middle and bottom: Sagittal view. Circulation 2008;118(10):1011–1020. For treated tumor versus contralateral striatum, \$\$ = P < .01, \$\$\$ = P < .001. Crossref, Medline, Google Scholar43 Uddin LQ, Kelly AM, Biswal BB, Xavier Castellanos F, Milham MP. Radiology 2005;235(3):969–976. Crossref, Medline, Google Scholar40 Parker SM, Gibson GJ. Crossref, Medline, Google Scholar12 van Randen A, Bipat S, Zwinderman AH, Ubbink DT, Stoker J, Boermeester MA. Comparison of digital mammography and screen-film mammography in breast cancer screening: a review in the Irish breast screening program. Crossref, Medline, Google Scholar22 Fracheboud J, de Koning HJ, Beemsterboer PMet al.. The numbers of our patients who did not receive a specific CT diagnosis (704 of 1571, 44.8%) and the numbers who did not receive a specific clinical diagnosis (672 of 1571, 42.8%) were similar (P = .2650). Altered spontaneous neuronal activity of the default-mode network in mesial temporal lobe epilepsy. 2010. Differences in mean perfusion between low-grade and high-grade RCC as well as tumor stage were assessed with the Student t test. The UK nephrostomy audit: can a voluntary registry produce robust performance data? In: Han J, Kamber M, eds. Diagnosis and treatment of uncomplicated urinary tract infection. Disorders of the cerebellum: ataxia, dysmetria of thought, and the cerebellar cognitive affective syndrome. Interobserver agreement for treatment decisions was substantial for intraarterial DSA (weighted κ = 0.73; 95% CI: 0.64, 0.82) and moderate for MR angiography (weighted κ = 0.53; 95% CI: 0.36, 0.70).These results show that the decisions to re-treat patients with coils based on findings of intraarterial DSA and MR angiography were, on a group level, comparable. Staging of differentiated thyroid carcinoma using diagnostic 131I SPECT/CT. SPECT/CT in addition to whole-body scintigraphy has been routinely performed for all patients treated with radioiodine therapy in our institution. SSDE did not statistically vary as a function of patient size (the linear regression model fit parameters were 0.02 mGy/cm; 95% CI: −0.14, 0.06 mGy/cm; P = .2). Concomitant coil treatment of aneurysms at the time of PED placement was performed for previously untreated aneurysms 20 mm or larger in size, after the occurrence of delayed rupture of aneurysms after PED placement in two aneurysms 20 mm or larger in diameter early in the study. AJR Am J Roentgenol 2002;178(2):367–372. The higher oxygen supply to the tumor (high BVf) could be associated with a higher oxygen extraction in the tumor tissue, in line with its higher cell density.MR imaging measurements (BVf and MR estimate of sO2) indicate that the antiangiogenic drug used in this study has a substantial effect on the tumor microvasculature. Dynamic contrast-enhanced magnetic resonance imaging pharmacodynamic biomarker study of sorafenib in metastatic renal carcinoma. There was one case of ipsilateral ischemic stroke due to a small left capsular infarct immediately after PED placement (mRS = 4). Inhibition of CD26/DPP IV attenuates ischemia/reperfusion injury in orthotopic mouse lung transplants: the pivotal role of vasoactive intestinal peptide. Research predating the widespread clinical use of CT demonstrated that the individual clinical signs and symptoms of appendicitis (abdominal pain, nausea, vomiting, anorexia, fever, chills, dysuria, diarrhea, and constipation) are either insensitive, nonspecific, or both (3).During the past decade, CT has become the study of choice in the setting of suspected acute appendicitis in adults, with rates of preoperative use increasing from approximately 20% in 2000 to greater than 90% in 2006 (4–7) and the subsequent reduction of negative appendectomy rate from greater than 20% to less than 10%. Adhesions between the heart and the left thoracic wall were dissected, and the thymus, with its overlying fatty tissue, was removed to allow clear identification of the ascending aorta and the root of the left pulmonary artery. The dependent variable was the indicator of concordance between the reference standard (histopathologic evaluation) diagnosis and the diagnosis derived for the same patient by using each qualitative and quantitative assessment; diagnostic test results for the quantitative assessments were based on the threshold levels from receiver operating characteristic analysis. Three centers used a 3.0-T and one center used a 1.5-T machine. Crossref, Medline, Google Scholar30 Park MJ, Cha ES, Kang BJ, Ihn YK, Baik JH. Key audit standards were met regarding sample adequacy for histologic assessment and diagnostic accuracy, although there were problems with documentation observed in relation to availability of consent form and postprocedural instructions in the patient record, with potential medicolegal implications. This situation arose, as it became apparent after receipt of initial departmental data that the pursuit of additional information surrounding patients and biopsy could be helpful; therefore, the coagulation questionnaire was distributed. For each group, four rats, called longitudinal subgroup, were imaged at each time (D9[T−1], D11[T1], D13[T3], D15[T5] and D18[T8]). Arch Surg 1999;134(6):622–626; discussion 626–627. Historically, performing WL evaluation, although more informative, has been technically challenging and hence not been adopted in clinical practice. MR angiography provides three-dimensional images in contrast to intraarterial DSA, the coil mesh configuration is visible on intraarterial DSA but not on an MR angiogram, and coil-induced artifacts may disturb evaluation of MR angiograms (4,8,9). The mean age of women diagnosed with cancer was also lower in the digital mammography group than in the screen-film mammography group (61.4 and 62.3 years, respectively). BMJ 2009;339:b2587. CA Cancer J Clin 2007;57(2):75–89. The Spearman rank-order correlation was used to assess the correlation between tumor size and tumor perfusion as well as ASL perfusion and DCE MR imaging parameters. Blunt abdominal trauma. Link, Google Scholar97 Santucci RA, McAninch JW, Safir M, Mario LA, Service S, Segal MR. Thyroid bed accumulation would be detected more frequently in patients who were undergoing initial radioiodine therapy than in patients who had already undergone radioiodine therapy because remnant normal thyroid tissue is likely to remain at the first therapy. This region was defined by using a sphere with a radius of 5 mm and the center in the coordinates corresponding to the maximum z score of cerebellar activation (Montreal Neurological Institute [MNI] space coordinates: 22, −54, −26 mm) of healthy control subjects for the interference condition. The distribution of clinical indications for MR imaging was not significantly different before (n = 253) and after (n = 175) exclusion of lesions because of missing or misregistered DW imaging data (χ2 = 0.9, P = .8). H.K.M.C. No relevant conflicts of interest to disclose. Alteration of brain functional network at rest and in response to YMCA physical stress test in concussed athletes: RsFMRI study. Google Scholar2 Hughes TM, Elton C. This decreases the heterogeneity of DMN patterns when using the seed-based method (28). Ionizing radiation exposure of the population of the United States. Intravenous administration of Gd-DTPA prior to DWI does not affect the apparent diffusion constant. The cocaine ‘body packer’ syndrome: diagnosis and treatment. Differentiation of renal cell carcinoma subtypes by multislice computerized tomography. Patients with a Chance-type vertebral fracture and large abdominal wall hematoma have a higher risk of injury to the bowel or mesentery (77–80).A variety of signs help diagnose bowel and mesenteric injuries with CT. For clarity, both contralateral striatum values for untreated and treated groups were merged and are presented in c and d. When compared with the first frame, there was a trend toward decline in both signal-to-noise ratio and contrast-to-noise ratio of the later frames (P < .05). A test bolus of 2 mL was used to time the first pass based on corticomedullary arrival (25). These ROIs were then transferred to the automatically coregistered precontrast and early nephrogenic phase images. Crossref, Medline, Google Scholar3 Migaud H, Putman S, Krantz N, Vasseur L, Girard J. For reliable grading and staging of diffuse liver disease processes, a minimum of 11 complete portal tracts within the specimen has been suggested (13). Recent hardware and software developments, especially multidetector technology (18,19), have further potentiated the methods used to evaluate the polytrauma patient in multiple facets: diagnostic capability, speed, and patient safety. Crossref, Medline, Google Scholar31 Stuber M, Botnar RM, Spuentrup E, Kissinger KV, Manning WJ. Overdiagnosis and overtreatment of breast cancer: progression of ductal carcinoma in situ: the pathological perspective. Crossref, Medline, Google Scholar26 Mohammed MA, Cheng KK, Rouse A, Marshall T. The median percent histologic fibrosis in all patients was 8.5% (interquartile range: 5.7–14.4). The abdominal aorta may be injured in high-speed automobile accidents, when it can be trapped between a lap belt and the lumbar spine. Factors such as chronic kidney disease, diabetes mellitus, periprocedural hemodynamic instability, and volume depletion may substantially increase the risk for contrast medium–induced AKI (2). Link, Google Scholar9 Le Bihan D. Further studies need to be conducted on the application of SSDE to DLP so that scan length can be accounted for in the patient dose equation. Radiology 1991;181(1):189–196. Spurious but systematic correlations in functional connectivity MRI networks arise from subject motion. In our prospective study, abdominal radiography achieved an overall sensitivity of 0.77 (41 of 53) and an overall specificity of 0.96 (267 of 277) in the depiction of packets when compared with low-dose CT. AJR Am J Roentgenol 2009;192(6):1514–1523. Our results show that perfusion with iodixanol has differential effects on afferent and efferent arterioles, leading to a significant constriction of afferent, while not significantly influencing efferent, arterioles. Portal phase and equilibrium phase images were obtained at 60–90 seconds and 120–180 seconds after injection, respectively. The use of contrast-enhanced magnetic resonance imaging to identify reversible myocardial dysfunction. All scans were performed by using the same AEC system and settings to adapt scanner output to changes in patient size. Treatment options are often discussed in multidisciplinary meetings together with neurologists and neurosurgeons. MR imaging of renal cell carcinoma: its role in determining cell type. Second, we did not use the T1 relaxation time of the tumor to calculate tumor perfusion. Crossref, Medline, Google Scholar23 Roes SD, Korosoglou G, Schär Met al.. Diagnosis of appendicitis in adults by ultrasonography or computed tomography: a systematic review and meta-analysis. Therefore, the purpose of this study was to evaluate the sensitivity of the perfusion parameters derived from Intravoxel Incoherent Motion (IVIM) in the human brain and MR imaging to hypercapnia-induced vasodilatation and hyperoxygenation-induced vasoconstriction.This prospective study was approved by the local ethics committee at the University of Lausanne. Crossref, Medline, Google Scholar18 Partridge SC, Demartini WB, Kurland BF, Eby PR, White SW, Lehman CD. Crossref, Medline, Google Scholar95 Ramchandani P, Buckler PM. Blood located adjacent to the source of the hemorrhage is typically partially clotted and tends to be higher in attenuation (45–70 HU); this finding is termed the sentinel clot sign (45). Kidneys were removed and sliced along the corticomedullary axis. Abdominal X-ray signs of intra-intestinal drug smuggling. Ann Intern Med 1988;108(5):710–717. Link, Google Scholar38 Peng MY, Parisky YR, Cornwell EE, Radin R, Bragin S. Occlusion rate of covered arterial side branches at 6 months was 1.4% (two of 140; 95% CI: 0.3%, 5.6%). Patients were excluded if they had more than one HCC (12 patients with 31 nodules), if they had previous treatment (three patients with 10 nodules), if they did not have MR imaging (nine patients with nine nodules) or if their lesions were hypovascular in the arterial phase (three patients with three nodules) (Fig E1 [online]). Normalized accurate measurement of longitudinal brain change. Diffusion tensor MR imaging and fiber tractography: technical considerations. Acta Radiol 2008;49(6):646–657. Link, Google Scholar42 Bhullar IS, Block EF. Kohlfuerst et al (14) showed that SPECT/CT had a diagnostic effect in 21 (64%) of 33 patients, and therapeutic planning was changed in eight (24%) of 33 patients. Acta Radiol 2008;49(6):658–667. Patient SSDEsize was categorized according to the body weight used to select the CT protocol.For age-based SSDE conversion (SSDEage), the age of the patient was determined at the time of the CT examination and was used to search for a typical patient size based on the patient’s age, according to ICRU Report 74 data. On the other hand, patients with low amounts of fibrosis (approximately 5%) in the biopsy specimen showed remote areas of focal LGE at MR imaging. Interpreting radiologists were not blinded to the clinical indication for the study and had full access to patient medical records. Note higher image noise in a and c, as compared with b, due to lower radiation dose delivered in a and c.Figure 1c: Axial CT images in a 25-year-old man who fell from a second floor. These additional sets of TRAPD images were used only to assess reproducibility. J Neurol Neurosurg Psychiatry 2001;71(2):161–168. Financial activities not related to the present article: was paid for travel reimbursement and honorarium by Radiology Advisory Board of GE Healthcare; was paid consultancy fees by the Medical Advisory Board of Elsevier; was granted stock options for service on advisory board by the Medical/Technical Advisory Board of Activate Networks; is a shareholder, as a member of the Board of Directors, of Montage Healthcare. Our study showed a finding different from what was reported previously. (e) Axial T2-weighted MR images show ROIs drawn to avoid as much cerebrospinal fluid as possible.Figure 2b: Box and whisker plots (median, 25th and 75th percentiles, minimum, maximum, outliers) compare variations of (a)f, (b)D*, (c)fD*, and (d)D, averaged in ROIs drawn in white matter (WM), gray matter (GM), thalamus (T), and lenticular nucleus (LN), in four to seven volunteers and in both sides of the brain. On the contrary, patients with benign MS and RR MS exhibited similar cognitive performances. One possibility is that the sample size

is relatively small in our groups, which warrants further investigation in a larger population. Crossref, Medline, Google Scholar26 Arendshorst WJ, Brännström K, Ruan X. The 16-cm-diameter phantom is much too small to measure absorbed dose to a volume that could be considered patient specific; the percentage difference of such an assumption is in excess of 65% (17.6/50.2), whereas use of the 32-cm-diameter phantom results in overestimation of absorbed dose to a patient volume because the density of the PMMA material is greater than that of the adipose tissue predominant in patients weighing more than 140 kg. Differentiation of clinically benign and malignant breast lesions using diffusion-weighted imaging. The former occurred 27 days after PED placement. Radiology 2004;232(1):164–172. Suboptimal apposition of device to vessel wall and acute or delayed thrombosis of parent artery were extremely uncommon or rare. In a series of experiments, TEMPOL (10^{-4} mol/L) was applied in the bath and perfusate 10 minutes before starting the recordings (Fig 1). Then, the value of each ex vivo pixel was set to one (necrotic), two (hypoxic), or three (normoxia), according to the staining (no cells, brown staining, and no staining, respectively). Financial activities not related to the present article: received consultancy fees from Bayer Schering Pharma, Merck Serono, Sanofi-Aventis, Biogen Dompè. Morphological, contrast-enhanced and spin labeling perfusion imaging for monitoring of relapse after RF ablation of renal cell carcinomas. Magn Reson Med 2006;55(5):1047–1057. Medline, Google Scholar14 Jørgensen KJ, Gøtzsche PC. Stroke 2010;41(10):2247–2253. Nonsurgical management of blunt splenic injury: use of CT criteria to select patients for splenic arteriography and potential endovascular therapy. Indeed, although CT has been reported to be the most accurate imaging method with which to display intraabdominal containers (6–11), the radiation dose typically delivered with this technique is a major limitation in its systematic use to screen persons suspected of conveying these containers. A, Pearson correlation analysis shows significant positive correlation (r = 0.60, P = .02) between functional connectivity in posterior regions and Trail Making Test B z score. Fibroadenomas are generally presumed to have higher ADCs because of stromal myxoid change and consequent higher water mobility (24). Stroke 2010;41(8):1736–1742. Trauma centers designated by the American College of Surgeons as level I are required to have CT available at all times. Using analysis of variance, we found a significant difference among histologic subtypes for both mean tumor perfusion (P < .001, F test) and peak tumor perfusion (P < .001, F test). A.G. No relevant conflicts of interest to disclose. Medline, Google Scholar30 Chong E, Poh KK, Liang S, Soon CY, Tan HC. Crossref, Medline, Google Scholar15 Matthies AK, Skinner JA, Osmani H, Henckel J, Hart AJ. J Forensic Sci 1995;40(5):811–815. Fatty muscle degeneration in cuff ruptures: pre- and postoperative evaluation by CT scan. This value is called the quality reference effective mAs, where effective mAs is defined as the tube current–time product (mAs) divided by the pitch. TEMPOL associated to iodixanol significantly blunted the median DHE ratio by 4.7% (25th and 75th percentiles, 1.0% and 7.1%, respectively), with P = .03, in comparison with iodixanol alone.Figure 9: Graph shows relative changes of DHE fluorescence ratio in afferent arterioles perfused with vehicle solution (control group, n = 5) or treated with iodixanol (n = 6) and TEMPOL (tempol) plus iodixanol (n = 5). (c) Eighty containers stuffed with cocaine were found at stool analysis.Figure 1c: (a) True-positive abdominal radiograph at admission in a 30-year-old man suspected of conveying drug packets shows multiple well-defined smooth and uniformly shaped oblong opacities (*) spread throughout the abdomen, with peripheral crescent of air or “double condom sign” (arrows) (3), consistent with drug packets. Follow-up consisted of comprehensive review of emergency department, inpatient, outpatient, procedural, laboratory, and imaging records. Ventricular mass was calculated by multiplying the myocardial volume at end-diastole by the specific gravity of myocardium (1.05 g/mL). Crossref, Medline, Google Scholar8 Schillaci O, Danieli R, Manni C, Simonetti G. A profile across the tumor was drawn for each modality (MR estimate of sO_2 map and pimonidazole image) (Fig 2). Hematocrit level (mean across all animals, 47.0% ± 3.3) was very stable, with no changes during the follow-up (Table 2).Figure 4a: (a–d) Representative T2-weighted (T2w) images, BVf, and MR estimate of sO_2(MR_SO2) maps and the corresponding pimonidazole (Pimo) staining presented as function of time for the untreated (a) and the treated (b) groups. Hepatobiliary scintigraphy is a simple and accurate test to detect biliary leaks and bilomas (72). These records need to be available for perusal at a later date, and a target of 100% was selected for both of these audit standards.The third standard was diagnostic adequacy; namely, that the sample was sufficient for histologic analysis and for a report to be issued. P.H. Financial activities related to the present article: none to disclose. Google Scholar17 Padia SA, Baker ME, Schaeffer CJet al.. In Table 7, the results are given for final histologic analysis, where available, in those patients with an initial insufficient biopsy (including necrotic tissue). Despite excluding poorly differentiated HCCs, the serum levels of these markers were also lower in the patients with hyperintense HCCs than in those with hypointense HCCs (P = .005, .019, and .08).Figure 3a: Graphs show serum levels of AFP, AFP-L3, and PIVKA-II. Currently defined CTDI phantoms have been shown to lead to underestimation of the dose to average-sized adult and pediatric torsos by 40%–70% (7–9). Radiology 2011;259(2):311–316. J Trauma 1995;39(3):514–518. Similarly, only 121 of 190 reports (63.68%) indicating unexplained free-intraperitoneal air had evidence of documentation of communications. Two holding pipettes held the free end of an arteriole and of an attached glomerulus, respectively. Crossref, Medline, Google Scholar9 Nelson PK, Lylyk P, Szikora I, Wetzel SG, Wanke I, Fiorella D. Women are invited according to postal code and assigned to the nearest screening center. Periprocedural death or major stroke rate was low and appeared to be further improved with concomitant coil treatment to prevent delayed rupture after PED placement. J Clin Gastroenterol 2005;39(10):900–903. Other relevant variables include the use of image guidance or assistance, biopsy technique, needle gauge, type of needle, number of biopsy passes, and nature of the underlying histology and lesion size (if focal).The coagulation questionnaire (questionnaire C) examined several aspects of the biopsy process; while it predominantly pertained to prebiopsy clotting assessment, it included presence of ascites, patient body habitus, and cooperation (Appendix E1 [online]). Am Heart J 2004;147(5):919–923. The majority of patients were adults (>16 years of age); however, data from 122 children were included. Liver 2001;21(6):391–397. Infect Dis Clin North Am 1997;11(3):551–581. Clin Radiol 2005;60(12):1280–1289. Radiology 2008;249(1):97–106. Crossref, Medline, Google Scholar35 Manson SC, Wegner C, Filippi Met al.. Two observers (K.Z.A., A.M.G., 5 and 10 years experience in coronary artery imaging, respectively) scored the visual quality of the vessel wall by consensus reading. Neural Comput 1995;7(6):1129–1159. Crossref, Medline, Google Scholar11 Schmahmann JD. J Am Coll Surg 2008;206(4):685–693. For patients weighing 10 kg or less, CTDIvol was calculated with the 16-cm-diameter CTDI phantom; for all other patients (ie, those weighing > 10 kg), CTDIvol was calculated with the 32-cm-diameter phantom.Figure 6c: Average CTDIvol calculations per weight category were converted to SSDEs for three anatomic scan locations: (a) chest, (b) abdomen, and (c) pelvis. The measurement, reporting and management of radiation dose in CT (Report #96). Thus, use of histogram distribution parameters may be a more appropriate comparator for across different MR systems as long as imaging is performed in the corticomedullary phase of enhancement.The accuracy of WL enhancement parameters was not significantly different from that of the ROI-based method in the ability to discriminate ccRCC from pRCC. Crossref, Medline, Google Scholar24 Vanhaudenhuyse A, Noirhomme Q, Tshibanda LJet al.. * = one patient had one ccRCC and one pRCC lesion, for a total of 74 lesions in 73 patients.ROI enhancement had significantly higher sensitivity (P = .01) for diagnosis of ccRCC when compared with qualitative assessment, but there was no significant difference in specificity or accuracy (P > .05). Clin Radiol 2009;64(3):284–290. SPECT/CT showed a radioactive focus localized in the uterine cervix, although clinical findings including MR imaging did not indicate any metastatic lesion except for Nabothian cysts. Reorganization in cognitive networks with progression of multiple sclerosis: insights from fMRI. Magn Reson Med 2002;47(3):601–606. Longer delays (75–80 sec) are advised when a CT scanner with 16 (or more) detectors is used. Approximately 10–15 patients per CT scanning weight category were retrospectively and consecutively selected from among patients who had undergone CT (Lightspeed VCT-XTe; GE Healthcare, Waukesha, Wis) at our institution between June and November 2011. Animals were approved by the institutional animal care committee (license number 177/2010) and received adequate care according to The Principles of Laboratory Animal Care (promulgated in 1985 and most recently revised in 1996) (14). J Gastroenterol 2009;44(Suppl 19):96–101. The origin of liver disease was viral hepatitis type B in 41 patients, type C in 85, types B and C in two, alcoholism in nine, and other origins in 43. Aneurysm size was smaller than 10 mm (n = 6), 10–25 mm (n = 4), or greater than 25 mm (n = 3). Crossref, Medline, Google Scholar13 Anthony SG, Prevedello LM, Damiano MMet al.. Radiology 2009;253(1):31–46. The observed increase of proton density and T2* relaxation time primarily indicated an increase of substance in the lung.Although we attributed the higher parenchymal density to either an increased cell accumulation or increased formation of edema, we were not able to distinguish the cause on the basis of the MR imaging pattern or T2* quantification. MR imaging was performed with fat-suppressed three-dimentional spoiled gradient-echo in the steady state T1-weighted sequences (liver acquisition with volume acceleration; generalized encoding matrix; repetition time, 3.2–4.0 msec; echo time, 1.6 msec; flip angle, 6–15 degrees; field of view, 42 × 42 cm; matrix, 192 × 320, interpolated to 512 × 512; section thickness, 4.2 mm; overlap, 2.1 mm). Of these lesions, 164 were malignant (24 were high-risk lesions that demonstrated malignancy at the subsequent excisional biopsy) and 253 were benign or high risk. Perlewitz, E.Y.L., P.B.P., A. So far, the results of attempts to improve or prevent such disturbances were disappointing (25), perhaps reflecting our incomplete understanding of how contrast medium–induced AKI comes about. One hundred sixteen patients with an mRS score of 0 before PED placement had a postprocedural mRS score that remained 0 throughout follow-up period. 2020. The coagulation questionnaire and its results are discussed in the companion article, which looks at biopsy complications (9).For statistical analysis (necrotic material excluded), findings were considered true-positive if initial biopsy yielded a malignant result, with no evidence of a subsequent amended benign diagnosis. The purpose of this study was to retrospectively determine the incremental diagnostic value of adding SPECT/CT to whole-body scintigraphy with ^{131}I compared with scintigraphy alone after radioiodine therapy in patients with well-differentiated thyroid carcinoma.This retrospective study was approved by the institutional review board, and the requirement of written informed consent was waived.One-hundred fifty-three consecutive patients with well-differentiated thyroid carcinoma who were treated with radioiodine therapy between October 2009 and August 2010 at our institution were included in this study. In the late 1990s, studies suggested that isolated free intraperitoneal fluid in male patients should be assumed to arise from a perforated hollow viscus and, therefore, that laparotomy was required (48). Brain tumor vessel response to synchrotron microbeam radiation therapy: a short-term in vivo study. The primary safety endpoint was periprocedural death or major stroke within 30 days. For data presentation, mean values from the mean of four measurements of each arteriole were calculated for the 4th, 8th, 12th, 16th, and 20th minutes of registration.To investigate the role of oxidative stress in the diameter changes induced by iodixanol in afferent arterioles, we measured the superoxide concentration estimated with DHE-derived fluorescence. Physiologist 1996;39(4):199, 208–211. ADC maps were created from the spatially registered DW images by using the following equation:where b = 600 sec/mm^2, SDWI is the combined DW image (geometric average of individual b = 600 sec/mm^2 DW images), and S0 is the b = 0 sec/mm^2 reference image.For each lesion detected at dynamic contrast-enhanced MR imaging, a region of interest (ROI) was defined at the corresponding location on the DW images. Crossref, Medline, Google Scholar55 Levine B, Kovacevic N, Nica EIet al.. One disadvantage of the very short TE technology is the relatively low soft-tissue contrast of this sequence type compared with conventional MR sequences. There are certain study parameters that have been evaluated in our study but not covered in the previous studies, including the evaluation of longer-term clinical outcome up to 3 years and longer-term angiographic outcome up to 6 months, evaluation of the effect of PED treatment on aneurysm-related cranial nerve palsy, and evaluation of the risk of side branch occlusion due to PED placement. The flexibility and speed of modern multidetector scanners mandate that a much more thoughtful approach be used when planning the optimal scan for each patient. Approximately one-third of patients with nonischemic cardiomyopathy have evidence of overt myocardial scarring by LGE, the presence of which is associated with a higher risk of sudden death and clinical decompensation (20). Crossref, Medline, Google ScholarPage 11Use of iodinated contrast media is becoming increasingly common. (Hematoxylin-eosin stain; original magnification, ×200.) No evidence of carcinoma was detected at excisional biopsy.Mean ADCs for the 28 high-risk lesions ([1.46 ± 0.39] × 10^{-3} mm^2/sec) were significantly lower than those for the 147 benign lesions ([1.83 ± 0.43] × 10^{-3} mm^2/sec; P < .0001; corrected α = .025). AJR Am J Roentgenol. Computed tomography of blunt abdominal trauma. Comparing screening mammography for early breast cancer detection in Vermont and Norway. Seventy-one patients underwent radioiodine therapy once, and the remaining 68 underwent radioiodine therapy two or more times. For weight categories between 10 and 36 kg, the SSDEs were approximately a factor of 2 times greater than the values, and for 48 and 77 kg, the SSDEs were approximately a factor of 1.5 and 1.2 times greater than the , respectively.Figure 6a: Average CTDIvol calculations per weight category were converted to SSDEs for three anatomic scan locations: (a) chest, (b) abdomen, and (c) pelvis. Improved intratumoral oxygenation through vascular normalization increases glioma sensitivity to ionizing radiation. Two cases in our series, one poorly differentiated urothelial carcinoma and one tubulocystic RCC, were not included in the statistical analysis because of their low prevalence.The maximum tumor diameter ranged from 1.4 to 15.7 cm (mean, 5.5 cm ± 3.5) and did not differ significantly among papillary RCC (mean, 7.9 cm ± 5.5), clear cell RCC (mean, 5.7 cm ± 3.3), chromophobe RCC (mean, 6.6 cm ± 3.4), unclassified RCC (mean, 3.6 cm ± 1.8), and oncocytoma (mean, 3.5 cm ± 1.6) (P = .31, F test) (Table 1).Table 1 Demographic Data and Average and Peak Perfusion Values for Different RCC Subtypes and OncocytomaTable 1 summarizes the perfusion of all renal masses tabulated on the basis of their histologic diagnosis. Rating neurologic impairment in multiple sclerosis: an expanded disability status scale (EDSS). We hypothesize that contrast media constrict afferent arterioles to a greater extent than efferent arterioles. J Arthroplasty 2011;26(4):511–518. Neuroimage 2007;35(1):175–184. Pediatr Res 1974;8(5):561–572. AJR Am J Roentgenol 2009;193(4):1010–1018. DAF-FM diacetate and DHE were dissolved in dimethyl sulfoxide and stored at −20°C.To investigate the effects of iodixanol on the nitric oxide bioavailability of afferent arterioles, we estimated nitric oxide by measuring the changes in the fluorescence of DAF-FM–loaded, perfused arterioles. Imaging near metal with a MAVRIC-SEMAC hybrid. AJR Am J Roentgenol 1992;159(3):591–599. Is mammographic screening justifiable considering its substantial overdiagnosis rate and minor effect on mortality? Radiology 1999;213(2):341–346. The organizational questionnaire was used to assess more generic aspects around biopsy relating to operator characteristics and the facilities available. Finally, more wall thickness precision was demonstrated by narrower standard deviations by using five frames (healthy subjects, 0.16 mm; subjects with CAD risk factors, 0.22 mm) than by using a single frame (healthy subjects, 0.20 mm; subjects with CAD risk factors, 0.26 mm).Friedman repeated-measures analysis of variance results showed that in healthy subjects and subjects with CAD risk factors separately, vessel wall thickness continued to decrease significantly (P < .05) when two or three images were used in calculations in comparison with single-frame measurements. and SSDE in the two lowest weight categories agreed to better than 14% (3.2/3.7) for the chest, 11% (4.8/5.4) for the abdomen, and 13% (4.8/5.5) for the pelvis CT protocols (Fig 6). Financial activities not related to the present article: received payment for board membership as cofounder and shareholder from Montage Healthcare Solutions; received consultancy fees from Infiniti Medical and Amirsys; received payment for lectures including service on speakers bureaus from Terumo Medical; received stock or stock options from Montage Healthcare Solutions; and received payment for travel, accommodations, or meeting expenses unrelated to activities listed as cofounder of Montage Healthcare Solutions. The hepatobiliary phase images were obtained 15–20 minutes after the injection.Image analysis was performed by two abdominal imaging radiologists (A.K. and O.M., with 10 and 40 years of experience, respectively) without information on clinical and pathologic results. Crossref, Medline, Google Scholar62 Broyd SJ, Demanuele C, Debener S, Helps SK, James CJ, Sonuga-Barke EJ. The Beck Depression Inventory (38) was used to assess depressive symptoms, fatigue was measured with the Fatigue Severity Scale (39), and subjective symptoms were assessed by using the Postconcussion Symptoms Scale (40). K.A. No relevant conflicts of interest to disclose. This can reduce coronary wall imaging reliability and success rate. Intraarterial DSA demonstrated adequate occlusion in this patient. However, recent rule-based algorithms were developed with overall accuracies (F1 score [harmonic mean of precision and recall, with equal weighting between the two values]) of greater than 90% for classifying unstructured radiology reports with certain critical results (7). R.I.G. No relevant conflicts of interest to disclose. Size-specific dose estimates (SSDE) in pediatric and adult body CT examinations. Acute appendicitis: meta-analysis of diagnostic performance of CT and graded compression US related to prevalence of disease. Most patients are treated with external fixation and endovascular embolization, with surgery reserved as a life-saving attempt in the most extreme circumstances. Crossref, Medline, Google Scholar9 Freislederer A, Bautz W, Schmidt V. Crossref, Medline, Google Scholar23 Yamashita T, Ji J, Budhu Aet al.. Each group combined their results to derive conversion factors as a means to correct the displayed CTDIvol value to SSDE. Repeated-measures analysis of variance (general linear model) with the Greenhouse-Geisser correction was used to assess differences in BVf and MR estimate of sO_2 between both ROIs (tumor and contralateral striatum) within each group (untreated and treated) by using the longitudinal subgroups. N Engl J Med 2008;358(9):972–973. Responses were incomplete in some parts of the questionnaires, and as such, numbers did not always add up to the expected total (including the response “don’t know,” as well as those sections that were incomplete or left blank).Image guidance was defined as the use of an imaging modality (usually US) for real-time depiction of both the liver and the biopsy needle during the procedure and to directly depict the needle during biopsy. Contrast-enhanced myocardial T1-weighted scout (Look-Locker) imaging for the detection of myocardial damages in hypertrophic cardiomyopathy. A thorough search for additional direct signs of organ injury is critical in these cases. R.L. No relevant conflicts of interest to disclose. The intrasubject reproducibility was not studied. Other relationships: none to disclose.Author ContributionsAuthor contributions: Guarantor of integrity of entire study, P.L.; study concepts/study design or data acquisition or data analysis/interpretation, all authors; manuscript drafting or manuscript revision for important intellectual content, all authors; approval of final version of submitted manuscript, all authors; literature research, all authors; clinical studies, P.L.; experimental studies, P.L.; statistical analysis, P.L., W.K.; and manuscript editing, all authorsReferences1 Kohn KT, Corrigan JM, Donaldson MS. J Comput Assist Tomogr 2009;33(1):63–69. 2006;91(8):2892–2899. The same strength setting was programmed into each of the scanners and was used for all protocols. It must also be noted that breast MR imaging performance varies by clinical indication (in our study, the dynamic contrast-enhanced MR imaging PPV3 for high-risk screening was lower than that for the other clinical indications), as well as between different centers and with reader experience. Radiology 2000;214(1):283–289. Making the diagnosis of acute appendicitis: do more preoperative CT scans mean fewer negative appendectomies? The leading CT diagnosis, as reported by the interpreting radiologist, was recorded for each patient. Interaction of angiotensin II and nitric oxide in isolated perfused afferent arterioles of mice. Radiology 2009;250(2):331–351. Crossref, Medline, Google Scholar13 Buckley DL. The annual rate of change was greatest in 1998 (34.31%). Crossref, Medline, Google Scholar18 Nacif MS, Turkbey EB, Gai Net al.. J Comput Assist Tomogr 2001;25(3):466–475. Crossref, Medline, Google Scholar11 Hunink MG, Krestin GP. Crossref, Medline, Google Scholar16 Liver Cancer Study Group of Japan. H. Crossref, Medline, Google Scholar27 Robson PM, Madhuranthakam AJ, Dai W, Pedrosa I, Rofsky NM, Alsop DC. Lesion types included five (3%) foci, 92 (53%) masses, and 78 (45%) areas of nonmasslike enhancement. Despite considerable interest in the DMN and its relationship with cognitive function, little is known about DMN connectivity changes in MTBI. Phase-sensitive signed-magnitude images were reconstructed (24) and used in all later analyses.All cine images were randomized, anonymized, and evaluated for image quality. The uptake transporter OATP8 expression decreases during multistep hepatocarcinogenesis: correlation with gadoxetic acid enhanced MR imaging. Crossref, Medline, Google ScholarPage 12The care of persons suspected of having swallowed drug containers is a complex procedure that usually integrates the results of specific investigations (1,2). Similar to the aforementioned approach to splenic trauma imaging, the AAST liver injury scale (Table 3) is commonly applied when assessing the severity of the acute hepatic injury (57,67). A craniocaudal view was added when indicated (in 40%–50% of cases) by using criteria based on breast density and visible abnormality. Medline, Google Scholar20 Muratet JP, Daver A, Minier JF, Larra F. The expression of OATP8 was significantly lower, but expression of AFP and PIVKA-II was significantly higher in hypointense HCCs than those in hyperintense HCCs (both P < .001). The contrast medium concentration was chosen on the basis of the estimation of the average iodine load during coronary angiography (12). Sorafenib exerts anti-glioma activity in vitro and in vivo. Brain 2010;133(Pt 1):161–171. Report STUK-A87. Data for control and iodixanol groups are the same as in Figure 3. Durante and co-workers (3) showed that the 10-year survival rate in well-differentiated thyroid carcinoma with ^{131}I uptake in metastases after radioiodine therapy was 56% versus a mere 10% in patients without any ^{131}I uptake.Radioiodine therapy with ^{131}I after a near-total or total thyroidectomy has been established as an effective treatment for patients with well-differentiated thyroid carcinoma (4,5). Imaging performance assessment of CT scanners:a medical devices agency evaluation group. Crossref, Medline, Google Scholar2 Ahn SS, Kim MJ, Lim JS, Hong HS, Chung YE, Choi JY. RadioGraphics 2002;22(6):1541–1553. 2005;234(2):323–329. We suspected that the transcription of OATP8 might change in accordance with the decrease of ligands to these receptors. Such diverging effects on afferent and efferent arterioles by iodixanol can explain the decreased GFR in contrast medium–induced AKI.The currently recommended diagnostic criteria for contrast medium–induced AKI rely on serum creatinine level measurements (3,4). However, women who had previously undergone digital screening mammography were always offered digital mammography. Google Scholar25 Sobin LH, Wittekind C. CT images should routinely be reviewed with lung or bone window settings, in addition to the routine soft-tissue settings. The five methodologies suggested for determining patient size were as follows: (a) use of the anteroposterior (AP) parameter as a measurement of body thickness from anterior to posterior, (b) use of the lateral (LAT) parameter as a measurement of the body thickness from left to right, (c) the summation of the AP and lateral dimensions (sum = AP + LAT), (d) the calculation of the effective diameter of the patient (), and (e) the association of the patient’s age with their effective diameter as determined by International Commission on Radiation Units (ICRU) Report 74 (11).Figure 2a: Conversion factors from Report 204: (a) Table 1 (32-cm CTDI phantom) and (b) Table 2 (16-cm CTDI phantom). In cases in which a specific diagnosis was made at CT, the diagnosis is confirmed or supported by the clinician in nearly 95% of cases.Among all patients receiving a specific CT diagnosis, acute appendicitis was the single most commonly diagnosed entity. One potential approach is to apply the algorithms to determine the documentation of communication rates for every radiologist in the department.To demonstrate the potential of using these algorithms for quality assurance initiatives, we ran the algorithms for cardiothoracic critical findings and sorted the data according to the radiologists in the Thoracic Imaging Division for 2009–2011. In this instance, it is tempting to develop a 24-cm-diameter phantom to calculate CTDIvol as an intermediate choice between 16-cm-diameter and 32-cm-diameter CTDI phantoms. Higher grade injuries (AAST grade III and higher) more often require surgical therapy. SPECT/CT identification of post-radioactive iodine treatment false-positive uptake in a simple renal cyst. Patient underwent laparotomy, and colonic injury was confirmed.Figure 6c: Axial contrast-enhanced CT images in a 35-year-old man, a pedestrian struck by a car, show (a) focal thickening of right colon (white arrows) with associated mesenteric hematoma (black arrow), (b) a moderate amount of hyperattenuation (measured attenuation, 30 HU) in the pelvis (arrow), and (c) pneumoperitoneum (arrow). LV end-systolic and end-diastolic volumes were calculated based on the summation of disks method, with subsequent derivation of stroke volume and global ejection fraction. (b) Photomicrograph of hematoxylin and eosin stained slide shows moderately differentiated HCC with fat deposition. AJNR Am J Neuroradiol 2008;29(5):843–852. (d) Histogram of WL enhancement demonstrates “peaked” distribution with high kurtosis value of 3.73; this distribution was positively skewed (skewness, 1.94).Figure 2d Findings in a 60-year-old man with a renal lesion (arrow) in the left kidney shown to be pRCC at pathologic evaluation. (a) Coronal T1-weighted MR image shows polylobulated pseudotumor on right side (arrowhead) and thick wall pseudotumor with adjacent foci of susceptibility artifact on left side (arrow). Crossref, Medline, Google Scholar74 Hagiwara A, Tarui T, Murata A, Matsuda T, Yamaguti Y, Shimazaki S. ESUR Web site. J Gastrointestin Liver Dis 2011;20(2):191–196. Crossref, Medline, Google Scholar6 Söderberg M, Gunnarsson M. Crossref, Medline, Google Scholar11 Berlin L. We recognize that even with correlation between all sequences, synovial hypertrophy and fluid can appear to be of similar signal intensity without administration of gadolinium-containing contrast material. Dynamic three-dimensional T1-weighted spoiled gradient-echo imaging was performed in the coronal plane after administration of a bolus of 0.1 mmol per kilogram body weight gadopentate dimeglumine (Magnevist; Berlex Laboratories, Wayne, NJ) at a rate of 2 mL/sec followed by a 20-mL saline flush. (Hematoxylin-eosin stain; original magnification, ×200.) No evidence of carcinoma was detected at excisional biopsy.Figure 3b: Images in 61-year-old woman with personal history of right-breast ductal carcinoma in situ. Prospective comparison of diagnostic peritoneal lavage, computed tomographic scanning, and ultrasonography for the diagnosis of blunt abdominal trauma. Patients in whom acute appendicitis was not the primary clinical concern or patients who were not referred to CT for evaluation would not have been captured. Crossref, Medline, Google Scholar47 Hutchinson EB, Stefanovic B, Koretsky AP, Silva AC. J Arthroplasty 2005;20(5):568–573. The animal bed was equipped with a pad with continuous warm water supply to prevent cooling of the mouse. The sensitivity, specificity, negative predictive value, and positive predictive value of CT for appendicitis in this study were 98.9% (346 of 350) (95% confidence interval: 97.0%, 99.7%), 98.0% (1196 of 1221) (95% confidence interval: 97.0%, 98.6%), 99.7% (1196 of 1200) (95% confidence interval: 99.1%, 99.9%), and 93.3% (346 of 371) (95% confidence interval: 90.2%, 95.4%), respectively.Our results confirmed that approximately three in four patients referred to diagnostic CT for the clinical suspicion of acute appendicitis prove not to have the disease. 1996;166(3):513–515. Crossref, Medline, Google Scholar33 Canadian Hip Resurfacing Study Group. Improved diagnostic accuracy of breast MRI through combined apparent diffusion coefficients and dynamic contrast-enhanced kinetics. Given the clinical importance of these results, they likely were communicated but not documented. Crossref, Medline, Google Scholar7 Neuberger J, Grant A, Day C, Saxseena S. Whole-brain histogram and voxel-based analyses of diffusion tensor imaging in patients with leukoaraiosis: correlation with motor and cognitive impairment. In each subject population, Friedman repeated-measures analysis of variance and trend analysis tests were used to examine the equality of the thickness measurements obtained with single-frame images and the thinnest vessel wall measurement from each subgroup. A trained investigator (Z.Z.L.) performed the imaging experiments.All experiments, including measurements of diameters, were analyzed by investigators experienced in experimental vessel physiology (Z.Z.L., M.M.S., A. Observer agreement regarding the necessity of retreatment of previously coiled recurrent cerebral aneurysms. The pathologist further divided the nonmalignant lesions into high-risk versus non high-risk major groups. First, this study was limited in scope to the DMN, a most reliable and robust network that supports the “default mode of brain function” during rest. Concomitant coil placement at the time of PED placement was performed in nine aneurysms that had not been treated previously, including four aneurysms 20 mm or larger in size and five aneurysms from 10 mm up to 20 mm (Table 2). After injection, the burr hole was filled, the skin incision was sewed, and animals were revived in an incubator prior to returning to the animal facility (16).Seven days after tumor implantation, or D7, T2-weighted anatomic imaging was performed to evaluate the volume of each tumor. Spin diffusion measurements: spin echoes in the presence of a time-dependent field gradient. Our findings are interesting, because we show that the decreases in GFR caused by contrast medium may involve differential effects of contrast medium on afferent and efferent arterioles.Impaired nitric oxide bioavailability appears to be the key to understanding afferent arteriolar constriction in response to iodixanol. Physicans should claim only the credit commensurate with the extent of their participation in the activity.Disclosure StatementThe ACCME requires that the RSNA, as an accredited provider of CME, obtain signed disclosure statements from the authors, editors, and reviewers for this activity. Financial activities not related to the present article: received consultancy fees from Bayer Schering Pharma and was paid for lectures including service on speakers bureaus by Biogen Dompè. J Am Coll Cardiol 2008;52(19):1574–1580. Crossref, Medline, Google Scholar17 Gai N, Turkbey EB, Nazarian Set al.. S.B. No relevant conflicts of interest to disclose. Ongoing technical development in thin-section CT has led to higher spatial resolution and improved signal-to-noise ratio (SNR), which, however, results in higher exposure to ionizing irradiation (5). Position Statement of the Health Physics Society. (b) Axial delayed phase CT image shows leakage of contrast-enhanced urine into perinephric space (arrow), caused by an injury to renal collecting system.Figure 9b: CT images in a 34-year-old man who was in a high-speed motor vehicle accident. Crossref, Medline, Google Scholar20 Boscak A, Shanmuganathan K. These three questionnaires would provide a wide range of contextual data, which would then be used to explore any potential relationship of importance to the chosen audit standards. Given our 1-year follow-up interval, it is reasonable to suggest that these patients likely had transient nonspecific abdominal pain, had resolution of symptoms spontaneously or with supportive care only, and avoided unnecessary medical intervention. Google Scholar2 Patient safety requirement 2C (standard NPSG.2a). Neuroimage 2004;23(Suppl 1):S208–S219. AJR Am J Roentgenol 2008;190(2):W100–W105. Bland-Altman plots (Fig E5 [online]) showed no systematic bias or relationship between ADCs and the magnitude of measurement error. Another reason could be the fact that the appropriate examinations were already carefully performed in our patients before radioiodine therapy. More details about the method used to measure wall thickness can be found in Appendix E3 (online).Wall signal-to-noise ratio (SNR), lumen-wall contrast-to-noise ratio (CNR), and vessel wall sharpness were calculated for all good- and excellent-quality TRAPD signed-magnitude images by using the following formulas: SNR = Mw/SDn and CNR = (Mw − Mb)/SDn, where mean signal intensity in the center of the lumen (Mb) was calculated, mean vessel wall signal (Mw) was calculated inside the vessel wall, and standard deviation of noise (SDn) was calculated inside the lung in a structure-free region. Observer agreement in the assessment of endovascular aneurysm therapy and aneurysm recurrence. While several studies reported negligible effects of contrast agent on ADC measurements (14,55–57), there have been conflicting reports on this topic (58,59), and this factor should also be considered when comparing our results with other studies.In summary, our findings show promise for using DW imaging to improve the specificity of breast MR imaging. When compared with DMN patterns in the control group (A), the patient group (B) showed significantly decreased connectivity in the posterior portion (arrowheads) and increased connectivity in the anterior portion (arrows) of the DMN (P < .01; cluster size, K ≥ 20). Error bars = 1 SD.Figure 4b: (a–d) Representative T2-weighted (T2w) images, BVf, and MR estimate of sO_2(MR_SO2) maps and the corresponding pimonidazole (Pimo) staining presented as function of time for the untreated (a) and the treated (b) groups. Automated immunofluorescence analysis defines microvessel area as a prognostic parameter in clear cell renal cell cancer. Crossref, Medline, Google Scholar10 Park YS, Moon YW, Lim SJ, Yang JM, Ahn G, Choi YL. The aim of this study was to determine the effect of the iodinated contrast medium iodixanol on the arteriolar tone in afferent and efferent arterioles of the glomerulus of mice and the functional interactions with the major modulators of arteriolar tone, angiotensin II and nitric oxide. ACR manual on contrast media, version 8. J.R. No relevant conflicts of interest to disclose. The mean interval between MR imaging and histologic analysis was 27.4 days ± 22.1. Histopathologic analysis revealed RCC in 28 patients, with clear cell RCC being the most common subtype (n = 15). Muratet et al (20) reported that it might occur even when 111 MBq of ^{131}I was used for the diagnostic scan. The highest correlations were associated with repeated measurements of the same data by the same observer (R^2 = 0.97, P < .001) and by different observers (R^2 = 0.96, P < .001). CT has high sensitivity for detection and determination of the size of a retroperitoneal or pelvic hematoma. In the definition of the European Society of Urogenital Radiology, contrast medium–induced AKI is an impairment in renal function detected by an increase in serum creatinine level by more than 25% or 44 mmol/L that occurs within 3 days after the intravascular administration of a contrast medium (3). Link, Google Scholar26 Dai W, Garcia D, de Bazelaire C, Alsop DC. A pRCC, on the other hand, demonstrates low-level homogeneous enhancement that may be progressive on images obtained at later phases (Fig 2) (17,19).Figure 1a Findings in a 38-year-old man with renal lesion (arrow) in the right kidney shown to be ccRCC at pathologic evaluation. We analyzed the average grades of the two investigators.Then, we compared hypointense and hyperintense HCCs for clinical and histologic features and AFP/PIVKA-II expression (serum level and immunohistochemical analysis). (b) Sagittal reformation shows the collar sign, in which a defect in the diaphragm creates a waistlike constriction of the herniated stomach (arrow).Injuries to the aorta and other major abdominal and pelvic vessels (inferior vena cava, renal vessels, celiac axis, superior mesenteric vessels, lumbar vessels, and iliac vessels) are uncommon but highly lethal, owing to the rapid rate of blood loss into the peritoneal cavity or retroperitoneal spaces. fMRI investigation of disinhibition in cognitively impaired patients with multiple sclerosis. While less common, hepatic abscesses can occur in patients who sustain high-grade injuries. Pre- and postcontrast corticomedullary phase acquisitions were transferred to a research application (MROncoTreat, Siemens Corporate Research). Link, Google Scholar101 Meyers BF, McCabe CJ. Crossref, Medline, Google Scholar32 Lyng H, Haraldseth O, Rofstad EK. Because noise is uniformly distributed in the difference ASL image, the mean signal intensity in an ROI outside the body should reflect the signal intensity that would be measured in the lesion ROI (mean signal intensity in the whole tumor) in the absence of perfusion. Patients with SP MS had lower NBV than did patients with RR MS (P = .04). (e) Axial T2-weighted MR images show ROIs drawn to avoid as much cerebrospinal fluid as possible.Figure 2d: Box and whisker plots (median, 25th and 75th percentiles, minimum, maximum, outliers) compare variations of (a)f, (b)D*, (c)fD*, and (d)D, averaged in ROIs drawn in white matter (WM), gray matter (GM), thalamus (T), and lenticular nucleus (LN), in four to seven volunteers and in both sides of the brain. The patients with hyperintense HCCs were significantly older than those with hypointense HCCs (P = .04).Table 1 Clinical Features of PatientsNone of the differences noted in the macroscopic growth patterns between the hypointense and hyperintense HCCs was significant (P = .77) (Fig E2a [online]). For visualization, the color-encoded parametric T2* maps were log-transformed. Crossref, Medline, Google Scholar46 Federle MP, Jeffrey RB. The CTDIvol data compared with both SSDE calculations were averaged as a function of patient age. “Soap-Bubble” visualization and quantitative analysis of 3D coronary magnetic resonance angiograms. 2009;34(8):537–538. Crossref, Medline, Google Scholar16 Lagios MD. The early and late nephrographic phases were started 20 seconds and 40 seconds, respectively, after completion of the initial (corticomedullary) acquisition.ASL MR imaging was performed before the administration of contrast material by using a single section through the center of the renal mass in the coronal plane in all but four patients, who underwent imaging in the axial plane owing to the location of the mass. Washington, DC: National Academies Press, 2006. Mann-Whitney tests showed significant differences between healthy subjects and those with CAD risk factors (P < .001), with a smaller P value associated with the use of more time frames.Image signal-to-noise ratio, contrast-to-noise ratio, and vessel wall sharpness measures are summarized in Table E1 (online). Registration was robust and no manual interactions were performed at this stage.Subsequently, lesions were segmented by using an interactive “random walk” approach on the registered data set (26). These five subgroups were created for each population (those with and those without CAD risk factors). This was based on the expectation that the lack of section-vessel orthogonality results in increased apparent wall thickness. Crossref, Medline, Google Scholar3 Villringer A, Rosen BR, Belliveau JWet al.. For the Dutch program, the focus is on a financially and socially acceptable balance between detection, recall, and false-positive rate, whereas the U.S. approach focuses more on a high detection rate, resulting in higher recall and false-positive rates. (b) Axial delayed phase CT image shows leakage of contrast-enhanced urine into perinephric space (arrow), caused by an injury to renal collecting system.Ruptures of the urinary bladder usually occur as a complication of pelvic fractures, especially in patients who have a distended bladder at the time of the impact. Such an analysis disclosed significant differences between healthy control subjects and patients with MS, and these differences were more pronounced in the SP phenotype.The regression analysis in each group between cerebral activations and RTs for the incongruent condition of the Stroop task highlighted that healthy control subjects recruit prefrontal, cingular, posterior parietal, and cerebellar regions. One patient with whole-body scintigraphic uptake thought to be in the thyroid bed was seen to be in the LN at SPECT/CT. Tensorial extensions of independent component analysis for multisubject FMRI analysis. Clinical features such as age and tumor size did not affect the recurrence and survival curves (Table E1 [online]). The conversion factor to correct each patient’s CTDIvol was based on the diameter of the CTDI phantom associated with the particular patient CT scan. If vitamin K decreases in HCC, the PIVKA-II production increases (20). The inclusion criterion for this study was for patients to be centered in the scanner (noncentered patients would have inaccurate AP and lateral measurements owing to radiographic magnification or minification effects); no patients identified in this study were excluded. G.J.E.R. No relevant conflicts of interest to disclose.Author ContributionsAuthor contributions: Guarantors of integrity of entire study, J.D.S., G.J.E.R.; study concepts/study design or data acquisition or data analysis/interpretation, all authors; manuscript drafting or manuscript revision for important intellectual content, all authors; approval of final version of submitted manuscript, all authors; literature research, J.D.S., O.E., R.T.H.L., J.C.B., G.J.E.R.; clinical studies, J.D.S., P.A.B., C.B.L.M.M., F.B., O.E., G.A.P.d.K., R.T.H.L., M.E.S.S., J.C.B., G.J.E.R.; experimental studies, G.J.E.R.; statistical analysis, J.D.S., W.J.v.R., G.J.E.R.; and manuscript editing, J.D.S., B.K.V., R.v.d.B., P.A.B., C.B.L.M.M., F.B., G.A.P.d.K., R.T.H.L., M.E.S.S., W.J.v.R., J.C.B., G.J.E.R.Supported by the Netherlands Organization for Scientific Research (NWO), the Netherlands Organization for Health Research and Development (ZonMw), grant 945-04-310.References1 Molyneux AJ, Kerr RS, Birks Jet al.. Although an alternative approach is to use iodine 123 (^{123}I), clinical usage of ^{123}I is limited in Japan. Note higher image noise in a and c, as compared with b, due to lower radiation dose delivered in a and c.Finally, patients suspected of having a bladder injury should undergo CT cystography. Most if not all of these diagnoses could have been made without the use of intravenous contrast material, but that a more focused examination for appendicitis (in terms of coverage) could conceivably have missed at least one of these.Figure 2d: Representative examples of alternative diagnoses made at abdominal multidetector CT in the setting of suspected appendicitis. In the respective ROIs, spin density (normalized to the dorsal normal lung) and T2* values were measured.For statistical analysis, mean values and standard deviations were computed. Inter- and intrareader reproducibility was not assessed. For maximum enhancement, an ROI of approximately 1 cm^2 was drawn in the area with the highest enhancement at visual assessment in the corticomedullary phase. Radiology 2010;256(1):64–73. Indeed, we observed some inconsistencies likely related to sampling error: Some biopsy specimens with a maximum of 19% fibrosis had no visually evident LGE at MR imaging. Eur Radiol 2011;21(10):2056–2066. Multiple-comparison corrections at the cluster level were performed on the whole brain on the basis of Gaussian random field theory by using FSL easythresh (minimum, z > 2.3; cluster significance, P < .05, corrected).Neuropsychologic measurements were input as covariants for second-level covariance analysis, and Pearson or Spearman rank correlations were performed between either the neurocognitive tests or posttraumatic symptoms (ie, anxiety, depression, fatigue, and PCS) scales and the ICA z images of DMN. R.T.H.L. No relevant conflicts of interest to disclose. W.K. No relevant conflicts of interest to disclose. Percutaneous biopsy of renal cell carcinoma underestimates nuclear grade. Regional differences in screening setup were foreseen and accepted because this study had to be purely observational to evaluate the digital program in daily practice. Good wall apposition was defined as perfect conformity of PED to vessel wall. T.Y. No relevant conflicts of interest to disclose. Crossref, Medline, Google Scholar91 Degiannis E, Boffard K. Anderson grade as designated by each reader was evaluated as a potential predictor of symptoms in the analysis described earlier, both as a normal versus abnormal classification and as an ordinal C1, C2, or C3 score.A total of 174 patients met our inclusion criteria; 88 patients were asymptomatic and 86 were symptomatic. Boxes depict interquartile ranges, bounded inferiorly by the first quartile and superiorly by the third quartile. Sangers (BBNN), as the then directors of the participating screening centers, for facilitating the digital pilots.Author ContributionsAuthor contributions: Guarantors of integrity of entire study, A.M.J.B., R.H., M.J.M.B.; study concepts/study design or data acquisition or data analysis/interpretation, all authors; manuscript drafting or manuscript revision for important intellectual content, all authors; manuscript final versions approval, all authors; literature research, A.M.J.B., R.H.; statistical analysis, A.M.J.B., R.H.; and manuscript editing, all authorsReferences1 Fracheboud J, Otto SJ, van Dijck JAet al.. Crossref, Medline, Google Scholar15 Benda P, Someda K, Messer J, Sweet WH. All exploratory analyses were performed by using statistical software (SAS, version 9.2; SAS Institute, Cary, NC).The responses to the departmental organizational questionnaire (questionnaire A) are included in Table 2. Bladder ruptures can be intraperitoneal, extraperitoneal, or combined intra- and extraperitoneal. We performed a preplanned subgroup analysis for patients imaged at 1.5 T and patients imaged at 3.0 T. Details of the contents of the three audit questionnaires as sent to departmental leads for audit are included in Appendix E1 (online). Google Scholar21 Gruskin AB, Auerbach VH, Black IF. To test the effect of nitric oxide synthesis inhibition on DAF-FM fluorescence, L-NAME (10^{-4} mol/L) was added to the bath solution 14 minutes before starting the recordings (Fig 1). (a) On precontrast T1-weighted fat-saturated gradient-echo VIBE MR image the tumor is hypointense, and (b) on postcontrast corticomedulary phase MR image it demonstrates avid enhancement. We investigated in two healthy volunteers (one man and one woman, mean age, 26 years) the variation of the IVIM parameters in the brain after inhalation of ambient air (22% O_2, 78% N_2), and a mixture of 5% CO_2 and air (5% CO_2, 22% O_2, 73% N_2), and in five healthy volunteers (four men and one woman; mean age, 28 years) after inhalation of ambient air, a mixture of 5% CO_2 and ambient air, and 8% CO_2 and ambient air (8% CO_2, 22% O_2, 70% N_2), and pure oxygen (100% O_2). Magn Reson Med 2009;61(6):1374–1387. The CT examinations within each weight category were separated according to scanning protocol (chest, abdomen, or pelvis); some patients underwent contiguous CT scanning of the chest and abdomen, abdomen and pelvis, or chest, abdomen, and pelvis. AJNR Am J Neuroradiol 2003;24(3):526–533. Delayed (or continued) hemorrhage can occur secondary to the formation of pseudoaneurysms, which are inherently unstable and can rupture through a laceration into the peritoneal cavity or the biliary system, resulting in hemobilia (32). Again, we emphasize that communication with the pseudocapsule is difficult to determine with MR imaging and thus may be underestimated. Under Minnesota state law, patients can prohibit the use of medical information for research purposes. Crossref, Medline, Google Scholar3 Beerman R, Nunez D, Wetli CV. This observation suggests that a dysfunction of cerebellar and prefrontal connections might be among the factors responsible for the clinical heterogeneity of MS. Pseudoglandular pattern was more frequently seen in hyperintense HCCs than in hypointense HCCs (Fig E2c [online]). The treated group received a daily oral administration of sorafenib (100 mg/kg) (17,18) during 8 days from D10(T0) to 18 days after tumor implantation (D18[T8]). Combined with the fact that the majority of nonmalignant lesions in our study had mixed histologic findings, this may explain the variability of ADCs observed in each subtype category. Crossref, Google Scholar39 Kety SS, Schmidt CF. Crossref, Medline, Google Scholar11 Togao O, Ohno Y, Dimitrov I, Hsia CC, Takahashi M. Oak Brook, Ill: Radiological Society of North America, 2008. The y intercept is lower for 8% CO_2 (ie, f is expected to be bigger for 8% CO_2).Figure 1d: (a–c) Graphs show mean ± standard deviation of percentage of variation of average brain (a)f, (b)D*, and (c)fD* as a function of pure O_2, 5% CO_2, and 8% CO_2 inhalation compared with inhalation of air for a 27-year-old male volunteer. Main results 2008–2009 breast cancer screening programme in the Netherlands. Some of the definitions for critical values were specific, including in tension or new/increasing large pneumothorax, unexplained free-intraperitoneal air, and malpositioned endotracheal and enteric tubes, which are defined in Table 1.Table 1 Algorithm Accuracies for Classifying Radiology Reports with Critical Values and Documentation of CommunicationsThe algorithms were designed to search for certain word and phrase patterns that indicated the presence of a critical result in the radiology report text. For male patients, the age range was 16–73 years, and the mean age was 52 years ± 14 (P = .84). Google Scholar2 Langdon DW. Cognitive control and right ventrolateral prefrontal cortex: reflexive reorienting, motor inhibition, and action updating. White = percent changes of pure oxygen compared with air, light gray = percent changes of 5% CO_2 compared with air, dark gray = percent changes of 8% CO_2 compared with air. By using a combined DMN template (a binarized image) from both core seeds, single-participant ICA (one-sample t test, P < .01; cluster size, K ≥ 20) showed a similar spatial connectivity pattern of DMN with seed-based analysis in healthy control subjects (Fig 2, A). Crossref, Medline, Google Scholar11 Möckel M, Radovic M, Kühnle Yet al.. Although noninvasive tools, such as imaging and blood tests, are available and may be able to replace histologic analysis in some cases, such as liver fibrosis, liver biopsy remains the reference standard for most diseases (1). Acquisition time for the VIBE sequence images averaged 17 seconds.Qualitative assessment.—Three radiologists (A.A.A., J. Link, Google Scholar27 Meyer CH, Pauly JM, Macovski A, Nishimura DG. R.M. No relevant conflicts of interest to disclose. As in clinical practice, all previous intraarterial DSA studies were available for assessment. Crossref, Medline, Google Scholar25 Wenkel E, Geppert C, Schulz-Wendtland Ret al.. Tucson, Ariz: Reitan Neuropsychology Laboratory, 1992. Therapeutic decision making is subjective and depends on the level of treatment experience, as well as on familiarity with the imaging techniques. High-resolution computed tomography and diffuse lung disease. AJR Am J Roentgenol 2010;195(6):1342–1346. This chapter also includes images and chart references of common spine measurements used in trauma and arthritis populations. Crossref, Medline, Google Scholar37 Foster BR, Anderson SW, Uyeda JW, Brooks JG, Soto JA. Most if not all of these diagnoses could have been made without the use of intravenous contrast material, but that a more focused examination for appendicitis (in terms of coverage) could conceivably have missed at least one of these.Figure 2b: Representative examples of alternative diagnoses made at abdominal multidetector CT in the setting of suspected appendicitis. Curve fitting of equation 1 was done on a voxel-by-voxel basis by using the Levenberg-Marquardt algorithm (42) implemented with standard Matlab functions (Mathworks, Natick, Massachusetts). World J Surg 2006;30(2):176–182. The feasibility of patient size-corrected, scanner-independent organ dose estimates for abdominal CT exams. Evaluation of the nitric oxide production in rat renal artery smooth muscle cells culture exposed to radiocontrast agents. Contrast medium–induced acute kidney injury (AKI) accounts for up to 10% of all hospital-acquired cases of AKI in the United States and Europe (1). J Magn Reson Imaging 2007;26(4):823–837. Ex vivo necrotic, hypoxic, and normoxic pixel values were set to one (necrotic), two (hypoxic), or three (normoxia) according to their staining (no cells, brown staining, and no staining, respectively).Figure 3a: Quantitative correlation between in vivo and ex vivo techniques of oxygenation assessments: MR estimate of sO_2(MR_SO2) map and pimonidazole staining. Furthermore, we placed small ROIs (approximately 1–2 cm^2) on images of the gray matter of the superior frontal and parietal gyri, in the white matter of the center semiovale, in the thalamus, and the lenticular nucleus on both sides. Detecting lung signal at MR imaging is more difficult with increasing magnetic field strength because the microscopic magnetic field inhomogeneities between air and lung parenchyma linearly correspond with the static magnetic field strength, resulting in increasingly faster signal decay. How significant is detection of ductal carcinoma in situ in a breast screening programme? Crossref, Google Scholar6 World Health Organization. A nonlinear least-squares fit of the signal intensities to the expression:was performed by using an algorithm that was based on the interior-reflective Newton method. Specimens were fixed in 10% formalin, embedded in paraffin, and stained with Masson trichrome. Learning Objectives:After reading the article and taking the test, the reader will be able to:• List imaging findings of important injuries that result from blunt abdominal trauma.• Explain current concepts of CT technique that are relevant to evaluation of patients with blunt trauma.• Apply CT findings for adequate therapy for patients with blunt abdominal trauma.Accreditation and Designation StatementThe RSNA is accredited by the Accreditation Council for Continuing Medical Education (ACCME) to provide continuing medical education for physicians. Other relationships: none to disclose.Author ContributionsAuthor contributions: Guarantor of integrity of entire study, B.D.P.; study concepts/study design or data acquisition or data analysis/interpretation, all authors; manuscript drafting or manuscript revision for important intellectual content, all authors; manuscript final version approval, all authors; literature research, all authors; clinical studies, B.D.P., P.J.P.; statistical analysis, B.D.P., E.M.L.; and manuscript editing, B.D.P., P.J.P.1 Current address: University of Cambridge, Cambridge, England.References1 Addiss DG, Shaffer N, Fowler BS, Tauxe RV. The percentage of departments from teaching hospitals in England differed from the percentage of district general hospitals by only 5% when comparing respondents (14 of 70 [20%]) and nonrespondents (14 of 94 [15%]). Uptake of Gd-EOB-DTPA by hepatocellular carcinoma: radiologic-pathologic correlation with special reference to bile production. Critics of breast cancer screening, on the other hand, often argue that high detection rates of DCIS represent overdiagnosis, claiming that many cases are biologically unimportant (13,14).Such criticism, however, seems to be unfounded without data about the characteristics of the detected lesions. It is difficult to explain this, however. As would be expected, increased fibrosis–and therefore decreased T1 time–correlated with LV hypertrophy and worsened LV systolic function. Another drawback is the missing radiology data for screen-film examinations in one pilot study. SSDE provides an estimate of the average dose in the scan volume for a patient of a specific size and is a reasonable and simple way to estimate organ dose for relatively large organs located in the scan volume (16,17). CTDIvol converted to SSDE accounts for two of the four parameters necessary to predict radiation dose to a patient for a given CT examination. Complete occlusion was found in 78 of 140 aneurysms (55.7%; 95% CI: 47.1%, 64%) at 6 months, 61 of 75 aneurysms (81%; 95% CI: 70.3%, 89.1%) at 12 months, and 49 of 58 aneurysms (84%; 95% CI: 72.1%, 92.2%) at 18 months (Table 3). Thus, the convenience of two-dimensional coronary vessel wall imaging and its relatively faster imaging time compared with three-dimensional imaging has led to its widespread use in clinical studies (2,6,14).In planning two-dimensional coronary artery wall imaging, the section to be imaged is prescribed orthogonal to the longitudinal view of the artery at the location of interest. Echo-planar imaging of intravoxel incoherent motion. Coil treatment was performed to induce a stable organized thrombus involving fibrin formation, not for complete coil occlusion of the aneurysm; therefore, dense packing was not performed. Blunt hepatic trauma in adults: correlation of CT injury grading with outcome. Crossref, Medline, Google Scholar60 Peitzman AB, Heil B, Rivera Let al.. A.A.W. Financial activities related to the present article: none to disclose. J Arthroplasty 2004;19(8, Suppl 3):5–11. Crossref, Medline, Google Scholar21 Kimura H, Takeuchi H, Koshimoto Yet al.. Thyroid. Circulation 2002;105(2):224–229. Radiology 2011;258(1):236–242. J Magn Reson Imaging 2001;14(4):368–373. An image with good or excellent quality was considered adequate for quantitative analysis. J Magn Reson Imaging 2008;28(1):74–79. Selective (rather than routine) acquisition of the delayed phase series is recommended to limit the amount of radiation delivered (31). The majority of traumatic renal injuries are treated conservatively with observation alone (96,97). Samples that were insufficient for histologic assessment (inadequate) or that were nonrepresentative were categorized as nondiagnostic for the purposes of the audit. Relationships between cycling hypoxia, HIF-1, angiogenesis and oxidative stress. Examples of TRAPD data sets from subjects with and those without CAD are shown in Figure 2. CT scanning at our center during the study period was performed with 120 kVp and modulated tube current (standard protocol noise index = 12, tube current range = 60–660 mA) with 16– and 64–detector row CT scanners (GE Healthcare, Waukesha, Wis). All examinations were processed by using a commercially available computer-aided evaluation software system (CADstream, version 3.0; Confirma, Bellevue, Wash). A negative interaction was found between the right cerebellum and the right MFG (Brodmann area 46, MNI coordinates: 26, 54, 28 mm; and Brodmann area 9, MNI coordinates: 30, 42, 42 mm).In patients with SP MS, a positive interaction was found between the right cerebellum and the bilateral MOG and left fusiform gyrus. Conversely, for large patient sizes, where fsize is less than 1, the variability in CTDIvol would be diminished after conversion to SSDE. Here, the relaxation of that constraint was a key factor in successful coronary wall time-resolved imaging. Crossref, Medline, Google Scholar21 Hauptfleisch J, Pandit H, Grammatopoulos G, Gill HS, Murray DW, Ostlere S. Patzak, M.M.S.; and manuscript editing, Z.Z.L., A. Crossref, Medline, Google Scholar13 Gottwald B, Wilde B, Mihajlovic Z, Mehdorn HM. Recently, a newer quantitative blood oxygen level–dependent approach has been introduced (13), which yields a high spatial resolution and provides MR estimates of sO_2 in the gray matter that correlates with blood sO_2 estimates obtained in the sagittal sinus. The opening chapter concisely offers an overview of normal presurgical anatomy. The SP2 and MLO measurements were performed 18 months after the SP1 measurements. For all sequences, the following parameters were used: field of view, 36 cm; matrix, 384 × 384; section thickness, 6 mm; no section gap; four signals acquired; zero-filled interpolation, 512; and receiver bandwidth, 250 kHz/pixel.Images were retrospectively reviewed with consensus interpretation by two fellowship-trained musculoskeletal radiologists (reader 1: J.L.M., 4 years of experience; reader 2: E.Y.C., 1 year of experience). Significant negative correlations were noted among the enhancement ratio and serum AFP (P = .023, R = −0.25), serum AFP-L3 (P < .001, R = −0.49) and serum PIVKA-II level (P = .018, R = −0.26) (Fig E7a, Fig E7b [online]). SPECT/CT scans from the skull base to the diaphragm were routinely obtained in all patients, and additional SPECT/CT scans of the abdomen and/or pelvis were obtained in 47 patients, depending on whole-body scintigraphy findings. Recanalization of aneurysm was defined as imaging evidence of incomplete aneurysm obliteration after an initial finding of complete obliteration. Biopsies performed with blinding or by nonradiologists outside of the radiology department were not included in the audit, mainly because of the anticipated logistical difficulties likely to be encountered by involving nonradiologists in data collection. Crossref, Medline, Google Scholar32 Smith AM, Walker LA, Freedman MS, DeMeulemeester C, Hogan MJ, Cameron I. Embolism or thrombosis of the transplanted lung seemed unlikely because the increase of opacity was equally and homogenously distributed in the graft.Our study had limitations. Arch Surg 2003;138(5):475–480; discussion 480–481. Intravoxel partially coherent motion technique: characterization of the anisotropy of skeletal muscle microvasculature. Diagnostic yield of MR-guided liver biopsies compared with CT- and US-guided liver biopsies. Between D15(T5) and D18(T8), the MR estimate of sO_2 in treated tumor increased (repeated-measures test, P < .05) and became comparable to the values observed in the contralateral striatum (62.6% ± 3.7 vs 69.8% ± 6.0, respectively) (Fig 4d).The results of this study show the feasibility to measure the local sO_2 by using MR imaging (MR estimate of sO_2) both in healthy and pathologic tissues. Simultaneous spatial and spectral selective excitation. Mol Cancer Ther 2007;6(6):1785–1792. Diffusion-weighted half-Fourier single-shot turbo spin echo imaging in breast tumors: differentiation of invasive ductal carcinoma from fibroadenoma. AJNR Am J Neuroradiol 2010;31(4):E43–E44. Ultrasound-guided fine-needle biopsy of focal liver lesions: techniques, diagnostic accuracy and complications: a retrospective study on 2091 biopsies. For 545 adult patients who received CT examinations of the torso and who varied in size by a factor of two, the AEC system that was used increased CTDIvol from 12 to 26 mGy, but the average estimated patient dose (SSDE) was 22 ± 3 mGy, independent of size. According to their reports, AFP-positive and epithelial cell adhesion molecule–positive HCCs showed stem and progenitor cell features with invasive character and poor prognosis compared with AFP-negative and epithelial cell adhesion molecule–negative HCCs that demonstrated mature hepatocyte-like features with a relatively good prognosis. This may occur, for example, in patients with preexistent anemia. The last two chapters review radiographic and cross-sectional imaging of postsurgical complications both within the surgical bed as well as at remote sites. Constriction of the vasa recta, the vessels supplying the area at risk for acute kidney injury, by four different iodinated contrast media, evaluating ionic, nonionic, monomeric and dimeric agents. In addition, no findings reached significance with respect to communication with pseudocapsule (analyzed as two or three binary categories), wall thickness, presence of synovial hypertrophy (analyzed as two or three binary categories), compartmentalization, soft-tissue erosion into muscle or tendon, osteolysis, or abductor muscle atrophy. C.P.L. Financial activities related to the present article: none to disclose. Ann Nucl Med 2005;19(2):65–74. It should be noted that these algorithms do not take into account radiologists who communicated results but failed to document such in the report. Google Scholar21 Committee to Assess Health Risks from Exposure to Low Levels of Ionizing Radiation, National Research Council. A functional magnetic resonance imaging study of patients with secondary progressive multiple sclerosis. With a cutoff value of 2.1 or less, ccRCC could be diagnosed with a sensitivity and specificity of 90.9% and 89.5%, respectively (Table 3).Figure 3a Boxplots of (a) kurtosis and (b) skewness in ccRCC and pRCC. Crossref, Medline, Google Scholar15 Kulcsár Z, Ernemann U, Wetzel SGet al.. Crossref, Medline, Google Scholar28 Roberts DA, Detre JA, Bolinger Let al.. The role of endomyocardial biopsy in the management of cardiovascular disease: a scientific statement from the American Heart Association, the American College of Cardiology, and the European Society of Cardiology. Staying up to date with these advances and their potential complications is crucial to the radiologist and surgeon reviewing images. J Bone Joint Surg Am 2011;93(24):2287–2293. Cancer yield of mammography, MR, and US in high-risk women: prospective multi-institution breast cancer screening study. AJR Am J Roentgenol 1999;173(5):1269–1272. The functional connectivity MR imaging abnormalities of other networks have not been investigated in the current study, and only the thalamic network was reported on previously in MTBI (69). At our institution, presence of any sign of intraabdominal traumatic injury prompts the decision to acquire delayed images.While not yet in widespread practice, there is growing evidence that supports the addition of an arterial phase series (25–30 seconds after injection) of the abdomen and/or pelvis in selected trauma patients: those with severe mechanisms of injury and those who have a displaced fracture of the pelvic ring on the portable radiograph of the pelvis obtained at the time of admission (20,32–35). No difference in 6-month aneurysm occlusion rate between single aneurysms and multiple aneurysms was observed (Table E1 [online]).Table 3 Angiographic OutcomeThe periprocedural death or major stroke rate was 3.5% (five of 143; 95% CI: 1.3%, 8.4%) (Table 4). Crossref, Medline, Google Scholar20 Kurtzke JF. Crossref, Medline, Google Scholar29 Jain RK. Benign multiple sclerosis? Crossref, Medline, Google Scholar58 Cicerone KD. Technical details are presented in Appendix E1 (online).T2 lesion volumes (LVs) were measured by using software (Jim 4.0; Xinapse Systems, Northants, England;). The original interpretations were not altered by retrospective image review to preserve the actual effect of the CT evaluation. Effect of CT on false positive diagnosis of appendicitis and perforation. Medline, Google Scholar22 de Bazelaire C, Alsop DC, George Det al.. Indeed, no prior series systematically included a CT examination or a stool analysis in every suspect after the negative result of abdominal radiography was reported. Intraobserver, interobserver, and interexamination correlations were evaluated by using the Pearson correlation coefficient (R). Our results show that in clinical practice, decisions for additional treatment during follow-up of coiled intracranial aneurysms can be made on the basis of MR angiographic findings alone. Crossref, Medline, Google Scholar47 Zhuang J, Hrabe J, Kangarlu Aet al.. Recently, a multidetector CT–based scale system that includes contained vascular injuries and active bleeding as part of the grading criteria (Table 2) has been proposed to improve the accuracy of predicting the need for intervention, as compared with the traditional AAST scale (62). A body-packer with a cocaine bag stuck in the stomach. C.K.K. No relevant conflicts of interest to disclose. Crossref, Medline, Google Scholar11 Pierot L, Spelle L, Vitry F; ATENA Investigators. Neurosurgery 2009;64(4):632–642. All individuals signed a consent form before undergoing MR imaging. Link, Google Scholar8 Boone JM. Recently, the American Association of Physicists in Medicine published Report 204 (10), which proposes the use of CTDI with size-specific dose estimate (SSDE) conversion factors to compute a more accurate dose estimate for pediatric and adult body CT imaging. H.H. No relevant conflicts of interest to disclose.We are indebted to Junji Kishimoto, MA, for supporting statistical analysis of this study.Author ContributionsAuthor contributions: Guarantors of integrity of entire study, Y.M., K.A., Y.T., H.H.; study concepts/study design or data acquisition or data analysis/interpretation, all authors; manuscript drafting or manuscript revision for important intellectual content, all authors; approval of final version of submitted manuscript, all authors; literature research, K.A., T.I., H.S., Y.T.; clinical studies, Y.M., K.A., S.B., T.I., H.S., Y.T., M.S.; experimental studies, K.A., Y.T.; statistical analysis, K.A., Y.T.; and manuscript editing, K.A., Y.T., M.S., H.H.References1 Eustatia-Rutten CF, Corssmit EP, Biermasz NR, Pereira AM, Romijn JA, Smit JW. Rofo 2011;183(5):441–447. No bleeding from an aneurysm occurred in cases of incomplete aneurysm occlusion, apart from two cases of delayed rupture after PED placement that occurred within 30 days in large-size aneurysms (≥20 mm). Recently, a study found that a region-of-interest (ROI)-based method of assessing enhancement demonstrated high accuracy in differentiating ccRCC from pRCC (19). In 1990, 89 of 468 reports (19.02%) with critical values had evidence of documentation of communication, compared with 1434 of 1980 (72.42%) radiology reports in 2010 (Table 2), with P < .001. Crossref, Medline, Google Scholar13 Scott AD, Keegan J, Firmin DN. To date, to our knowledge, T1 mapping for diffuse fibrosis quantification has been validated relative to histologic findings only in small numbers of patients with hypertrophic cardiomyopathy, aortic valve disease

(11,12), and in the postoperative cardiac transplantation setting (13).The purpose of our study was therefore to determine the utility of cardiac MR T1 mapping for quantification of diffuse myocardial fibrosis compared with the reference standard of endomyocardial biopsy in patients referred for evaluation of cardiomyopathy.Our Health Insurance Portability and Accountability Act (HIPAA)-compliant study was approved by our institutional review boards. Bartels-Kortland (Preventicon), J. Crossref, Medline, Google Scholar4 Schaafsma JD, Velthuis BK, Majoie CBet al.. Crossref, Medline, Google Scholar13 Cholongitas E, Senzolo M, Standish RAet al.. Non-invasive measurement of perfusion: a critical review of arterial spin labelling techniques. An uptake in the nose and symmetrical uptake in salivary glands were considered normal and indicative of physiologic uptake. J Am Soc Nephrol 1992;3(1):58–65. However, in a recent head-to-head study comparing US and CT in the setting of acute abdominal pain, CT demonstrated better performance overall, including a significantly higher sensitivity for acute gynecologic conditions and equal sensitivity for cholecystitis (26).Comparison of the prevalence of specific alternative diagnoses between male and female patients revealed few differences. Computed tomography grading systems poorly predict the need for intervention after spleen and liver injuries. This method has resulted in an improved success rate (95%) in obtaining good- to excellent-quality vessel wall images compared with the traditional single-image dual inversion-recovery technique (76%). London UK. Link, Google ScholarPage 2Ross's text is the first comprehensive book to address the interpretation of images of the postoperative spine. Patient-to-patient variations are also expected because of differences in body habitus, for example, variations in the proportion of muscle to adipose tissue and the spatial distribution of body fat. More solid-appearing portions of pseudotumor (defined as hypointense on all pulse sequences) and pseudotumors with foci of susceptibility artifact within the walls were also recorded.Figure 2a: Images in a 66-year-old woman with symptomatic bilateral metal-on-metal total hip arthroplasty and bilateral pseudotumors. Because the sensitivity of low-dose CT in the detection of intraabdominal packets is unknown, we cannot completely rule out the possibility that some intracorporeal containers may have been missed at both abdominal radiography and low-dose CT. The inferior pulmonary ligament was incised up to the inferior branch of the pulmonary vein. Crossref, Medline, Google Scholar11 Valable S, Lemasson B, Farion Ret al.. Furthermore, the median fluorescence in iodixanol-perfused arterioles was similar to that of L-NAME–treated arterioles (3.7% [25th and 75th percentiles, 2.2% and 5.0%, respectively], P = .049), indicating a marked suppression of nitric oxide bioavailability by iodixanol (Fig 6).Figure 5: Pseudocolor presentation of fluorescence intensity in an isolated perfused afferent arteriole loaded with DAF-FM, a fluorescent dye for imaging nitric oxide. Thirty-four of 178 aneurysms (19.1%; 95% CI: 13.8%, 25.8%) had been treated previously, with clipping procedure (n = 1), wrapping procedure (n = 1), clipping procedure and coil treatment (n = 2), stent-assisted coil treatment (n = 7), and coil treatment (n = 23). The presence of hematuria (gross or microscopic) after abdominal trauma is a good predictor of the presence of a urinary tract injury (95–97). Pimonidazole is a 2-nitroimidazole reductive chemical probe that undergoes reduction at PO_2 of approximately 10 mm Hg or less, releasing reactive species which form adducts with cellular components, and that can be detected immunohistochemically to assess tumor hypoxia (20). (a) T2-weighted single-shot fast spin-echo image shows that tumor has predominantly high signal intensity relative to renal cortex. Diagnostic peritoneal lavage versus abdominal computed tomography in blunt abdominal trauma: a review of prospective studies. One of the limitations of such ROI-based methods as previously mentioned is inter- and intraobserver variability in ROI placement. Impact of SPECT and integrated low-dose CT after radioiodine therapy on the management of patients with thyroid carcinoma. Usefulness of contrast enhanced ultrasound guidance in percutaneous biopsies of liver tumors. Wall thickening of pseudotumor on left side is less apparent than in a.Figure 3a: Images in a 72-year-old asymptomatic woman after metal-on-metal total hip arthroplasty. Additional exclusion criteria were (a) smoking (seven patients excluded) and (b) a previous history of drug or alcohol abuse (one patient excluded).We studied 57 MS patients (41 women, 16 men; mean age, 41.6 years; standard deviation, 8.5 years; median disease duration, 16 years; range, 2–31 years; median Expanded Disability Status Scale score (20), 4.0; range, 1.0–7.0) and 18 age- and sex-matched healthy control subjects. By using multiple CT scanner models and including the four major CT manufacturers, four independent research groups evaluated dose as a function of size by using four different methods: measurements in tissue-equivalent torso-shaped phantoms or polymethyl-methacrylate cylindrical phantoms and Monte Carlo simulations in cylinders or voxelized patient models. Central pathologic review was not carried out. Contrast Media Mol Imaging 2010;5(4):201–207. Myocardial T1 mapping with MRI: comparison of look-locker and MOLLI sequences. Crossref, Medline, Google Scholar14 Alsop DC, Detre JA. Quantitative measurement of enhancement may improve overall accuracy as well as overcome subjective interreader variability in making a diagnosis of ccRCC. Recently, in patients with essential tremor (17) the overactivation of posterior lobules of the cerebellum during high-load working memory trials was associated with better response time (RT) and accuracy, suggesting that it may represent a brain compensatory mechanism that contributes to maintaining normal behavioral performances.In the current study, we evaluated the involvement of the cerebellum and prefrontal areas during an attention and inhibition task (ie, the Stroop task) in patients with MS and to assess how the functional interaction among these cerebral areas varies across the different disease phenotypes by applying a psychophysiologic interaction (PPI) analysis (18). Three basic mechanisms explain the damage to the abdominal organs: deceleration, external compression, and crushing injuries (2). Crossref, Medline, Google Scholar14 Hirohashi S, Ishak KG, Kojiro Met al.. All donor lungs were exposed to 6 hours of ischemia followed by reperfusion at the time of implantation. Fat was suppressed with a frequency-selective saturation routine. College Park: American Association of Physicists in Medicine, 2011. Radiology 1997;203(3):733–736. Crossref, Medline, Google Scholar49 Vialatte FB, Cichocki A. The report states that, because patient size is included in the calculation of SSDE, SSDE gives a more meaningful estimate of patient dose, and therefore patient risk, than the value of CTDIvol, which is currently saved in patient records. The necroticohypoxic tumoral fraction was obtained by calculating the following ratio: N + H/N + H + NM, where NM is normoxic and N + H + NM signifies the total surface area of the tumor. A fast and complete constriction in response to a bath of a physiologic salt solution with high potassium chloride (KCl) (100 mmol/L) was used as a criterion to identify afferent arterioles suitable for the subsequent experiments (Fig 1). The inverse correlation between T1 time and fibrosis remained significant after adjusting for LV mass, stroke volume, and ejection fraction.Table 3 Correlation between Myocardial Fibrosis, T1 Time, and Cardiac Structure and FunctionOur results provide histologic validation for the use of postcontrast T1 mapping to noninvasively assess interstitial myocardial fibrosis in patients with clinically evident cardiomyopathy. Other treatment characteristics are shown in Table 2. (c) Eighty containers stuffed with cocaine were found at stool analysis.Once the abdominal radiographic findings were interpreted, the suspect underwent abdominal low-dose CT. In addition, the variable length and orientation of the appendix means that a focused scan may not always completely demonstrate the appendix, leading to the need for further testing.Ultrasonography (US) is utilized much less frequently in our clinical practice for suspected appendicitis in adults; there are studies to suggest that US should be the first-line imaging test for acute appendicitis in selected populations, including pediatric patients and thin adults. In this TRAPD approach, each cine frame is then reconstructed into a PS-DIR sign-preserved magnitude image (24).Figure 1: Black-blood pulse sequence diagrams for, A, conventional dual inversion-recovery and, B, TRAPD imaging. Crossref, Medline, Google Scholar41 Smith SM, Jenkinson M, Woolrich MWet al.. This algorithm was previously validated in a different published study as having an overall accuracy of 98%, with precision of 97% and recall of 99% (Table 1) (8). Because of the low incidence of these angiographic endpoints, difference between single aneurysms and multiple aneurysms was unlikely and not analyzed. Medline, Google Scholar3 Berry J, Malt RA. Cancer statistics, 2007. The hyperintense HCCs showed a significantly lower rate of portal vein invasion than that of hypointense HCCs (P = .039) (Fig E2e [online]).The serum levels of tumor markers AFP, AFP-L3, and PIVKA-II were significantly lower in the patients with hyperintense HCCs than in those with hypointense HCCs (P = .003, .004, and .026) (Figs 3, E3 [online]). J Trauma 1994;36(3):385–389; discussion 390. Communication with the pseudocapsule was recorded, but only the size of the collection was measured (rather than the combined pseudocapsule and pseudotumor size). Link, Google Scholar12 Kaufmann TJ, Huston J, Mandrekar JN, Schleck CD, Thielen KR, Kallmes DF. In addition, the decision to avoid biopsy for lesions that were positive at dynamic contrast-enhanced MR imaging and negative at DW imaging cannot be entirely supported on the basis of the results of our study. Crossref, Medline, Google Scholar39 Bonnet MC, Dilharreguy B, Allard M, Deloire MS, Petry KG, Brochet B. Third, the results of disrupted DMN connectivity can be caused by structural connectivity abnormalities (eg, axonal injury), which were not investigated in the current study. Circulation 2000;102(21):2582–2587. B, Spearman rank correlation shows significant negative correlation (r = −0.56, P = .01) between functional connectivity of the anterior MPFC and depression scores in patients with MTBI.Our results show significantly decreased intrinsic functional connectivity in the PCC and parietal regions and increased functional connectivity in the MPFC regions at functional MR imaging in patients shortly after MTBI. Crossref, Medline, Google Scholar25 Thomsen HS, Morcos SK, Barrett BJ. Ann Nucl Med 2001;15(2):111–116. Examples of nonmalignant lesions exhibiting ADCs above and those exhibiting ADCs below the threshold are shown in Figures E1–E4 (online). Only one variable was associated (P < .10) with nondiagnostic samples at multivariate analysis; this was the number of passes (P = .059), which showed fewer passes are associated with lower odds of nondiagnostic sampling.Overall, diagnostic sensitivity was 97.58% (886 true-positive findings, 22 false-negative findings) for metastases and 86.76% (59 true-positive findings, nine false-negative findings) for hepatoma. Crossref, Medline, Google Scholar24 Lemke A, Laun FB, Klauss Met al.. Intraobserver agreement in ADC measurements according to the CCC was 0.91 (95% confidence interval: 0.83, 0.96), and the CCC for the interobserver agreement between the SP1 and the MLO ADC measurements was 0.90 (95% confidence interval: 0.80, 0.95). Top and bottom of boxes = 25th and 75th percentiles, line in box = median.Figure 3b Boxplots of (a) kurtosis and (b) skewness in ccRCC and pRCC. Diffusion-weighted MRI in the body: applications and challenges in oncology. J Magn Reson Imaging 2007;26(2):235–249. Larger hematomas and mesenteric vascular injuries carry the risk of subsequent bowel ischemia and usually require surgical repair, although endovascular therapy with coil embolization can be attempted in patients with injuries to smaller vessels (80).Blows to the mid–upper abdomen with a steering wheel or bicycle handlebars are the typical mechanisms that injure the pancreas and/or the duodenum, often involving the left hepatic lobe and spleen as well. In each spectrum, numbers at left and right represent lower limit and upper limit, respectively, of the intensity within a 1024-bit range.Figure 6: Graph shows relative changes in the DAF-FM fluorescence measured in afferent arterioles perfused with vehicle solution (control group, n = 5) or treated with iodixanol (n = 5) and L-NAME (n = 4). Crossref, Medline, Google Scholar22 Lee JS, Heo J, Libbrecht Let al.. Likewise, there was no significant difference in biopsy adequacy or accuracy according to lesion histology, although final diagnosis of metastasis (in nine patients) or hepatocellular carcinoma (in six patients) was most likely with an initial sample insufficient for diagnosis. Removal of local field gradient artifacts in T2*-weighted images at high fields by gradient-echo slice excitation profile imaging. Atherosclerosis 2010;208(1):69–74. TEMPOL is a superoxide dismutase mimetic and so reduces the superoxide concentration in the arteriolar wall. Crossref, Medline, Google Scholar18 Garvin JL, Hong NJ. Descriptive statistics were applied to explore the radiologic and pathologic characteristics of the lesions. We used the average setting.CTDIvol was calculated by the scanner by using the average tube current throughout the entire scan and was recorded for each scan series. The cerebellum contributes to higher functions during development: evidence from a series of children surgically treated for posterior fossa tumours. In most patients, the liver is readily amenable to ultrasonographic (US) assessment, and this modality has become the biopsy technique of choice in most patients (2–4). All imaging sequences were inspected for the presence of smearing, pulsation, movement, and Gibbs ringing artifacts (definition in Morelli [16]). Hyperintense marrow signal on all pulse sequences was considered an artifact. The standard intravenous contrast material regimen consists of 100 mL of iohexol with a 50-mL saline chaser at a rate of 3 mL/sec, with portal venous phase imaging. Differences in the clinical, radiologic, and neuropsychological characteristics of the patients enrolled, statistical approaches used for the analysis, and choice of the control group to define abnormalities are likely to account for heterogeneity and discrepancies among the available studies and between these and our results (4,6,7,9,26). There were discordant readings in nine (12%) cases between readers 1 and 2, in eight (11%) cases between readers 1 and 3, and in 12 (16%) cases between readers 2 and 3.ccRCC had significantly higher ROI enhancement compared with pRCC for reader 1 (mean ± standard deviation, 277.3 ± 129.7 vs 55.9 ± 51.2; P < .001) and reader 2 (344.7 ± 145.7 vs 59.7 ± 50.4; P < .001). PMID: 32228707 Free PMC article. To evaluate the incremental effect of the additional TRAPD cine frames on vessel wall thickness measurement, five image subgroups containing progressive numbers of cine phases were created for each subject. Five-year results of the ASR XL Acetabular System and the ASR Hip Resurfacing System: an analysis from the Australian Orthopaedic Association National Joint Replacement Registry. All imaging was performed during suspended respiration. Generalized estimating equation based on a binary logistic regression model was used to model the likelihood of a correct diagnosis as a function of the type of information on which the diagnosis was based. S.A. No relevant conflicts of interest to disclose.We deeply appreciate Dr. Taro Yamashita (Department of Gastroenterology, Kanazawa University Graduate School of Medical Science, Kanazawa, Japan), Dr. Yoh Zen (Institute of Liver Studies, King's College Hospital, London, United Kingdom) and Dr. Seiko Kitamura-Sawada (Division of Pathology, Kanazawa University Hospital, Kanazawa, Japan) for their support to our study.Author ContributionsAuthor contributions: Guarantors of integrity of entire study, A.K., O.M., K.K., S. Conversely, 15 patients (5%) would undergo further follow-up based on intraarterial DSA findings, while on the basis of MR angiographic findings, these aneurysms seemed adequately occluded (Table 2). The concern is increased in animal studies with micro-CT, because animals are exposed to relatively large radiation doses (6). The radiograph was immediately interpreted by the radiologist on call (a fellow or a senior resident). Consequences of digital mammography in population-based breast cancer screening: initial changes and long-term impact on referral rates. R: a language and environment for statistical computing, reference index version 2.8.1. . Circulation 2003;107(18):2290–2293. Pathology and genetics of tumours of the digestive system. Foci in the mediastinal region were categorized as positive for LN metastases. DW imaging studies of the breast have demonstrated significantly lower ADCs for breast carcinomas than for benign breast lesions or normal tissue (12,14,18–20,22–31). Kobayashi, S. Eur Radiol 2006;16(6):1226–1236. We observed a range in the number of biopsies performed per operator over 1 year from a minimum of one biopsy to a maximum of 134 biopsies. Diffusion-weighted imaging of malignant breast tumors: the usefulness of apparent diffusion coefficient (ADC) value and ADC map for the detection of malignant breast tumors and evaluation of cancer extension. These data should reassure the clinician that a surgically urgent or emergent cause for symptoms can be safely ruled out when CT imaging findings support a nonspecific clinical picture.On the basis of our experience, we use and advocate a nonfocused (entire abdomen and pelvis) CT protocol when acute appendicitis is clinically suspected. Coronary artery anomalies and variants: technical feasibility of assessment with coronary MR angiography at 3 T. J Surg Oncol 2005;92(1):32–38. Crossref, Medline, Google Scholar62 Marmery H, Shanmuganathan K, Alexander MT, Mirvis SE. MR estimate of sO_2 measurements obtained in the healthy striatum are reproducible and consistent with values reported in the literature. J Trauma 1998;44(6):1000–1006; discussion 1006–1007. 2000;41(6):1082–1085. The quality of liver biopsy was determined by the length and width of the specimen, the degree of sample fragmentation, and, frequently, the number of complete portal tracts contained within the specimen (12). J Bone Joint Surg Am 2004;86-A(9):1947–1954. Patient underwent laparotomy, and colonic injury was confirmed.Figure 6b: Axial contrast-enhanced CT images in a 35-year-old man, a pedestrian struck by a car, show (a) focal thickening of right colon (white arrows) with associated mesenteric hematoma (black arrow), (b) a moderate amount of hyperattenuation (measured attenuation, 30 HU) in the pelvis (arrow), and (c) pneumoperitoneum (arrow). Two women were pregnant and thus were excluded. Arch Neurol 1989;46(10):1121–1123. Stenosis of parent artery at 6 months and delayed posttreatment aneurysm were also extremely rare. Traumatic laceration of the liver limited to the bare area: CT findings in 25 patients. Neurologic complications were rare beyond 30 days and did not occur beyond the 1st year. A tidal volume between 0.6 mL and 0.9 mL was applied, depending on the body weight of the animal. However, there were no differences in ADC between the high-risk and malignant lesion types (P = .1).All MR imaging examinations were performed with a 1.5-T imaging unit (LX; GE Healthcare, Waukesha, Wis) using a dedicated eight-channel bilateral breast coil in the axial orientation. Continuous flow-driven inversion for arterial spin labeling using pulsed radio frequency and gradient fields. Crossref, Medline, Google Scholar11 Drost TF, Rosemurgy AS, Kearney RE, Roberts P. Magn Reson Med 2002;47(3):539–548. To ensure unimpaired ventilation, the bronchial lumen was cleared of any residual fluid or tissue remnants shortly before insertion into the recipient's bronchus. The study was wholly funded by the intramural research program of the National Institutes of Health. (b) Graph shows calculation of SSDEs separately on the basis of effective diameter measurements from CT radiographs (SSDEsize) and from ICRU 74 data provided in Report 204 (SSDEage). M.S.N. No relevant conflicts of interest to disclose. Qualitative assessment resulted in discordant diagnosis in 14.9% of cases when compared with third quartile enhancement.Figure 4a Findings in a 58-year-old woman with an enhancing lesion in the lower pole of the right kidney (arrow), which on review of (a) precontrast and (b) postcontrast T1-weighted fat-saturated gradient-echo VIBE MR images was diagnosed as pRCC by all three radiologists, owing to low-level homogeneous contrast enhancement at corticomedullary phase. Crossref, Medline, Google Scholar15 Grewal RK, Tuttle RM, Fox Jet al.. Link, Google Scholar8 Shope TB, Gagne RM, Johnson GC. These test results were reported in z scores. 2010;195(3):730–736. However, the presence of a combination of these findings increases the likelihood of a clinically important injury (ie, one that necessitates surgical management). E.L. No relevant conflicts of interest to disclose. Hoboken, NJ: Wiley-Interscience, 2003. Reperfusion was restored and the lung was inflated with a brief application of positive inspiratory pressure of a maximum of 20 mbar (2 kPa). Furthermore, only a small increase of T2* relaxation time to approximately 1 msec showed persistent tissue-air interfaces. Note also collapsed inferior vena cava and hyperenhancement of adrenal glands. MR results derived from semiautomated analyses (mass, volume, and ventricular function) or qualitative analysis (presence of LGE) were reported as a single consensus reading of two radiologists blinded to histology with 5 (E.B.T.) and 3 (R.A.N.) years of experience in cardiac MR.Images were processed by using MASS research software (MASS V2010-EXP; Leiden University Medical Center, Leiden, the Netherlands). Study design for concurrent development, assessment, and implementation of new diagnostic imaging technology. Neurology 2012;78(13):969–975. We retrospectively identified patients who had undergone both cardiac MR and endomyocardial biopsy as part of evaluation for cardiomyopathy at a single center between 2005 and 2010. Therefore, we investigated whether enhanced oxidative stress has influence on the constriction of afferent arterioles caused by iodixanol. Low-dose versus standard-dose CT protocol in patients with clinically suspected renal colic. The greatest discrepancy was in distinguishing a normal seroma (grade A lesion) from a fluid-filled periprosthetic cavity (grade C lesion). (Hematoxylin-eosin stain; original magnification, ×200.) No evidence of carcinoma was detected at excisional biopsy.Figure 3d: Images in 61-year-old woman with personal history of right-breast ductal carcinoma in situ. JACC Cardiovasc Imaging 2009;2(1):34–44. Barboriak Laboratory, Duke University School of Medicine, Durham, NC) image processing tools. S.Kobayashi. The dangling diaphragm sign: sensitivity and comparison with existing CT signs of blunt traumatic diaphragmatic rupture. However, in each interexamination reproducibility acquisition, the TRAPD vessel wall technique was replanned, not merely reexamined, at a similar location of the coronary segment. Proc Natl Acad Sci U S A 2004;101(13):4637–4642. Crossref, Medline, Google Scholar9 Kang HS, Moon WJ, Roh HGet al.. Timely and accurate diagnosis and characterization of liver trauma is important in guiding clinical management decisions (65,66). All measurements and calculations were performed by observer 1 (K.Z.A.).The differences in body mass index and age between healthy subjects and those with CAD risk factors and the difference in age between men and women with CAD risk factors were analyzed by using the unpaired Student t test. The PPV3 for dynamic contrast-enhanced MR imaging alone was 39% (164 of 417) overall and 47% (120 of 253) for evaluation of extent of disease, 21% (24 of 112) for high-risk screening, 39% (18 of 46) for problem solving, and 33% (two of six) for short-term follow-up. The pneumothorax could not be identified in either sequence because of the missing MR imaging signal in the lung parenchyma and pneumothorax.Figure 3: Conventional T2-weighted fast spin-echo image (2500/33) and images with TE of 50 µsec, 500 µsec, and 1.5 msec are displayed. Our results demonstrated that f, D*, and fD* change in a gradual way under hypercapnia and hyperoxygenation stimuli in the full brain and in smaller ROIs. It is an important step in confirming the feasibility of IVIM imaging as a quantitative method to measure brain perfusion.The measurement of IVIM perfusion parameters in the full brain seems to be robust in this small cohort, with an intersubject standard deviation of approximately 10% of the mean for f, D*, and fD*, which is similar to the standard deviation obtained for D. Application of recently developed computer algorithm for automatic classification of unstructured radiology reports: valdation study. SSDE conversion factors were created for two CTDI phantom diameters (16 and 32 cm). Crossref, Medline, Google Scholar28 Navar LG, Nishiyama A. Patients in whom acute appendicitis was not clinically suspected, or in whom acute appendicitis was not the primary clinical concern, were not included. Magn Reson Med 2011;65(1):71–82. The mean, standard deviation, and median of these variables for each tumor type were calculated. Crossref, Medline, Google Scholar53 Zhang Z, Lu G, Zhong Yet al.. Radiology 2004;232(2):373–378. Crossref, Medline, Google Scholar13 Iles L, Pfluger H, Phrommintikul Aet al.. Int J Technol Assess Health Care 2005;21(3):368–379. However, SPECT/CT clearly revealed that they were physiologic and benign uptake. Biopsy specimens from patients with shorter myocardial postcontrast T1 times contained significantly greater amounts of histologic fibrosis (r = −0.57; 95% confidence interval [CI]: −0.74, −0.34; P < .0001) (Fig 2). First, the total number of hyperintense HCCs examined was small because such tumors are relatively rare (8). Resting-state functional connectivity in major depression: abnormally increased contributions from subgenual cingulate cortex and thalamus. At the time of data analysis in January 2012, the patients had been observed for an average of 17.6 months ± 10.8 (median, 18.2 months; range, 3–39.2 months).The primary effectiveness endpoint was angiographic evidence of complete aneurysm occlusion at 6, 12, and 18 months and recanalization of the aneurysm. Radiology 2004;233(3):830–849. They also found that dose to the liver increased with an essentially linear relationship (slope = 1.2 mGy/kg; R^2 = 0.66), ranging from a dose of about 5 mGy for a 45-kg patient to about 40 mGy for a 130-kg patient. 2021 May 6;4(1):39. Crossref, Medline, Google Scholar27 Yoshikawa MI, Ohsumi S, Sugata Set al.. On the basis of both intraarterial DSA and MR angiographic findings, additional coil placement was recommended because of incomplete occlusion with both imaging modalities.Figure 1b: (a) Intraarterial DSA image and (b) three-dimensional time-of-flight MR angiogram at 3.0 T in a 46-year-old woman with a coil-treated anterior communicating artery aneurysm (arrow). For this study, histopathologic slides were re-reviewed by a pathologist (J. Posttherapeutic (131)I SPECT-CT offers high diagnostic accuracy when the findings on conventional planar imaging are inconclusive and allows a tailored patient treatment regimen. Its presence portends an adverse prognosis and may provide important therapeutic guidance with regard to revascularization (4), device implantation (5), and medical therapy.Cardiac magnetic resonance (MR) with delayed imaging after administration of a gadolinium-based contrast agent (late gadolinium enhancement [LGE]) has become a reference standard for visualization of focal myocardial scar/fibrosis (6,7). Crossref, Medline, Google Scholar5 Suzuki A, Suzuki MN. Crossref, Medline, Google Scholar3 Kwong RY, Chan AK, Brown KAet al.. Typical case examples are illustrated in Figure 2.Table 2 Alternative Diagnoses at CT according to SexTable 3 Alternative Diagnoses according to Age GroupFigure 2a: Representative examples of alternative diagnoses made at abdominal multidetector CT in the setting of suspected appendicitis. J Surg Oncol 1998;69(2):60–62. Neither risk nor organ doses were determined in this work. Although group ICA is a robust measure (66), it is limited by its inapplicability in individual quantification and correlation with clinical measures. Contrast agent—associated nephrotoxicity. Proc Natl Acad Sci U S A 2003;100(1):253–258. Intermediate-signal-intensity late gadolinium enhancement predicts ventricular tachyarrhythmias in patients with hypertrophic cardiomyopathy. Pelvic CT angiography: application to blunt trauma using 64MDCT. However, this study and others also demonstrated that the prevalence of acute appendicitis is only about 25% among patients in routine clinical practice referred to CT because of clinical suspicion of the disease (16–18).In addition to evaluating for appendicitis, nonfocused CT of the abdomen and pelvis—a scan that images the entirety of the abdomen and pelvis—offers the opportunity to diagnose other acute disease processes that may be indistinguishable from appendicitis on the basis of clinical presentation alone (19). To estimate this noise-induced offset in the perfusion measurement, we took advantage of the linearity of blood flow quantification, that is, blood flow = calibration constant × difference ASL signal, where the calibration constant is dependent on the signal intensity on the reference image and other parameters unrelated to the ASL difference signal (27). J Hepatol 1999;30(4):580–587. Attentional activation of the cerebellum independent of motor involvement. Guidelines for the use of liver biopsy in clinical practice. Individuals were instructed to close their eyes for better relaxation but to stay awake during the imaging protocol. A variety of methods exist to measure brain perfusion by using magnetic resonance (MR) imaging. Systematic review: computed tomography and ultrasonography to detect acute appendicitis in adults and adolescents. Crossref, Medline, Google Scholar16 Maurer MH, Niehues SM, Schnapauff Det al.. Link, Google Scholar20 Herts BR, Coll DM, Novick ACet al.. However, treatment depends more on the hemodynamic status of the patient, the rate of growth of the hematoma, and the presence of active extravasation of contrast-enhanced blood. (c) Serum level of PIVKA-II was in normal range (17%) (21) were excluded. Crossref, Medline, Google Scholar30 Chang YC, Huang CS, Liu YJ, Chen JH, Lu YS, Tseng WY. To our knowledge, no study to date has focused primarily on alternative diagnoses suggested at CT in patients suspected of having acute appendicitis.Our purpose was to assess alternative diagnoses in adults undergoing CT for suspected acute appendicitis in routine clinical practice.This Health Insurance Portability and Accountability Act–compliant retrospective study was approved by our institutional review board. Studies (6,7) indicate that radioiodine therapy improves the clinical prognosis of patients even though they have distant metastases, provided there is accumulation of 131I in the metastatic foci. Crossref, Medline, Google Scholar21 Koh DM, Collins DJ, Orton MR. Heparin was administered intravenously during the procedure to maintain an activated clotting time between 250 and 300 seconds and was not reversed at the end of procedure.Subgroup analysis of correlation between the occurrence of complete occlusion of aneurysm within 6 months and six potential predictors was performed by using the Pearson χ^2 test and the Fisher exact test. Coccolini F, Coimbra R, Ordonez C, Kluger Y, Vega F, Moore EE, Biffl W, Peitzman A, Horer T, Abu-Zidan FM, Sartelli M, Fraga GP, Cicuttin E, Ansaloni L, Parra MW, Millán M, DeAngelis N, Inaba K, Velmahos G, Maier R, Khokha V, Sakakushev B, Augustin G, di Saverio S, Pikoulis E, Chirica M, Reva V, Leppaniemi A, Manchev V, Chiarugi M, Damaskos D, Weber D, Parry N, Demetrashvili Z, Civil I, Napolitano L, Corbella D, Catena F; WSES expert panel. The background liver was normal in 28 patients, whereas 70 patients had chronic hepatitis and 82 had cirrhosis. Rev Invest Clin 2000;52(2):125–131. The first 50 consecutive unique patients in each department, including adult (>16 years of age) and pediatric patients, who had undergone image-guided or image-assisted liver biopsy after January 1, 2008, were to be identified retrospectively from radiology departmental databases. Patient size explained less than 1% of the variation in SSDE (R^2 = 0.003), supporting the conclusion that SSDE was independent of size.Figure 2a: Scatterplots show (a) CT scanner output, as indicated by CTDIvol, and (b) SSDE as function of patient size, which is indicated by sum of AP thickness and LAT width (AP+LAT). K.O. No relevant conflicts of interest to disclose. Crossref, Medline, Google Scholar19 Leopold SS. In the remaining sections of this article we will review the current elements of CT technique that are relevant today for evaluating blunt abdominal trauma, including some that remain somewhat controversial at this time, and describe the most important CT signs of trauma in the various organs. In patients with MTBI, such increased connectivity in the frontal (anterior) regions significantly correlated with decreased connectivity in the posterior regions (r = −0.44, P = .03) (Fig 3), suggesting that these opposite within-network changes are essentially associated.Figure 2: Group t test maps of single-subject ICA results and comparison between patients with MTBI and control subjects. Crossref, Medline, Google Scholar2 Cheville JC, Lohse CM, Zincke H, Weaver AL, Blute ML. MGESE = multiple gradient-echo (GRE) and spin-echo (SE) imaging, MGE3D = multiple GRE three-dimensional (3D) imaging, MR_SO2 = MR estimate of sO_2, MSME = multiple SE two-dimensional, T2 = T2-weighted imaging, T2* after = T2* imaging after ultrasmall superparamagnetic iron oxide (USPIO) injection, T2* before = T2*-weighted imaging before ultrasmall superparamagnetic iron oxide injection.Figure 1b: (a) Diagram shows experimental protocol. Knowledge of these common patterns of injury and the associations of the organs involved are helpful when interpreting computed tomographic (CT) studies of trauma victims (4).Appropriate care of the trauma patient entails a multidisciplinary effort that requires speed and efficiency. Diffusion tensor MRI: preliminary anisotropy measures and mapping of breast tumors. The radiologist on call reported on a standardized electronic form whether an abdominal radiograph was considered positive or negative for the presence of packets. Each patient had four SSDEs calculated per anatomic scan region. The results of these previous studies have suggested that the safety and treatment effectiveness of flow diverters are promising. Breast magnetic resonance imaging for preoperative locoregional staging. In other cases, the assigned screening location determined the modality used.All women invited for screening were informed in writing about the possibility of undergoing digital mammography. Comparisons of outcome and prognostic features among histologic subtypes of renal cell carcinoma. Patient data were handled and stored in compliance with Health Insurance Portability and Accountability Act requirements. The intensity of the radioactive uptake in the thyroid bed of this patient was too weak to detect at whole-body scintigraphy, but at SPECT/CT, an uptake in the thyroid remnant was clearly revealed. Mean weight was 37.7 kg ± 33.1, with range of 3.4–146.6 kg (Fig 3).Figure 3: Correlation plot of patient weight and age in this study.The coefficients of variation between SSDEs for each scan protocol, based on AP and lateral measurements, were as follows: chest, 2% (range, 1%–5%); abdomen, 3% (range, 1%–7%); and pelvis, 7% (range, 4%–11%). Magn Reson Med 2009;62(1):66–76. For example, de Bazelaire et al (22) showed that early changes in ASL perfusion of RCC metastases 1 month after initiation of antiangiogenic therapy correlated with changes in tumor size at 4 months as well as with progression-free survival. Spiral CT: applications in the emergency patient. J Cardiovasc Magn Reson 2011;13(1):75. By dichotomization of the occlusion level, information is lost on the exact degree of occlusion.Besides a different occlusion grade, variability in treatment advices among interventional neuroradiologists may explain discrepancy in policy decisions based on intraarterial DSA and MR angiographic findings. Crossref, Medline, Google Scholar2 Wen SW, Naylor CD. Traumatic brain injury and atrophy of the cingulate gyrus. Sample calculations of SSDE from fsize, CTDIvol, and AP+LAT are shown for small and large patients.Patient dimensions such as anteroposterior (AP) thickness at the midline and lateral (LAT) width can be determined from the CT radiograph before the scan or from CT images after the scan. Motion in cardiovascular MR imaging. The geographic distribution of departments differed by only 4% when we compared respondents and nonrespondents in England (70 of 87 [80%] vs 94 of 123 [76%]), and it differed by less than that in Wales (five of 87 [6%] vs eight of 123 [7%]), Scotland (10 of 87 [11%] vs 16 of 123 [13%]), and Northern Ireland (two of 87 [2%] vs five of 123 [4%]). Also, new effective dose conversion coefficients need to be assessed for use with SSDE-derived DLP values.The findings of this study must be considered in the context of the limitations of the population sampled. All types of contrast media have cytotoxic effects on various cell lines and cause functional impairment of kidney tubules and vasa recta in vitro (5). Significance of intra-abdominal extraluminal air detected by CT scan in blunt abdominal trauma. Hemoperitoneum studied by computed tomography. . New methods in diffusion-weighted and diffusion tensor imaging. Radiol Clin North Am 1998;36(2):399–411. Patient underwent emergent splenectomy.In an effort to improve the ability of CT to help predict successful nonsurgical management in splenic trauma and, ultimately, to improve patient care, several additional CT features of splenic trauma are important considerations. Median luminal diameter of the afferent arterioles decreased in response to iodixanol perfusion when compared with that of the control group (97.5% of initial diameter [25th and 75th percentiles, 89.2% and 106.2%, respectively] vs 104.3% of initial diameter [25th and 75th percentiles, 102.2% and 110.2%, respectively], P = .008) (Fig 3). Left ventricular (LV) structure and function were assessed by using a steady-state free-procession sequence (temporal resolution, ≤50 msec; section thickness, 8 mm; in-plane resolution, ≤1.5 × 2 mm). Defining the current negative appendectomy rate: for whom is preoperative computed tomography making an impact? According to the previous studies, the incremental diagnostic value of SPECT/CT has varied widely from 15% (15) to 73.9% (11); these percentages represent the rate of findings or patients who had findings whose interpretations were changed from whole-body scintigraphy to SPECT/CT. Crossref, Medline, Google Scholar52 Cauda F, Micon BM, Sacco Ket al.. They have also recently been reported as useful in demonstrating the presence of an intracorporeal drug packet (16,17).The purpose of this study was to evaluate the diagnostic performance of abdominal radiography in the detection of illegal intracorporeal containers (hereafter, packets), with low-dose CT as the reference standard.This research was approved by the research ethics committee of our institution (CER 06–023); written informed consent was obtained before any radiologic investigation was performed. Contusions are focal areas of low attenuation or enlargement (Fig 7). For the complete assessment of the pulmonary status of the transplanted lung, additional conventional T2-weighted fast spin-echo sequences were necessary for identifying pleural effusion.The visualization of pulmonary parenchyma at MR imaging remains problematic because physiologically perfused and ventilated lung parenchyma appears black on conventional MR images because of extremely fast decay of the transverse magnetization (17). However, such differences did not reach statistical significance (two-sample t test) regarding the voxel numbers of DMN or average z values.Figure 1: DMN templates created with the seed-based method in healthy control subjects. However, in human studies, the issue of respiratory motion might become more important. Acute appendicitis: comparison of low-dose and standard-dose unenhanced multi-detector row CT. Superoxide increased more in afferent arterioles perfused with iodixanol than in the control group. Real-time imaging is not performed.An audit standard is an explicit specification of an outcome of clinical care against which performance can be measured, and it involves setting a target indicating the anticipated level of performance to be achieved. Error bars = 1 SD.In the contralateral striatum, the mean BVf and MR estimate of sO_2 were stable over time and across groups (for BVf, the mean across all animals and times was 2.9% ± 0.5, and that for MR estimate of sO_2 was 68.2% ± 6.5) (Table 2; Fig 4c, 4d).In the untreated animals, the pimonidazole staining indicated that tumors exhibited hypoxic areas from D13(T3) to D18(T8) (Fig 4a). The transplanted lung showed a statistically significant increase in spin density (approximately 51%, P = .006) and longer T2* transverse TR (1041 µsec ± 424, P = .016).Figure 5: Typical T2* decay curves with measurement points from 50 µsec to 5 msec. Y.G. No relevant conflicts of interest to disclose.The authors thank Kelly-Anne McGorty, BS, RT, for technical support and Damon Kenul, BS, for manuscript preparation.Author ContributionsAuthor contributions: Guarantors of integrity of entire study, Y.W.L., Y.G.; study concepts/study design or data acquisition or data analysis/interpretation, all authors; manuscript drafting or manuscript revision for important intellectual content, all authors; approval of final version of submitted manuscript, all authors; literature research, Y.Z., M.P.M., Y.W.L., R.I.G., Y.G.; clinical studies, Y.Z., L.M., J.R., R.I.G., Y.G.; experimental studies, Y.Z., M.P.M.; statistical analysis, Y.Z., Y.G.; and manuscript editing, Y.Z., M.P.M., Y.W.L., Y.G.2 Current address: Center for the Developing Brain, Child Mind Institute, New York, NY3 Current address: Nathan S. Crossref, Medline, Google Scholar12 Powles T, Chowdhury S, Jones Ret al.. We cannot confidently identify specific risk factors for given complications, given the small sample size and rare nature of these events. Eur Radiol 2008;18(6):1206–1214. Magn Reson Med 2000;43(6):828–836. Table 4 shows that most invasive cancers were small and nonadvanced, as judged by the proportion classified as T1N0. R.J.v.d.G. Financial activities related to the present article: none to disclose. To date, to our knowledge, there are limited data as to the subtypes of nonmalignant lesions that exhibit lower ADCs. Results of prior studies (19,40,41) suggest that papillomas and lymph nodes are two benign lesion types that frequently show restricted diffusion; this is attributed to their higher cellularity. Crossref, Medline, Google Scholar21 Sclafani SJ, Weisberg A, Scalea TM, Phillips TF, Duncan AO. Medical Electrical Equipment. Contemporary approach to the classification of renal epithelial tumors. In particular, only 539 of 924 (58.33%) radiology reports indicating malposition of an endotracheal or enteric tube had evidence of documentation of communications. This is consistent with the observed reduction of tumor BVf, which limits the oxygen supply to the tumor. J Am Coll Cardiol 2006;47(10):2027–2033. Large black typeset letters on clear white paper make for easy reading, and the appropriate-sized margins allow the reader to jot down any notes while reading this fine book. Crossref, Medline, Google Scholar18 Langton DJ, Jameson SS, Joyce TJ, Hallab NJ, Natu S, Nargol AV. Cholecystitis and small-bowel obstruction become major considerations in both sexes starting in middle age.A specific clinical diagnosis was made in 17.3% of patients who did not receive a specific diagnosis at CT. The segments affected most commonly are the proximal jejunum (distal to the ligament of Treitz) and the distal ileum (proximal to the ileocecal valve). Crossref, Medline, Google Scholar26 Brooks A, Schinde V, Bateman AC, Gallagher PJ. Crossref, Medline, Google Scholar7 Young AN, Dale J, Yin-Goen Qet al.. As an expansion of this work, a method to estimate patient dose that accounts for patient size was introduced in the American Association of Physicists in Medicine (AAPM) Report 204 in collaboration with the International Commission on Radiation Units and Measurements and the Image Gently campaign of the Alliance for Radiation Safety in Pediatric Imaging (16). The AAPM Report 204 provides tables based on AP+LAT that are used to find the fsize that, when multiplied by CTDIvol, yields SSDE. Coccolini F, et al. Ratio of men to women was 138 (76.7%) to 42 (23.3%). McMenamy No relevant conflicts of interest to disclose. Link, Google Scholar17 Lanzman RS, Wittsack HJ, Martirosian Pet al.. Kline Institute for Psychiatric Research, Orangeburg, NYFunding: This research was supported by the National Institutes of Health (grants R01 NS039135 and NS039135-08S1).References1 Sosin DM, Sniezek JE, Thurman DJ. Frequency is defined as reports with critical results that also contain documentation of communication. Crossref, Medline, Google Scholar10 Schär M, Kim WY, Stuber M, Boesiger P, Manning WJ, Botnar RM. Magn Reson Med 2003;50(3):531–540. Radiology 2012;262(2):495–502. Radiology 2001;218(1):215–223. Crossref, Medline, Google Scholar29 Greicius MD, Srivastava G, Reiss AL, Menon V. ADC measurements are affected by the size and density distribution of cells, features that may be heterogeneous even within a lesion. Magnetic resonance imaging for the assessment of myocardial viability. Med Phys 1978;5(6):536–539. The last time was defined as 5 days before the median survival time previously observed in the 9L gliosarcoma model (19). C.M.C. No relevant conflicts of interest to disclose. We used arterioles with a minimum length of approximately 55 µm up to a maximum of approximately 100 µm. Google Scholar3 American College of Radiology. . CT scan evaluation of blunt hepatic trauma. In 10 of 84 departments, clinicians from other specialties perform biopsy with image guidance, and this does reflect current moves in gastroenterology training. Crossref, Medline, Google Scholar10 Ho C, Hitchens TK. The bath solution was then changed to DMEM. Diagnosis generally relies on clinical and laboratory findings (27–31), underscoring the importance of thorough clinical evaluation in these patients. Crossref, Medline, Google Scholar28 Otten JD, Karssemeijer N, Hendriks JHet al.. Splenic studies. Arterial phase images facilitate detection of trauma to the major vessels and demonstrate vascular injuries of the solid organs that are not apparent on portal venous or delayed phase images. NMR Biomed 2010;23(7):849–864. Radiology 2010;256:209–218. Furthermore, these two subtypes respond differently to available targeted therapies in advanced disease; tyrosine kinase inhibitors are more effective in patients with advanced ccRCC, whereas mammalian target of rapamycin inhibitor temsirolimus has been recently shown to be more effective against advanced pRCC (11–13).These differences in biologic behavior and response to targeted therapies underscore the need to accurately differentiate between these two common subtypes of RCC. More recent work with newer generations of CT scanners has shown a higher sensitivity for detecting small amounts of free peritoneal fluid. Radiol Clin North Am 2004;42(5):793–806, v. Regional differences in vascular response to changes in arterial partial pressure of CO_2 have been reported in humans with positron emission tomography as well (47).This study had some general limitations. (c) ASL image shows heterogeneous perfusion of tumor (mean perfusion = 152.4 mL/min/100 g).Figure 3b: Coronal images in 68-year-old man with clear cell RCC (arrow) in lower pole of left kidney. Lacerations may be superficial or extend through the entire pancreas, resulting in a transection (also termed fracture). A study of 204 cases (1996-2000). No effects of in vivo micro-CT radiation on structural parameters and bone marrow cells in proximal tibia of wistar rats detected after eight weekly scans. For data sets where the variability in y depends on the value of x, a property called heteroscedasticity, linear regression analysis could give misleading results because the assumption of uniform variation is violated. Link, Google Scholar11 Baltzer PA, Dietzel M, Vag Tet al.. Breast Cancer Res 2006;8(2):204. Bile leaks and bilomas must be suspected in all patients with severe liver injury and are seen on CT images as low-attenuating fluid collections, often enlarging over time. Suboptimal vessel wall apposition of PED occurred in two cases, one at the curvature of the carotid siphon, and the other at a preexisting stent (Neuroform; Boston Scientific) placed for stent-assisted coil treatment. Link, Google Scholar3 Kalra MK, Rizzo SM, Novelline RA. A statistically significant difference in mean ADC among subtypes was identified with the Kruskal-Wallis test (P = .006). A retrospective review of our prospectively populated MR imaging database was performed to identify all consecutive suspicious breast lesions detected at breast MR imaging from October of 2005 to December of 2008 that were subsequently sampled at core needle or surgical biopsy. The bronchus was cut at the tracheal bifurcation, and the vein was cut within the wall of the left atrium. J Am Soc Nephrol 1999;10(suppl 11):S149–S161. Prognosis for mild traumatic brain injury: results of the WHO Collaborating Centre Task Force on Mild Traumatic Brain Injury. All tumors were classified into one of the following categories: (a) low-grade clear cell RCC (Fuhrman I–II), (b) high-grade clear cell RCC (Fuhrman III–IV), (c) papillary RCC, (d) chromophobe RCC, (e) unclassified RCC, or (f) oncocytoma. ESUR guidelines on contrast media. Occult marker of serious injury. Crossref, Medline, Google Scholar37 Hofvind S, Vacek PM, Skelly J, Weaver DL, Geller BM. T1 time correlated inversely with LV mass (r = −0.29; P = .05), end-systolic volume (r = −0.31; P = .04), stroke volume (r = −0.44; P < .01), and ejection fraction (r = −0.52; P < .001) (Table 3). J.R.V.H. No relevant conflicts of interest to disclose. The lack of a straightforward reference standard explains the wide range of sensitivities (from 0.40 to 1.00) that has been reported in the detection of intracorporeal containers with abdominal radiography (3,7,23,25). Functional MR imaging correlates of neuropsychological impairment in primary-progressive multiple sclerosis. Acute rupture of the diaphragm due to blunt trauma: diagnostic sensitivity and specificity of CT. Our results help explain results in previous reports (11,12,21,22) in which diminished blood flow in the renal cortex was observed in clinical and experimental studies.Several phenomena can contribute to decreased GFR in contrast medium–induced AKI (eg, intrarenal regional circulatory disturbances, leading to hypoxia more prominently to the renal medulla; increased oxidative stress; cytotoxicity of contrast media; and derangements of several autocrine or paracrine substances, such as endothelin, nitric oxide, renin-angiotensin system components) (5,23,24). Crossref, Medline, Google Scholar22 Lemasson B, Christen T, Tizon Xet al.. N.C. No relevant conflicts of interest to disclose. Whether our results can be extrapolated to other packet content (such as heroin or liquid cocaine) remains an open question.Another limitation of our study was that the experience of the radiology residents or fellows in interpreting abdominal radiographs was not evaluated, and interobserver variability was not assessed. Evidence for widespread movement-associated functional MRI changes in patients with PPMS. Black lines on T2-weighted images delineate the tumor ROI. A repetition time of 6 seconds was used to allow for recovery of blood signal, and patients were instructed to breathe in the quiet periods between the 6-second acquisitions. A multispectral three-dimensional acquisition technique for imaging near metal implants. Liver Int 2007;27(9):1166–1173. Radiology 2011;260(3):616–620. Usefulness of multidetector computed tomography for the initial assessment of blunt abdominal trauma patients. Fifty-two of the nonmalignant lesions in our study, as well as a group of 31 malignant lesions (used for the ADC comparisons with benign lesion subtypes in Fig 1), were included in a prior study investigating the clinical utility of breast DW imaging (20).Figure 1: Graph shows comparison of ADCs of benign, high-risk, and malignant breast lesions. Daily oral clopidogrel (75 mg) was given for 3 days before PED treatment and for 3 months afterward for each patient. MRI of tumor angiogenesis. Detection and characterization of focal liver lesions: a Japanese phase III, multicenter comparison between gadoxetic acid disodium-enhanced magnetic resonance imaging and contrast-enhanced computed tomography predominantly in patients with hepatocellular carcinoma and chronic liver disease. Furthermore, we evaluated the two most common subtypes of RCC and did not evaluate other subtypes, which have lower incidence of occurrence. With automated dose modulation, the radiation delivered fluctuates during the CT acquisition (by means of modulation of the tube current), on the basis of patient size determined in the longitudinal (z-axis) and axial (in-plane) planes (41). Thus, their estimate of patient dose was dependent on patient size. Renal NO production and the development of hypertension. Google Scholar8 Rockey DC, Caldwell SH, Goodman ZD, Nelson RC, Smith AD; American Association for the Study of Liver Diseases. Each of these structures was then provided with a cuff made by W.J. Cuffs were made of a Teflon intravenous catheter (BD Insyte, Becton Dickinson, Madrid, Spain) and designed as we described in a previous study (15). (c) ASL image shows heterogeneous perfusion of tumor (mean perfusion = 152.4 mL/min/100 g).Figure 4a: Coronal images in 64-year-old man with papillary RCC (arrow) in lower pole of left kidney. All were minor, including two transient ischemic attacks within 1 day after PED placement (mRS = 1), one small ipsilateral occipital infarction immediately after PED placement (mRS = 1), one small contralateral thalamic and corona radiata infarct 1 week after self-withdrawal from aspirin (mRS = 1), one cranial nerve palsy that occurred after the procedure and subsided after 1 week (mRS = 1), and one retroperitoneal hematoma related to femoral arterial puncture (mRS = 0).Beyond 30 days, there were two neurologic complications (1.4%; two of 134; 95% CI: 0.2%, 5.5%). Crossref, Medline, Google Scholar4 Glagov S, Weisenberg E, Zarins CK, Stankunavicius R, Kolettis GJ. (c) There were differences in the interval time between injury and MR imaging, with a mean of 11.5 days postinjury in their study versus 22 days in our study.A few potential limitations of the current study should be considered. Operators other than radiologists, radiographers (a departmental assistant with no formal medical training), or gastroenterologists performed the biopsy in 20 cases; a nurse performed the biopsy in 11 cases, and interns in pediatric and renal medicine performed biopsy in the remainder of cases.Table 3 Primary Indication for Liver Biopsy from Original Request Form by Type of Lesion at ImagingTable 4 Preprocedural Aspects of BiopsyTable 5 Technical Aspects of Biopsy by Type of Lesion at ImagingA breakdown of initial liver biopsy results is provided in Table 6. BOLD signal compartmentalization based on the apparent diffusion coefficient. B, Disrupted DMN pattern is shown in the patient group. Crossref, Medline, Google Scholar27 Clark B, McKendrick M. In addition, relatively more invasive cancers were detected with digital mammography, but the difference was only significant for initial screening examinations (P < .001) (Table 3). Nat Rev Neurosci 2007;8(9):700–711. The effect of posttherapy 131I SPECT/CT on risk classification and management of patients with differentiated thyroid cancer. After multiplying different CTDIvol values by the same fsize, the corresponding SSDE would also vary.For a given patient size, the absolute variability of SSDE will not, in general, be the same as the variability of CTDIvol because fsize is a function of patient size. Link, Google Scholar32 Toms AP, Smith-Bateman C, Malcolm PN, Cahir J, Graves M. Eur Radiol 2006;16(2):365–373. Surg Clin North Am 2011;91(1):233–248. Combination of histogram enhancement and distribution parameters did not improve the ability to use each measure to independently predict whether a patient had papillary or clear cell subtype of RCC. Grading the severity of soft tissue changes associated with metal-on-metal hip replacements: reliability of an MR grading system. Teva Pharmaceutical,Industries, and Novartis Pharmaceuticals. Therefore, ADC ranges for nonmalignant lesions obtained in our study at b = 600 sec/mm^2 may not be the same as those obtained by using higher, lower, or multiple b values, and ADC threshold values should be interpreted with caution depending on the approach. Prognostic impact of histological subtype on surgically treated localized renal cell carcinoma. J Magn Reson Imaging 2011;34(3):539–546. SPECT/CT showed that 13 of 20 equivocal areas of uptake on whole-body scintigraphic images in 10 patients were uptake in metastatic LNs (three of them had 131I accumulation in each of two metastatic LNs simultaneously). Furthermore, change in signal intensity after contrast agent injection depends on the type, dose, and rate of gadolinium-based contrast agent injected. Randomized trial of screen-film versus full-field digital mammography with soft-copy reading in population-based screening program: follow-up and final results of Oslo II study. Clin Radiol 2008;63(8):888–894. Crossref, Medline, Google Scholar4 Kim RJ, Wu E, Rafael Aet al.. Blunt intestinal injury in children. AJR Am J Roentgenol 2010;194(6):1664–1673. There was no significant change in diagnostic accuracy with increasing size of lesion, number of needle passes, needle gauge, or needle type. C.B.C. No relevant conflicts of interest to disclose.Author ContributionsAuthor contributions: Guarantors of integrity of entire study, E.Y.C., S.S.; study concepts/study design or data acquisition or data analysis/interpretation, all authors; manuscript drafting or manuscript revision for important intellectual content, all authors; approval of final version of submitted manuscript, all authors; literature research, E.Y.C., J.R.V.H., S.S.; clinical studies, E.Y.C., J.L.M., J.R.V.H.; statistical analysis, S.S., T.W., A.G.; and manuscript editing, all authorsReferences1 Campbell P, Urban RM, Catelas I, Skipor AK, Schmalzried TP. P ≤ .05 was considered indicative of a statistically significant difference.During the study period, 1 198 493 screening examinations were performed, which consisted of 1 045 978 screen-film mammography examinations (87.3%) and 152 515 digital mammography examinations (12.7%). Comparing measures of sample skewness and kurtosis. The content of the packets was isoattenuated compared with the bowel content at low-dose CT in 16 (30%) of the 53 positive cases and as hyperattenuated in 37 (70%) cases. Healthy volunteers provided written informed consent. This was reflected in our study population, where screen-film mammography represented 87.3% of the cases. Overall, in a total of 21 radioactive foci in 17 patients, the interpretation of whole-body scintigraphic findings was altered in light of SPECT/CT findings (Table 1). The target was to place one device for each patient, unless an additional device was necessary for stent placement across the aneurysmal segment from normal artery to normal artery. Of these, 18 patients had bilateral hip replacements. The hypothesis is that two compartments exist: a slow moving compartment, where particles diffuse in a Brownian fashion as a consequence of thermal energy, and a fast moving compartment (the vascular compartment), where blood moves as a consequence of pressure gradient. CT was used in only 58 cases, transjugular biopsy was used in 68, and MR imaging was used in none. In FAST, the following spaces are evaluated with ultrasonography for the sole purpose of detecting hemorrhage: pericardium, hepatorenal fossa, left subphrenic space, right and left paracolic gutters, and pouch of Douglas (5,6). The frequency of radioiodine therapy might affect the uptake in the thyroid bed or metastatic LNs adjacent to the thyroid bed at both whole-body scintigraphy and SPECT/CT. Experiments were recorded by using software (VisiView; Visitron Systems, Munich, Germany). Means and standard deviations were also computed separately for AP and LAT. J Natl Cancer Inst 2005;97(10):748–754. Full-field digital versus screen-film mammography: comparative accuracy in concurrent screening cohorts. What mechanisms underlie diastolic dysfunction in heart failure? Spatially, we observed along the profile across the tumors that necrotic (no cells), hypoxic (pimonidazole staining), and normoxic (unstained cells) areas observed ex vivo correspond to three oxygenation levels significantly different from each other, with a mean of 12.9% ± 8.7, 42.1% ± 4.9, and 68.8% ± 4.9, respectively (P < .001) (Fig 2b). MR imaging parameters have been previously published (4) (Appendix E1 [online]).Intraarterial DSA was performed on single or biplane angiographic units with a transfemoral approach by using standard hospital-specific protocols. Link, Google Scholar12 Palmowski M, Schifferdecker I, Zwick Set al.. Diffusion maps were created by using in-house software that incorporates the ImageJ (National Institutes of Health, public domain) and JDTI (Daniel P. Crossref, Medline, Google Scholar54 Pereira FP, Martins G, Figueiredo Eet al.. Crossref, Medline, Google Scholar23 Hayter CL, Koff MF, Koch KF, Shah P, Su EP, Potter HG, eds. TNM classification of malignant tumours. In fact, of all the findings analyzed, only marrow edema and high-grade tendon tearing were associated with pain symptoms. Three patients with visually evident LGE had amyloidosis. 6, Abdominal radiograph deemed positive (level of confidence, 2). Crossref, Medline, Google Scholar75 Buck GC, Dalton ML, Neely WA. Eur J Nucl Med Mol Imaging. However, several studies showed very diverse responses of blood vessels to contrast media, depending on the investigated species and the vascular bed (5).In our study, isolated, perfused renal arterioles were investigated. Therefore, a total of four aneurysms (1%) in three patients (1%) were not interpretable at either intraarterial DSA or MR angiography (Table 2). Use of a flat 45° flip angle, reduced navigator efficiency, and cardiac motion artifacts are potential causes for reduction of signal-to-noise ratio and image quality in later TRAPD cine frames. Crossref, Medline, Google Scholar29 Manning AP, Thompson WG, Heaton KW, Morris AF. Int J Radiat Oncol Biol Phys 2010;76(5):1537–1545. Radiology 2007;244(2):381–388. sO_2 is known to decrease in tumors, as demonstrated with optical imaging techniques (3). Pain is included as a component of both hip scores, and presence of mechanical symptoms (including grinding, clicking, and other noise) is a component of the Hip Disability and Osteoarthritis Outcome Score. I.P. No relevant conflicts of interest to disclose.Author ContributionsAuthor contributions: Guarantor of integrity of entire study, I.P.; study concepts/study design or data acquisition or data analysis/interpretation, all authors; manuscript drafting or manuscript revision for important intellectual content, all authors; manuscript final version approval, all authors; literature research, R.S.L., D.C.A., I.P.; clinical studies, M.R.S., K.M., E.M.G., D.C.A., I.P.; experimental studies, P.M.R., I.P.; statistical analysis, R.S.L., A.D.P., D.C.A., I.P.; and manuscript editing, R.S.L., P.M.R., M.R.S., A.D.P., A.A.W., E.M.G., N.M.R., D.C.A., I.P.Supported in part through the Harvard Catalyst/The Harvard Clinical and Translational Science Center (NIH grant 1 UL1 RR 025758-01, principal investigator: I.P.).Funding: This research was supported by the National Institutes of Health (grant 1 UL1 RR 025758-01).References1 Jemal A, Siegel R, Ward E, Murray T, Xu J, Thun MJ. AJR Am J Roentgenol 1992;159(6):1217–1221. Traumatic diaphragmatic hernia. One control subject was excluded due to an incidental finding of brain lesions at MR imaging, and another two control subjects were excluded due to excessive movement. These included the following:Abdominal radiography.—For a field of 35 × 43 cm, the entrance doses delivered by abdominal radiography ranged from 6.0 mGy (66 kV and 50 mA) to 12 mGy (73 kV and 120 mA), with a mean dose of 9 mGy ± 3.0 (standard deviation). There was a significant negative correlation between AFP expression and OATP8 expression (P = .002, R = −0.22) (Fig E5c [online]). Crossref, Medline, Google Scholar48 Cunningham MA, Tyroch AH, Kaups KL, Davis JW. Diagnosis of blunt intestinal and mesenteric injury in the era of multidetector CT technology—are results better? Indirect signs of pancreatic injury include fluid in the peripancreatic fat or in the plane separating the pancreas from the splenic vein and thickening of the left anterior renal fascia. Crossref, Medline, Google Scholar7 Karhunen PJ, Suoranta H, Penttilä A, Pitkäranta P. (d) Frontal DSA image shows complete obliteration of the aneurysm (arrow) 6 months after treatment.Apart from major stroke or death, there were six other cases of periprocedural complications occurring in five patients (3.5%; five of 143; 95% CI: 1.3%, 8.4%). For the heaviest weight category (average, 113 kg ± 11), and SSDE agreed to within 7% (18.8/17.6) for the chest, 3% (24.9/24.1) for the abdomen, and 2% (24.4/25.0) for the pelvis CT protocols. Crossref, Medline, Google Scholar7 Tangcharoen T, Jahnke C, Koehler Uet al.. Link, Google Scholar85 Wong YC, Wang LJ, Lin BC, Chen CJ, Lim KE, Chen RJ. Studies in clear cell RCC have highlighted the connection between tumor angiogenesis and prognosis and its ability to metastasize (36,37). Of these, nearly half are hospitalized, and one in four undergoes surgery or other invasive intervention. Published 2007. Longitudinal studies are warranted to further evaluate whether the DMN can serve as a biomarker to monitor disease progression and recovery in MTBI.Advances in Knowledge• In patients with mild traumatic brain injury (MTBI), as compared with healthy control subjects, the integrity of default-mode network (DMN) functional connectivity was disrupted, as evidenced by significantly reduced connectivity in the posterior cingulate cortex and parietal regions and increased frontal connectivity around the medial prefrontal cortex (P < .01).• These opposed changes were significantly correlated with each other (r = −0.44, P = .03), suggesting that frontoposterior DMN nodes are not only intrinsically interdependent but also highly complementary and dynamically equilibratory in their functions after mild injury.• The reduced posterior connectivity correlated clinically with neurocognitive dysfunction (eg, cognitive flexibility), while the increased frontal connectivity correlated with posttraumatic symptoms (ie, depression, anxiety, fatigue, and postconcussion syndrome [PCS]).Implication for Patient Care• Our results of disrupted DMN synchrony and connectivity in MTBI suggest that resting-state functional MR imaging can be used as an additional clinical tool for detecting subtle brain injury that is not apparent with conventional MR imaging and for better understanding the underlying disease pathophysiology of PCS.Disclosures of Conflicts of Interest: Y.Z. No relevant conflicts of interest to disclose. Crossref, Medline, Google Scholar15 Karlsson M, Nordell B. Digital pictures were serially acquired from the digital movie of each experiment and were used to measure arteriolar luminal diameter, as described previously (17). Past research has validated the use of such inventories in the use of assessing individuals after minor head injuries (41).All data pre- and postprocessing were performed by an imaging scientist (Y.Z.) with 11 years of experience in functional MR imaging data analysis and interpretation.Preprocessing.—The three-dimensional magnetization-prepared rapid gradient-echo imaging data were first reoriented, skull stripped, and segmented into gray matter, white matter, and cerebrospinal fluid regions. Perforator infarction did not occur. G.K.C.W. No relevant conflicts of interest to disclose. A large hemoperitoneum does not mandate laparotomy (46). The amount of hemoperitoneum has been shown to predict the eventual success of nonsurgical management; patients with smaller degrees of hemoperitoneum have higher rates of successful nonsurgical management (60). Of five equivocal findings at whole-body scintigraphy, three were in the thyroid bed and two were in metastatic LNs at SPECT/CT. Detecting functional connectivity in the resting brain: a comparison between ICA and CCA. J Urol 2005;173(6):1853–1862. Crossref, Medline, Google Scholar45 Jin T, Kim SG. In vivo ADC measures are influenced by the degree and number of diffusion sensitizations (b values) applied during DW imaging (49–52). Assessment of multiparametric MRI in a human glioma model to monitor cytotoxic and anti-angiogenic drug effects. Only US assistance was used in a small number (n = 33) of focal lesion biopsies. Radiology 2007;244(3):708–717. Therefore, the increased contraction that we observed in afferent arterioles can be caused by reduced angiotensin II–induced nitric oxide release because of iodixanol. J Urol 2005;174(2):451–455; discussion 455. MGESE = multiple gradient-echo (GRE) and spin-echo (SE) imaging, MGE3D = multiple GRE three-dimensional (3D) imaging, MR_SO2 = MR estimate of sO_2, MSME = multiple SE two-dimensional, T2 = T2-weighted imaging, T2* after = T2* imaging after ultrasmall superparamagnetic iron oxide (USPIO) injection, T2* before = T2*-weighted imaging before ultrasmall superparamagnetic iron oxide injection.Experiments were performed at 4.7 T at a nuclear MR spectrometer console (Avance III; Bruker, Wissembourg, France) by using a volume coil for excitation and a surface coil for detection (B.L., R.S., A.B., C.M., C.R., and E.L.B., with 4, 7, 0, 0, 20, and 15 years of experience in MR imaging, respectively). AJR Am J Roentgenol 2001;176(2):289–296. Note in B and C that increase in f is predominantly in cortex and that f in cerebrospinal fluid decreases. J Neurosurg 2005;103(2):298–303. Approximate distribution of adrenal hemorrhage secondary to blunt trauma is the right adrenal in 75% of cases, the left adrenal in 15% and both adrenals in 10% (99). Similarly, our initial results showed that the 32-cm-diameter phantom was a good surrogate for CTDIvol values for patients weighing 113 kg; however, calculations for patients weighing more than 10 kg and 36 kg or less underestimated the SSDE calculation by approximately 50%, which implied that if CTDIvol were measured with a 16-cm PMMA phantom, the CTDIvol values would agree with these SSDE calculations. World Health Organization: tumours of the breast and female genital organs. Radiology 2007;244(2):494–504. One of the main reasons why the findings of whole-body scintigraphy were changed with addition of SPECT/CT findings at a lower rate in our study, compared with the data in other previous articles, is that all posttherapy patients were routinely imaged, not just those with equivocal findings at whole-body scintigraphy. Mean duration was not associated with pain (P = .2928) or mechanical (P = .2734) symptoms.MR imaging results are summarized in Table 3. In the L-NAME group, as well as in the iodixanol group, the diameter was decreased significantly, compared with the control group (P < .0001 for both comparisons). The Bland-Altman method was used to study systematic mean differences and 95% limits of agreements. Although our seed-based method did not show statistical significance between patients with MTBI and control subjects when we used the significance level of corrected P < .05, the direct visual inspection of seed-based results indeed revealed a similar pattern of differences as when ICA approaches were used. Crossref, Medline, Google Scholar9 Jung D, Hagenbuch B, Gresh L, Pontoglio M, Meier PJ, Kullak-Ublick GA. Link, Google Scholar22 Shanmuganathan K, Mirvis SE. Crossref, Medline, Google Scholar33 Messroghli DR, Greiser A, Fröhlich M, Dietz R, Schulz-

Menger J. It allows the reader to receive highlights without getting buried in verbose text and paragraphs. Crossref, Medline, Google Scholar5 Stattaus J, Kuehl H, Ladd Set al.. However, administering L-NAME and iodixanol together had an additive vasoconstrictor effect in comparison with iodixanol alone, and also adding iodixanol during L-NAME treatment enhanced vasoreactivity to angiotensin II compared with L-NAME alone, suggesting that the constriction caused by iodixanol is not simply caused by a lower nitric oxide bioavailability. Compared with SP1, MLO reclassified three lesions as having ADCs below the threshold (one hemangioma, one case of apocrine metaplasia, and the same case of focal fibrosis) and one lesion (a case of apocrine metaplasia) as having an ADC above the threshold.Previous studies (12,14,19,22–26,35) have shown promising differences in ADCs between malignant and nonmalignant breast lesions and improved diagnostic accuracy through a multivariate combination of ADC and dynamic contrast-enhanced MR imaging features (18,20,36,38). Therefore, the added value of DW imaging must be further studied in larger multicenter trials.The mean ADC for nonmalignant lesions was (1.77 ± 0.45) × 10−3 mm2/sec, which compares well with that in prior reports (18,20). Ann Surg 1995;221(6):744–753; discussion 753–755. Increasing TE results in signal loss in lung at TE of 1.5 msec (lower right), thereby giving an image impression similar to the conventional T2-weighted sequence. AJR Am J Roentgenol 2007;189(6):1421–1427. Although the vast majority of bowel injuries have associated abnormalities in the mesentery (Fig 6), the converse is not always true. J Bone Joint Surg Am 2005;87(7):1515–1521. A 1-mL test bolus was administered to determine TTP arterial enhancement of the aorta at the level of the renal artery. de Freitas RK, et al. In crushing injuries, massive forces crush the abdominal contents between the abdominal wall and the spine or bones of the chest wall. Acad Radiol 2008;15(7):867–872. Analysis of variance was used to evaluate size and perfusion differences between the different histologic subtypes of renal masses. Perfusion MR imaging with FAIR true FISP spin labeling in patients with and without renal artery stenosis: initial experience. Role of radiology in a national initiative to interdict drug smuggling: the Dutch experience. Google Scholar4 Hripcsak G, Austin JH, Alderson PO, Friedman C. RadioGraphics 2009;29(7):2033–2053. IVIM parameter maps were generated to demonstrate the voxel-by-voxel percentage variations under the various gases in comparison to those under ambient air.Normal data distribution was assumed and not tested owing to the low number of data. A.K.S.W. No relevant conflicts of interest to disclose. Without another diameter CTDI phantom to rely on for physical measurements, continued reliance on SSDE conversion factors is necessary to correct for the underestimation of patient dose with .For CTDIvol values in patients weighing more than 140 kg, the data demonstrate increasing differences between SSDE and CTDIvol when measured with either the 16- or the 32-cm-diameter phantom. Crossref, Medline, Google Scholar13 Ishii K, Yoshida Y, Akechi Yet al.. Most if not all of these diagnoses could have been made without the use of intravenous contrast material, but that a more focused examination for appendicitis (in terms of coverage) could conceivably have missed at least one of these.Figure 2c: Representative examples of alternative diagnoses made at abdominal multidetector CT in the setting of suspected appendicitis. We also analyzed the correlation among enhancement ratio and serum levels and immunohistochemical AFP and PIVKA-II expression for 79 HCCs.We compared the two groups for recurrence (including all local recurrence and intrahepatic and extrahepatic metastasis) and survival duration from the operation day. For example, oral and intravenous contrast media were used in 75.2% (1181 of 1571) and 87.3% (1372 of 1571) of cases, respectively, with no contrast material used in 121 (7.7%) cases. CT angiography or magnetic resonance (MR) angiography was used alternatively if digital subtraction angiography (DSA) was refused by the patient. Magnetic resonance imaging findings in painful metal-on-metal hips: a prospective study. The receiver operating characteristic curve associated with confidence in the analysis of abdominal radiographic findings considered as an ordinal eight-level variable showed good discrimination (Fig 4) because the area under the curve was 0.95. In the normal liver, OATP8 is expressed on the sinusoidal side of the hepatocyte membrane and takes up many intrinsic and extrinsic organic anions from blood into hepatocytes.On the other hand, Jung et al (9) showed that OATP8 was up-regulated by hepatocyte nuclear factor 1α. Crossref, Medline, Google Scholar35 Taouli B, Thakur RK, Mannelli Let al.. To assess the magnitude of association, the squared coefficients of determination (R2) were computed. Hepatocellular carcinoma may be low-grade or poorly differentiated, making diagnosis difficult outside of specialist centers.The study did have limitations. Crossref, Google Scholar11 Report Committee. In our study, the mobilization of the precuneus could be a sign of an inability of patients with MS to deactivate such a cerebral region during cognitive solicitations secondary to disease progression (as also supported by the correlation with NBV), which in turn might lead to an impairment of cognitive performances. Extent of left ventricular scar predicts outcomes in ischemic cardiomyopathy patients with significantly reduced systolic function: a delayed hyperenhancement cardiac magnetic resonance study. Then, a second-level (ie, a group-level) random-effect analysis was performed to assess comparisons among groups (24,25) (analysis of variance model). Crossref, Medline, Google Scholar2 Kalra MK, Maher MM, Toth TLet al.. Crossref, Medline, Google Scholar60 Christodoulou C, DeLuca J, Ricker JHet al.. The contralateral MR estimates of sO2 obtained in the present study are comparable to those reported by Christen et al (13) in healthy rats. Crossref, Medline, Google Scholar5 Berg WA, Gutierrez L, NessAiver MSet al.. Crossref, Medline, Google Scholar6 McKenney KL, Nuñez DB, McKenney MG, Asher J, Zelnick K, Shipshak D. Radiology 2002;222(3):604–614. However, for very small organs and organs only partially included in or located outside of the scan volume, SSDE will not provide a reasonable estimate of organ dose.In summary, use of an AEC system to adjust scanner output for patient size in CT examinations of the torso resulted in a linear relationship between patient size and scanner output. (d) Histogram of WL enhancement demonstrates “peaked” distribution with high kurtosis value of 3.73; this distribution was positively skewed (skewness, 1.94).Figure 2b Findings in a 60-year-old man with a renal lesion (arrow) in the left kidney shown to be pRCC at pathologic evaluation. However, the underlying pathophysiology of PCS is still poorly understood.In recent years, resting-state functional magnetic resonance (MR) imaging has enabled evaluation of critical brain networks on the basis of baseline energy expenditure in awake and resting states of the brain. Thus, T1 mapping provided an independent and noninvasive correlate of histologic fibrosis in this patient population.There has been limited foregoing data comparing quantitative T1 measurement methods with histopathologically demonstrated fibrosis, to our knowledge. One dual inversion-recovery image is acquired at the nominal blood-nulling inversion time (TI*) when blood magnetization is nulled. For each patient, AP and LAT dimensions at the mid-liver level were measured from axial CT images by using digital calipers on the scanner console. The pipeline embolization device for the intracranial treatment of aneurysms trial. Multiple sclerosis: effects of cognitive rehabilitation on structural and functional MR imaging measures—an explorative study. Bilateral hemorrhage occasionally manifests as adrenal insufficiency. Patzak, M.M.S.; study concepts/study design or data acquisition or data analysis/interpretation, all authors; manuscript drafting or manuscript revision for important intellectual content, all authors; approval of final version of submitted manuscript, all authors; literature research, all authors; experimental studies, Z.Z.L., V.U.V., P.B.P., A. 3rd ed. The estimated perfusion offset was averaged across lesions to estimate the contribution to perfusion from noise.In addition, another radiologist with 4 years of experience in body MR imaging (M.R.S.), who was blinded to the histopathologic and ASL results, analyzed the enhancement patterns of the renal masses on dynamic three-dimensional T1-weighted spoiled gradient-recalled images. Br J Sports Med 2002;36(1):6–10. Investigation of relationships between fMRI brain networks in the spectral domain using ICA and Granger causality reveals distinct differences between schizophrenia patients and healthy controls. Pathophysiology of contrast medium-induced nephropathy. Crossref, Medline, Google Scholar18 Poletti PA, Platon A, De Perrot Tet al.. Necrotic granulomatous pseudotumours in bilateral resurfacing hip arthoplasties: evidence for a type IV immune response. (a) Whole-body scintigraphic image shows radioactive foci in the left side of the neck (arrowhead) and the right buttock (arrow), which are considered to be neck LN and pelvic or femoral bone metastases, respectively. Artifacts, anatomical and physiological variants, and unrelated diseases that might cause false-positive whole-body 131-I scans in patients with thyroid cancer. Detection of drugs in the urine of body-packers. Metal ion levels after metal-on-metal proximal femoral replacements: a 30-year follow-up. Oral contrast material for evaluating patients is no longer administered at most large trauma centers in the setting of blunt trauma (25–27).An ideal trauma CT protocol would be one that maximizes detection of important abdominal injuries while at the same time minimizing patient risks. Small isolated mesenteric hematomas are not always an indication for immediate surgery and can be treated with observation alone. “Pseudopneumoperitoneum,” air confined between the abdominal wall and the parietal peritoneum, is another potential cause of a false-positive diagnosis of bowel rupture. Reliance on SSDE conversion factors to correct for the overestimation of patient dose with is necessary for patients weighing more than 140 kg. AJR Am J Roentgenol 1997;169(5):1275–1280. The Expanded Disability Status Scale score was higher in patients with SP MS versus patients with RR MS (P < .0001) and with benign MS (P < .0001). Delays in diagnosis as short as 8–12 hours increase the morbidity and mortality from peritonitis and sepsis (76). Link, Google Scholar51 Koh DM, Collins DJ. While the ADC threshold we used (1.81 × 10−3 mm2/sec) was determined for maximal sensitivity in a prior study (20), other investigators who used MR imaging with similar b values have suggested a lower ADC threshold of 1.6 × 10−3 mm2/sec (18,35) to optimize both sensitivity and specificity. While there was a greater frequency of reports with critical results containing documentation of communication after implementing the policy in 2005, it is unclear if this increase was directly related to policy implementation because the linear trend plot demonstrates a relatively continuous rise in documentation of communication rates beginning in 1997, many years before policy implementation. Am J Cardiol 2006;98(6A):27K–36K. Finally, angiotensin II (Sigma-Aldrich, St Louis, Mo), at 10−12 mol/L to 10−6 mol/L, was applied in the bath to construct concentration-response curves, with 2-minute intervals for each concentration. Crossref, Medline, Google Scholar29 Danias PG, McConnell MV, Khasgiwala VC, Chuang ML, Edelman RR, Manning WJ. J Rehabil Res Dev 2007;44(7):951–962. The perfusate was then exchanged either to contrast medium (iodixanol, GE Healthcare, Munich, Germany; ioxaglate, Guerbet, Sulzbach, Germany), at 23 mg of iodine per milliliter, or to vehicle solution (control group, DMEM), and treatment was performed for 20 minutes. An important component of the audit involved examination of all of the patients’ records to see if a subsequent and amended diagnosis was reached after the initial biopsy. Current trends in molecular classification of adult renal tumors. Arenson, MD, and Cathy Garzio, MBA, who are the chairman and administrative director, respectively, of the Department of Radiology and Biomedical Imaging, University of California, San Francisco, Calif. Diagnostic value of diffusion-weighted magnetic resonance imaging (DWI) compared to FDG PET/CT for whole-body breast cancer staging. The slope (−D) between b = 200 sec/mm2 and b = 1000 sec/mm2 were almost identical, but the slope (−D*) between b = 0 sec/mm2 and b = 200 sec/mm2 was decreased while volunteers inhaled 8% CO2. These data also demonstrate that the average SSDE for patients weighing between 100 and 140 kg correlates well (r = 0.999) with CTDIvol calculated with a 32-cm CTDI phantom (Fig 6b).Figure 7a: Comparison between patient and . Radiol Med (Torino) 2010;115(1):51–69. However, approximately 6%–15% of hypervascular HCCs demonstrate iso- or hyperintensity, which is uncommon among hepatic malignant tumors (5–8). There were two cases of major hemorrhagic stroke due to a large left parieto-occipital intracerebral hemorrhage (mRS = 5) and a large cerebellar hemorrhage (mRS = 6), which occurred in vascular territories independent from locations of instrumentation or PED placement for aneurysms in the right carotid siphon and left internal carotid artery, respectively. In one patient there were two lesions, one in either kidney, and hence 74 renal lesions were evaluated. Note that the positive interaction between the right cerebellum and the bilateral middle occipital gyrus (MOG) and left lingual gyrus in benign MS (BMS) is not shown.In healthy control subjects, a positive interaction was found between the right cerebellum and the bilateral MOG and left SPL. 2010;20(9):2067–2073. Diagnosis of chlamydia trachomatis genitourinary infections. It is likely that the ASR XL is a relatively high-wear prosthesis and that it leads to increased pseudotumor formation from reaction to high-wear particles (18,35).An unexpected finding was the high frequency of pseudotumor in our asymptomatic population, which was not significantly different with respect to prevalence or size compared with the symptomatic population. Improvements in the certainty of parameter estimates should be pursued. The performance of the ADC threshold was also compared within each clinical indication and age group by using the χ2 test. Link, Google Scholar17 Martirosian P, Boss A, Fenchel Met al.. Patients with SP MS had a longer RT than did patients with RR MS (P = .004) and with benign MS (P = .02).Table 1 Main Demographic, Clinical, Radiologic and Behavioral Characteristics of Healthy Control Subjects and Patients with MSFigure 1 shows the patterns of brain activations in each group during the interference condition. Longitudinal imaging of such changes could be applied to individualization of therapy by assessing treatment response in a given patient, and to the evaluation of prospective therapies for heart failure.We observed significant relationships of similar magnitude between both myocardial fibrosis and T1 time with cardiac structure and function. The advantage of the local cross-correlation cost function is that it allows for correlations to be established over images of different MR modalities or varying contrast enhancement. Discrepancy was settled by using consensus.PED placement was the sole intervention without coils in most cases. (b) Contrast-enhanced image obtained in the excretory phase shows that tumor has low levels of enhancement compared with renal parenchyma. Although our study did not explicitly determine diagnostic quality, on the basis of a decade of clinical experience with the AEC used in this study, we assumed that the criterion of acceptable diagnostic performance in different patient sizes was met. J Digit Imaging. Additional imaging findings that have been found to be useful in guiding clinical management decisions include (a) extension of the injury to involve the major hepatic veins, which usually requires surgery to control ongoing hemorrhage; (b) the presence of active bleeding into the peritoneal cavity, which can usually be treated with endovascular intervention (65); and (c) the presence of a large hemoperitoneum (71).The growing trend toward nonsurgical management of hepatic injuries has increased the relevance and frequency of delayed complications such as bile leaks, biliary strictures, hepatic abscess, delayed hemorrhage, and other vascular complications. The associations in the different study subgroups are summarized in Table 3.In agreement with the results of previous studies (4,6,7,9), patients with MS in our current study demonstrated different recruitment of several brain areas as compared with healthy control subjects. For this reason, bedside radiographs of the chest and pelvis are usually included in the initial set of tests performed in polytrauma patients, shortly after arrival at the hospital. Crossref, Medline, Google Scholar84 Gupta A, Stuhlfaut JW, Fleming KW, Lucey BC, Soto JA. This also implies that the lack of a specific diagnosis at CT largely excludes important conditions that may require immediate invasive therapy.In addition to helping direct management when alternate diagnoses are discovered, the use of CT in these cases facilitates avoidance of invasive interventions when they are not needed. Eur Radiol 2010;20(7):1657–1666. The key change is for the standard error of the slope and intercept, which influence the CIs. For the fit of SSDE as a function of AP+LAT, when heteroscedasticity was appropriately accounted for, the 95% CI of the slope was −0.020 to 0.069 mGy/cm, which was slightly larger than if heteroscedasticity were ignored (95% CI: −0.014, 0.063 mGy/cm). Given the role of the spleen in immune function and the potential for overwhelming infection after splenectomy (53), splenic preservation after trauma is the current standard of care. Crossref, Medline, Google Scholar35 Ei Khouli RH, Jacobs MA, Mezban SDet al.. We previously reported about the assessment of the occlusion status at MR angiography versus intraarterial DSA of this patient population (4).MR angiography consisted of three-dimensional unenhanced time-of-flight, as well as contrast material–enhanced, images by using gradient-echo techniques. Acta Orthop Belg 2009;75(4):477–483. Incidence and prognostic implication of unrecognized myocardial scar characterized by cardiac magnetic resonance in diabetic patients without clinical evidence of myocardial infarction. A receiver operating characteristic curve was obtained. Once the patient size is determined, fsize can be found from the appropriate table in the AAPM Report 204 or computed from a mathematical equation (16).The purpose of this retrospective study was to determine the relationships among patient size, scanner radiation output, and SSDE for adults who underwent CT of the torso at our institution.This institutional review board–approved, retrospective study was performed by using routine CT examinations of the torso performed in adults for clinical indications with patient waiver of informed consent. Radiology (in press) Google Scholar10 Haynes AB, Weiser TG, Berry WRet al.. Age-related changes in the default mode network are more advanced in Alzheimer disease. Crossref, Medline, Google Scholar13 Greicius MD, Supekar K, Menon V, Dougherty RF. Proc Natl Acad Sci U S A 1988;85(24):9533–9537. For single-participant ICA, one- and two-sample t tests were implemented by applying SPM8 software (Statistical Parametric Mapping, to the z image of the DMN made up of ICA components from the two participant groups to generate statistical maps. J Magn Reson Imaging 2009;30(4):778–784. A university hospital experience. J Urol 2007;178(4 Pt 1):1184–1188; discussion 1188. Mice received ventilation at a respiratory rate of 120 breaths per minute and anesthesia was maintained by ventilation with a positive end-expiratory pressure of 0.1 mbar (0.01 kPa) and a maximum inspiratory pressure of 10 mbar (1 kPa). The diaphragm was cut along the ventral costal attachment toward the spine, and the thoracic cavity was exposed by retracting both sides of the chest wall laterally. Searching for a baseline: functional imaging and the resting human brain. For this reason, the robust variance estimator, which is designed to account for nonuniform variance, was used to fit SSDE as a function of size. J Neurosurg 1971;34(3):310–323. Diagnostic accuracy and short-term surgical outcomes in cases of suspected acute appendicitis. The sample of screen-film mammography cases was appropriately weighted by initial and subsequent examinations. These patients had APs of 32.6 cm ± 1.3, LATs of 39.1 cm ± 1.6, AP+LATs of 71.7 cm ± 0.4, effective diameter of 35.7 cm ± 0.1; and equivalent CTDIvol and SSDE values (20.1 mGy ± 3.2).Descriptive Statistics for Patients, CT Scanner Output, and SSDENo significant deviations from regression assumptions were observed when modeling CTDIvol as the dependent variable. I highly recommend this fine book to those interested in academic radiology careers.Reviewed by Robert D. Financial activities not related to the present article: author and/or institution received consultancy fees from Bayer-Schering Pharma, Sanofi-Aventis, Biogen-Idec, UCB, Merck-Serono, Novartis, Roche, Synthon BV, Jansen Research, and Lundbeck; author received honoraria for consultancy; author received payment from Serono Symposia Foundation. Although the graded response indicates sensitivity to cerebral perfusion, the high intrasubject standard deviations, which were of more than 100% of the mean, could be due to the limited precision of the method, but could also be explained by the physiologic heterogeneity of the brain.Interestingly, in the smaller ROIs in various brain regions, the variability increases significantly for f, D*, and fD*, but not for D, in comparison with the full-brain results. Crossref, Medline, Google Scholar72 Fleming KW, Lucey BC, Soto JA, Oates ME. More recently, the incorporation of CT into the early resuscitative efforts by installing scanners inside modern trauma bays, where patients are assessed initially and triaged, has been proposed (14).Shortly after its introduction into clinical practice nearly 3 decades ago, CT redefined our understanding of the appearance and importance of abdominal organ injuries (15). Hepatocellular carcinoma: signal intensity at gadoxetic acid-enhanced MR Imaging—correlation with molecular transporters and histopathologic features. When CTDIvol was the dependent variable, a model consisting of only patient size had a slope of 0.34 mGy/cm (95% CI: 0.31, 0.37 mGy/cm; P < .001) and explained 48% of the variation in CTDIvol (R2 = 0.48). (a) Coronal reformation of portal venous phase CT images shows grade IV renal injury with multiple large renal lacerations (arrow). When the screening of body packers was based on abdominal radiography alone, our results showed that the optimal ratio for sensitivity (0.85) and specificity (0.94) was obtained by considering a negative abdominal radiograph with a lower level of confidence (1 of 4) as a positive result (cutoff point). In the setting of myocardial scar due to infarction, the inversion-recovery cardiac MR technique allows visual identification of the extent of myocardial scar compared with normal myocardium. (c) At immunohistochemical evaluation (magnification, ×200), tumor shows intense expression of OATP8 but (d) no definite expression of either AFP or (e) PIVKA-II.Figure 2e: HCC in a 65-year-old man shows hyperintensity in hepatobiliary phase of gadoxetic acid–enhanced MR images (serum AFP level, 23 ng/mL [23 μg/L]; AFP-L3, 5.8%; and PIVKA-II 30, mAU/mL) (a) On hepatobiliary phase image, almost entire 30-mm tumor (arrow) showed higher SI than that of background liver (tumor SI/background SI = 1.09). Ann Surg 1993;218(6):783–790. Thus, for instance, a delayed series should be limited to patients with abnormalities seen on the portal venous phase images. Postcontrast myocardial T1 time in heart failure patients ranged from 220 to 560 msec (mean, 351 msec ± 76). Two additional categories (for a total of 11) were used to sort patients weighing between 55 and 100 kg (n = 17) and those weighing more than 100 kg (n = 20). The following results were provided by the program: For women, dose-length product was 84 mGy · cm ± 10.5 and effective dose was 1.7 mSv ± 0.2; for men, dose-length product was 84 mGy · cm ± 10.5 and effective dose was 1.2 mSv ± 0.1.Abdominal radiographic findings were compared with results of low-dose CT (used as reference standard) to estimate sensitivity, specificity, and positive and negative predictive values for depiction of foreign bodies. Quantitative diffusion-weighted MR imaging in the differential diagnosis of breast lesion. A negative interaction was found between the right cerebellum and the left IFG (Brodmann area 45).Compared with patients with RR MS, healthy control subjects had a higher interaction between the right cerebellum and left SPL (MNI coordinates: −26, −72, 56 mm) and right MFG (MNI coordinates: 36, 40, 40 mm) (Fig 3).Figure 3: Color-coded statistical maps overlaid on single-subject T1-weighted statistical parametric mapping software (SPM8) templates show areas with significant differences of functional interactions (color-coded with red to yellow t values [t test]) during the Stroop interference condition of the right cerebellum with other brain areas among the different study groups (analysis of variance; P < .05, corrected at a cluster level). By using a third quartile enhancement cutoff value of greater than 100, diagnosis of ccRCC could be made with sensitivity and specificity of 96.4% and 89.5%, respectively (Table 3).Table 2 Quantitative WL Enhancement Histogram Parameters in ccRCC and pRCCTable 3 Receiver Operating Characteristic Analysis of WL Enhancement Histogram Parameters in Discriminating ccRCC from pRCCThe WL enhancement histogram distribution parameter kurtosis was significantly lower in ccRCC compared with pRCC (0.46 ± 1.37 vs 7.42 ± 5.96; P < .0001) (Table 2, Figs 1c and 2d). Data from some centers were incomplete due to a slight delay in sending out the coagulation questionnaires and due to our encouragement to submit cases with severe complications even if notes were unavailable (however, in such cases, we asked for alternative data sources to be interrogated); this may have resulted in incomplete data in some areas in some cases. Whether treatment with flow diverters is reliable for this vasculopathy remains unknown at the moment. Monitoring blood-brain barrier status in a rat model of glioma receiving therapy: dual injection of low-molecular-weight and macromolecular MR contrast media. Despite that these areas are expected to be active during the Stroop task, this latter finding suggests that such an overrecruitment seen in patients with MS might represent a maladaptive mechanism that contributes to the severity of the clinical manifestations. Cases 3 and 4 subjects with CAD risk factors and short cardiac cycles in whom it was impossible to acquire the fifth frames. The patients were imaged by using the GE Color Coding for Kids weight-based CT scanning categories: 6.0–7.5 kg (n = 4), 7.5–9.5 kg (n = 13), 9.5–11.5 kg (n = 13), 11.5–14.5 kg (n = 19), 14.5–18.5 kg (n = 23), 18.5–22.5 kg (n = 18), 22.5–31.5 kg (n = 22), 31.5–40.5 kg (n = 15), and 40.5–55.0 kg (n = 22). J Magn Reson Imaging 2007;26(4):838–847. The impact of O2 availability on human cancer. The percentage of cases with adequate-quality images increased from 76% with the traditional single-frame method to 95% with five consecutive frames. J Bone Joint Surg Am 2008;90(9):1988–1993. Furthermore, the majority of the aneurysms were located at the internal carotid artery and were small. SPECT/CT showed that 31 of the 32 foci positive for uptake were metastases to the extrathyroidal organs, such as lungs and bones. The change in the interpretations of foci from whole-body scintigraphic to SPECT/CT images was analyzed in the thyroid bed, LN, and distant metastases. Link, Google Scholar36 Kul S, Cansu A, Alhan E, Dinc H, Gunes G, Reis A. Radiology records for all patients receiving emergency department or urgent care were electronically searched for those who underwent nonfocused abdominopelvic CT and whose study indication contained the terms appendicitis, right-lower quadrant pain, or appendix. The figure shows that for diagnostic accuracy, all departments lie within the control limits, exhibiting common cause variation. Many analyses were performed, so all P values should be considered descriptive. Data acquisition was conducted between February 2009 and March 2009, and data processing occurred between May 2009 and March 2011.The 9L gliosarcoma cells (15) were implanted in the brains of 48 male Fisher 344 rats (Charles River Laboratories, L’Arbresle, France) weighing 120–150 g, as previously described (16), by three authors (B.L., R.S., and A.B., with 4, 8, and 1 year of experience in tumor models). Images of each sequence type were assessed regarding discrimination of thoracic wall, lung, heart, presence of pneumothoraces or effusion, and pulmonary infiltration. Crossref, Medline, Google Scholar24 Loupatatzis C, Schindera S, Gralla Jet al.. Eur Radiol 2012;22(2):484–492. Link, Google Scholar5 Dreyer KJ, Kalra MK, Maher MMet al.. This could be due to low signal-to-noise ratio, slight motion during the acquisition, partial volume effects with cerebrospinal fluid, or could reflect true physiologic variability. Apparent diffusion coefficients of breast tumors: clinical application. All ASL acquisitions were prescribed following directions of a radiologist (I.P.) who selected the best imaging plane based on the anatomic location of the mass. Survival and death causes in differentiated thyroid carcinoma. Rev Sci Instrum 2009;80(7):074301. Briefly, one measures T2* before, or T2*before, and 1 minute after, or T2*after, the injection of ultrasmall superparamagnetic iron oxide. Interestingly, US guidance rather than assistance was used in the majority (n = 1665) of cases in which no focal lesion was present. Crossref, Medline, Google Scholar19 Mahrholdt H, Wagner A, Judd RM, Sechtem U, Kim RJ. Myocardial magnetic resonance imaging contrast agent concentrations after reversible and irreversible ischemic injury. Crossref, Medline, Google Scholar7 McGee MC, Hamner JB, Williams RFet al.. Data for absorbed dose in the center of the scan region were normalized to CTDIvol, combined among the four research groups, and fit to an exponential relationship as a function of size. Report of AAPM Task Group 204. These parameters were indexed to adjust for patient size by dividing by body surface area.T1 values were derived from postcontrast Look-Locker inversion-recovery sequences by using a balanced steady-state free-precession sequence over two R-R intervals with 30–45 phases acquired. Neuroradiology 2003;45(9):592–597. It is unlikely, however, that this had any effect on the distribution of detected cancer subtypes. J Comput Assist Tomogr 2009;33(1):1–7. Differentiation of subtypes of renal cell carcinoma on helical CT scans. First, whole-body scintigraphy was performed by using a dual-head gamma camera (Symbia T6; Siemens Healthcare, Malvern, Pa). The results of our study on these study parameters were all favorable. Staging data were recorded according to the TNM classification system developed by the International Union against Cancer (25). College Park, Md: American Association of Physicists in Medicine, 2008. Among these patients, the most common disease entities included conditions that generally lack specific findings at CT (eg, nonspecific infectious or inflammatory gastrointestinal conditions, constipation, irritable bowel syndrome, uncomplicated urinary tract infection, and pelvic inflammatory disease). The pilot studies were part of the national screening program in which all women aged 50–75 years receive a personal invitation to participate in screening every 2 years. Crossref, Medline, Google Scholar64 Jones DT, Machulda MM, Vemuri Pet al.. Phase-sensitive black-blood coronary vessel wall imaging. The Rao’s Brief Repeatable Battery and Stroop test: normative values with age, education and gender corrections in an Italian population. CT is superior to clinical evaluation and diagnostic peritoneal lavage for diagnosing important abdominal injuries (12,13). Brain 2006;129(Pt 3):747–753. Therefore, detailed pathology data had to be extracted from reports obtained from the individual pathology laboratories. Crossref, Medline, Google Scholar16 Amano Y, Takayama M, Kumita S. This situation would result in patient selection bias.Our study had a number of limitations. Neurology 2008;70(10):771–778. These posttraumatic symptoms, referred to as postconcussion syndrome (PCS), manifest as a history of traumatic brain injury along with the presence of three or more common symptoms (ie, headache, dizziness, fatigue, irritability, insomnia, poor concentration, memory difficulty, or an intolerance of stress, emotion, or alcohol) that have lasted at least 3 months (6), as well as evidence of deficits in attention and memory (7). Vessel size imaging. Persons who declined to participate in the study, those younger than 18 years of age, and pregnant women were excluded from the study. Incidence of mild and moderate brain injury in the United States, 1991. CTDI is not a metric of patient-specific dose but a measurement of machine output. World J Emerg Surg. Link, Google Scholar3 Ichikawa T, Saito K, Yoshioka Net al.. The detection of DCIS on the basis of microcalcifications tended to be better as well.With digital mammography, in both initial and subsequent examinations, significantly more DCIS was detected (P = .002 and P < .001, respectively). The mean signal intensity in the whole tumor and the mean signal intensity in an ROI outside the body, in an area without apparent ghosting artifacts, were measured on the difference ASL images. (a) Coronal T1-weighted and (b) coronal short inversion time inversion-recovery MR images show pseudotumor (arrow) with wall thickening more apparent on a and large solid component inferiorly with minimal surrounding soft-tissue edema (arrowhead).Figure 5b: Images in a 65-year-old asymptomatic man after metal-on-metal total hip arthroplasty. Crossref, Medline, Google Scholar25 Bogusz MJ, Althoff H, Erkens M, Maier RD, Hofmann R. However, acquiring images at only the blood signal nulling time makes it difficult to maintain section-vessel orthogonality, as this condition is highly sensitive to any cardiac rhythm variation or unaccounted for bulk displacement. An information-maximization approach to blind separation and blind deconvolution. Therefore, modifications of cerebellar connectivity in cognitively impaired patients needs to be investigated. Sonography as the primary screening technique for blunt abdominal trauma: experience with 899 patients. All MR experiments were performed with the rats anesthetized with the following: 5% isoflurane for induction and 2% for maintenance in air. Washington, DC: National Academies Press; 1999. Perfusion levels in papillary RCCs were significantly lower than those for all other RCC subtypes. Blunt bowel and mesenteric injuries: the role of screening computed tomography. MR imaging was performed with fat-suppressed two-dimensional or three-dimensional gradient-echo T1-weighted sequences (repetition time, 3.2–4.0 msec; echo time, 1.6–2.3 msec; flip angle, 10–15 degrees; field of view, 33–42 cm; matrix, 128–192 interpolated to 256–512; section thickness, 4.0–8.0 mm). AJNR Am J Neuroradiol 2008;29(4):688–693. Effect of patient size on radiation dose for abdominal MDCT with automatic tube current modulation: phantom study. The worst performance during the task in patients with SP MS could contribute explaining the observed differences in patients with RR MS. Crossref, Medline, Google Scholar9 Ekeh AP, Saxe J, Walusimbi Met al.. If a greater range of patient sizes were studied (eg, from children to large adults), the influence of heteroscedasticity would correspondingly increase.The purpose of this study was not to evaluate the SSDE metric, which has already been validated by the data reported in AAPM Report 204. Independent component analysis using an extended infomax algorithm for mixed subgaussian and supergaussian sources. Crossref, Medline, Google Scholar30 Duffy SW, Tabar L, Olsen AHet al.. Alterations of the blood-brain barrier status have an effect on brain edema and on drug delivery and should thus be characterized in addition to BVf and MR estimates of sO2.Practical applications: The findings of this study suggest that the MR estimate of sO2 is a reproducible method that could be used as an in vivo probe of hypoxia in brain tumors and as a sensitive reporter of the hypoxic effects of antiangiogenic therapies. Crossref, Medline, Google Scholar11 Kim WY, Stuber M, Kissinger KV, Andersen NT, Manning WJ, Botnar RM. Diffusion-weighted imaging of mucinous carcinoma of the breast: evaluation of apparent diffusion coefficient and signal intensity in correlation with histologic findings. Thalamic resting-state functional networks: disruption in patients with mild traumatic brain injury. M.F. Financial activities related to the present article: none to disclose. Crossref, Medline, Google Scholar12 Takahashi M, Togao O, Obara Met al.. There were four false-negative findings among the 1200 patients in whom appendicitis was not diagnosed at CT. Beyond perfusion, the IVIM method is dependent on the capillary microarchitecture (51), a property that could prove useful, for example, in the study of tumor neoangiogenesis, where the capillary bed structure could differ significantly from the norm.In conclusion, the results of this study show that IVIM can measure perfusion quantitatively in the human brain. Link, Google Scholar10 Kuhl C. Other technical problems such as misregistration between pre- and postcontrast acquisitions and difficulty with appropriate ROI placement on a precontrast image for T1-isointense tumors can also lower interobserver agreement. Mechanism of the abnormal vitamin K-dependent gamma-carboxylation process in human hepatocellular carcinomas. Per group, the 20 remaining rats, called single-time subgroup, were imaged once and then euthanized at the end of the imaging session for ex vivo studies (four animals per time). In addition, a high-activity (1.4–9.77 GBq) posttherapy scan could yield a higher detection rate of radioactive foci than a low-activity (37–185 MBq) diagnostic 131I scintigraphic scan. Furthermore, findings at CT in the setting of suspected acute appendicitis in adults appear to positively affect management in cases in which an alternative diagnosis is made. Link, Google Scholar67 Mirvis SE, Whitley NO, Vainwright JR, Gens DR. Conversely, approximately one-fourth of recalled masses only or microcalcifications only were true positive (24.6% and 23.3%, respectively).The detection of invasive carcinoma based on masses associated with microcalcifications was significantly better with digital mammography than with screen-film mammography (P = .047). Gastroenterol Hepatol 2009;24(suppl 2):A294–A295. Specifically, we used axial T1-weighted images to grade the gluteus minimus and gluteus medius as follows: Grade 0 indicated that no intramuscular fat was present; grade 1, that some fat streaks were present; grade 2, that fat was evident but there was less fat than muscle tissue; grade 3, that there were equal amounts of fat and muscle tissue; and grade 4, that there was more fat than muscle.Finally, on the basis of consensus imaging findings, a previously published MR grading scale for use with metal-on-metal hip replacements (22) was independently used by the two readers (Table 2). However, full active distention of the bladder through a Foley catheter is still required.Figure 2: CT cystography in a 52-year-old man who was in a motorcycle accident. Increased gadolinium concentration causes T1 shortening and high signal intensity on T1-weighted images relative to areas of normal myocardium. Cholinergic agonism alters cognitive processing and enhances brain functional connectivity in patients with multiple sclerosis. Our results may not be generalizable to patients with cardiomyopathies that result in rapid progression of myocardial injury, such as fulminant myocarditis, that were not represented in this population. Because well-differentiated thyroid carcinoma is a slow-growing neoplasm, a long follow-up period is needed to make a more accurate clinical diagnosis. All images were registered to the image with a b value of 0. As a result, we expected that PIVKA-II expression and OATP8 expression might be correlated.However, there were many patients that showed low AFP and PIVKA-II expression in hypointense HCCs. We attribute this to the fact that OATP8, AFP, and PIVKA-II have several direct and indirect regulatory mechanisms other than the hepatocyte nuclear factor route (21). Because of these reasons, a pretherapeutic diagnostic scan is not routinely performed at our institute. Increased MPFC activation has been reported previously in moderate and severe traumatic brain injury (60) and is hypothesized to represent brain neuroplasticity operating in recovery and neural repair after injury (61). These hepatocyte nuclear factors are indispensable transcription factors that relate to primitive embryonal differentiation of hepatocytes and to hepatocarcinogenesis. Crossref, Medline, Google Scholar36 Bonavita S, Gallo A, Sacco Ret al.. Ann Surg 1984;200(5):567–575. These low-dose CT protocols have been reported to be accurate in screening for well-defined medical conditions, such as renal colic (12) and appendicitis (13–15). The κ coefficient was calculated to assess interreader agreement.An exact Mann-Whitney test was used to compare lesion subtypes (ccRCC and pRCC) with respect to quantitative measures. Crossref, Medline, Google Scholar31 Taub E, Cuevas JL, Cook EW, Crowell M, Whitehead WE. The most common clinical diagnoses among these patients included infectious or inflammatory gastroenteritis, colitis, or adenitis (26 of 122, 21.3%); constipation (15 of 122, 12.3%); irritable bowel syndrome (12 of 122, 9.8%); urinary tract infection (10 of 122, 8.2%); pelvic inflammatory disease (eight of 122, 6.6%); cholecystitis (six of 122, 4.9%); pancreatitis (five of 122, 4.1%); and musculoskeletal pain (five of 122, 4.1%). Before study initiation, all were accustomed to reading abdominal radiographs for the screening of drug packets; they were also familiar with interpreting findings at abdominal low-dose CT because this test is routinely used in our institution (12,14,18). The CT scan parameters were 130 keV, 30 mAs or less (due to the minimization of radiation exposure), a 512 × 512 matrix, a 2 × 2.5-mm collimation, and a 5-mm section thickness.Whole-body scintigraphic and SPECT images were reviewed by two nuclear medicine physicians (Y.M., with 6 years of experience, and K.A., with 20 years of experience) in consensus. In our study, the mean number of included voxels was 310 ± 163 (after excluding a mean of 0.8% ± 1.1 of voxels) and 910 ± 988 (after excluding a mean of 6.4% ± 7.5 of voxels) for the contralateral striatum and the tumor ROI, respectively (mean ± SD across all times and both groups).Correlation between MR imaging findings and histologic findings.—Each pimonidazole slice was digitized with a 1200-dot-per-inch resolution by using a photo scanner (Perfection 4870; Epson, Long Beach, Calif) with backlighting, and image analyses were performed by using ImageJ software (. Continued intraabdominal hemorrhage in the setting of a compromised hemodynamic status, despite aggressive resuscitation efforts, is usually an indication for emergent surgery. In the iodixanol group, afferent arteriolar diameter was decreased significantly, compared with the control group (P = .008).Afferent arterioles perfused with iodixanol showed a significantly stronger response to angiotensin II compared with the control group (median constriction at angiotensin II concentration at 10−6 mol/L, 43.6% [25th and 75th percentiles, 31.4% and 63.1%, respectively] vs 74.9% [25th and 75th percentiles, 67.0% and 88.3%, respectively]; P = .03) (Fig 4). Lateral patient dimensions were measured on the AP CT radiograph (Fig 1b), and AP dimensions were measured on the lateral projection of the CT radiograph (Fig 1c). Crossref, Medline, Google Scholar8 Agid R, Willinsky RA, Lee SK, Terbrugge KG, Farb RI. The remainder of the CT study showed no evidence of solid or hollow visceral organ injury. Crossref, Google Scholar45 Rombouts SA, Barkhof F, Hoogenraad FG, Sprenger M, Valk J, Scheltens P. R.I.P. No relevant conflicts of interest to disclose.Author ContributionsAuthor contributions: Guarantor of integrity of entire study, K.Z.A., study concepts/study design or data acquisition or data analysis/interpretation, all authors; manuscript drafting or manuscript revision for important intellectual content, all authors; approval of final version of submitted manuscript, all authors; literature research, K.Z.A..; clinical studies, all authors; experimental studies, K.Z.A., A.M.G.; statistical analysis, K.Z.A., A.M.G.; and manuscript editing, all authorsFunding: The authors are employees of the National Institutes of Health.References1 Botnar RM, Stuber M, Kissinger KV, Kim WY, Spuentrup E, Manning WJ. BI-RADS: magnetic resonance imaging. NMR Biomed 2011;24(5):473–482. For each participant, we acquired images of nine axial brain sections with the following parameters: section thickness, 4 mm; field of view, 297 × 297 mm2; matrix, 256 × 256, in-plane resolution, 1.2 × 1.2 mm2; repetition time/echo time, 4000/99 msec; parallel imaging with an acceleration factor of two; and 75% partial Fourier encoding. Crossref, Medline, Google Scholar103 Murray JG, Caoili E, Gruden JF, Evans SJ, Halvorsen RA, Mackersie RC. Diagnostic accuracy of computed tomography–guided percutaneous biopsy of renal masses. 10th ed. N Engl J Med 2000;343(20):1445–1453. Reactive oxygen species and the pathogenesis of radiocontrast-induced nephropathy. The site of the strongest response of the arteriole was chosen for analysis of the diameter (Fig 2). K.Y.P. No relevant conflicts of interest to disclose. Additionally, 28 (11%) of 253 lesions that had been imaged with DW imaging were excluded from the study because of misregistration within the DW imaging sequence owing to patient motion and/or eddy current–based distortions. This included algorithms for acute appendicitis, acute cholecystitis, ectopic pregnancy, unexplained free-intraperitoneal air, tension or new or increasing large pneumothorax, acute pulmonary embolism, acute scrotal torsion, and malpositioned endotracheal and enteric tubes, the accuracies of which are denoted in Table 1 (7). The amount of radiation a CT scanner delivers during an examination (ie, the radiation output) can be quantified by using the volume CT dose index (CTDIvol), which allows measurement of the dose in an acrylic cylinder for a very specific set of conditions (7–10). Subjects with CAD risk factors were significantly older than healthy subjects (P < .001), while there was no significant difference in age between men and women with CAD risk factors (P = .7).All data sets except two had at least one time frame image with good or higher-quality scores. The test characteristics and cost-effectiveness of MR angiography compared with those of intraarterial DSA are good (4,5), but more insight in the subsequent image-based additional treatment decisions is desirable before MR angiography is implemented as a standard follow-up imaging technique.We investigated whether therapeutic decision making can be solely based on MR angiographic findings by comparing treatment decisions based on findings of MR angiography and intraarterial DSA in the follow-up of patients with coil-treated aneurysms who were examined by using both imaging techniques.The institutional review boards of the participating centers approved this study. Conventional respiratory triggering with one excitation per respiratory cycle results in a strong increase of the acquisition time of the very short TE sequence. Heart 2003;89(10):1255–1256. Pixels in color were included in the mean myocardial T1 time reported. J Hepatol 2004;40(2):212–218. Crossref, Medline, Google Scholar102 Desser TS, Edwards B, Hunt S, Rosenberg J, Purtill MA, Jeffrey RB. Overall, degree of hemorrhage and increase in size over the three phases of image acquisition are indicative of a large arterial bleed. Crossref, Medline, Google Scholar6 Höckel M, Vaupel P. Specific written informed consent for this study was not required.In anticipation of the nationwide transition from conventional to digital mammography in the Dutch screening program, three pilot studies were set up in 2003–2004 to test the quality of digital screening and the organizational consequences of implementation.The results of one of these pilot studies have been used to analyze the screening performance of digital mammography and led to previous publications (10,21). Google Scholar7 American Psychiatric Association. Imaging of genitourinary trauma. N Engl J Med 2001;344(7):495–500. Mean ADCs were also compared between specific nonmalignant lesion subtypes by using the same method. (a) Axial contrast-enhanced image shows herniation of stomach (arrow) into the thoracic cavity secondary to traumatically induced diaphragmatic injury. The T1 values of pixels with χ2 goodness-of-fit with level of significance α ≤ 0.05 were averaged for a final mean postcontrast T1 value to reduce noise and to reduce partial volume effects at myocardial borders.Use of this Look-Locker sequence and T1 measurement method in a four-chamber view has previously been demonstrated to have excellent intrasequence agreement with short-axis views and other cardiac MR T1 mapping sequences (18).Data are presented as mean ± standard deviation or median with interquartile range, as appropriate. Error bars = 1 SD.Figure 4d: (a–d) Representative T2-weighted (T2w) images, BVf, and MR estimate of sO2(MR_SO2) maps and the corresponding pimonidazole (Pimo) staining presented as function of time for the untreated (a) and the treated (b) groups. We compared the original ADC measurements by S.P. (SP1) with repeat measurements by S.P. (SP2) and with measurements by M.L.O. (MLO) (with 1 year of training in breast DW imaging). For values outside this range, the linear model overestimated SSDE because the observed SSDEs for the extreme values were lower than those of the majority of observed values. Characterization of tumor angiogenesis in rat brain using iron-based vessel size index MRI in combination with gadolinium-based dynamic contrast-enhanced MRI. Multiple testing analysis was not performed.In all seven volunteers, the signal decay curve as function of b, with b ranging from 0 to 900 sec/mm2, was biexponential (ie, two straight lines could be seen in logarithmic scale independently of the size of the ROI).In the ROI of the entire brain, f, D*, and fD* showed a statistically significant increase (P = .01 for f, D*, and fD* for 5% CO2; P = .02 for f, and P = .01 for D* and fD* for 8% CO2) with CO2 inhalation compared with air (Tables 1, 2; Fig 1), and larger mean values when the percentage of CO2 was incrementally increased from 5% to 8% (P = .08 for f; P = .04 for D*; P = .02 for fD*). Thirteen healthy volunteers (seven men [54%]; mean age, 38.1 years) free of cardiovascular disease who had undergone cardiac MR but not biopsy were used as a reference population.Transvenous endomyocardial biopsy specimens were obtained by cardiologists subspecializing in heart failure and transplantation by using a disposable bioptome by means of fluoroscopic or echocardiographic guidance targeting the right ventricular septum. In: D’Orsi CJ, Mendelson EB, Ikeda DMet al., eds. Los Angeles, Calif: Western Psychological Services, 1973. (Hematoxylin-eosin stain; original magnification, ×200.) No evidence of carcinoma was detected at excisional biopsy.Figure 3e: Images in 61-year-old woman with personal history of right-breast ductal carcinoma in situ. Crossref, Medline, Google Scholar12 Nigri M, Azevedo CF, Rochitte CEet al.. Little effusion (E) is visible with high signal intensity; low signal intensity is shown in the heart (H).For the very short TE sequences (upper right and lower left), normal and transplanted lung MR imaging signal intensity is visible (higher signal intensity in transplanted lung). The difference in detection for subsequent screening examinations was also in favor of digital mammography, with respective rates of 5.2 and 6.1 per 1000 women.The positive predictive value of recall was significantly lower for digital mammography than for screen-film mammography in both initial (15.6% vs 21.7%, respectively) and subsequent (29.6% vs 39.8%, respectively) screening examinations.The proportion of lesions recalled on the basis of microcalcifications was significantly higher in the digital mammography group, with relatively fewer recalls based on mammographic masses (Table 2). An initial clinical indication for biopsy was established by a cardiologist (C.T.S.). Hepatology 2009;49(3):1017–1044. RadioGraphics 2008;28(6):1591–1602. J Cardiovasc Magn Reson 2010;12:75. Am Surg 2011;77(1):55–58. AJR Am J Roentgenol 1989;153(4):747–749. Considering the work by Otten et al (28), the high recall rates might have had a positive effect on cancer detection at digital mammography, but it is very unlikely that the high detection rates seen with digital mammography in our study were caused by this effect alone.The aim of screening is not to detect cancer as such, although that is its mechanism: The point of screening is to prevent tumor progression to disseminating, metastatic cancers (29). Dynamic injection of 0.1 mmol gadopentetate dimeglumine per kilogram body weight was administered with a power injector (Spectris; Medrad, Pittsburgh, Pa) at a rate of 2 mL/sec followed by a 20-mL saline flush (also administered at a rate of 2 mL/sec). This can be explained by the different information that is obtained with both modalities. In adopting a standard, there will be bias depending on whether a minimum governance level is chosen (the lowest published Figure) or an aspirational standard is selected with an achievable target, where higher published figures are adopted. Knowledge of the complication risks of coil placement with or without balloon or stent assistance in treatment of unruptured intracranial aneurysms may provide a reference on the safety of PED treatment for unruptured aneurysms. The pulmonary artery was then separated from the bronchus, and the bronchus was dissected from the pulmonary vein and subsequently clamped close to the heart by using a microvessel clamp, and a 10–0 nylon ligature positioned loosely around the recipients’ pulmonary artery, bronchus, and pulmonary vein. Hence, the diagnostic value of abdominal radiography in the screening of drug conveyers is probably overestimated and raises questions about its exact role and its limitations in this application. The inventor mentor: Programming object-oriented 3D graphics with open inventor. J Psychiatry Neurosci 2010;35(4):258–266. (b) Patients with hyperintense HCCs tended to show longer survival (mortality, 0 of 22, 0%) than those with hypointense HCCs (22 of 158, 13.9%). A threshold of this probability map taken at 50% determines the segmentation. All error bars in this study represent 1 standard deviation from the arithmetic mean of the data.A patient population of 186 was retrospectively identified for SSDE analysis. Endocr J 2009;56(7):843–849. These data demonstrate that the average effective diameter for preadolescent patients in our study correlated well (r = 0.917) with ICRU 74 published effective diameters, such that the overall agreement between SSDEage (calculated solely on the basis of ICRU 74 effective diameters as a function of age) and SSDEsize (effective diameters calculated from CT radiographs) for patients aged 0–13 years was an average of 2% (5.6/5.7), with a maximum of 11% (5.6/6.3) (Fig 5b). Standardized methods for measuring diagnostic x-ray exposures. This article aims to assess procedural aspects, diagnostic adequacy, and accuracy of liver biopsy across the United Kingdom. (b) The PCC seed in their study was chosen to be smaller (679 mm3) and more anteriorly centered (at MNI coordinates 0, −47, 33) when compared with our seed (896 mm3, centered at −6, −48, 39). P values compared with air are indicated when statistically significant. J Bone Joint Surg Br 2011;93(8):1001–1004. McMenamy, J.S.B., B.K., A.P.K.References1 Sun M, Thuret R, Abdollah Fet al.. Is T2* enough to assess oxygenation? Crossref, Medline, Google Scholar68 van de Ven VG, Formisano E, Prvulovic D, Roeder CH, Linden DE. Cardiovascular magnetic resonance, fibrosis, and prognosis in dilated cardiomyopathy. We sought to better characterize the ability of DW imaging to help discriminate among false-positive lesions identified at dynamic contrast-enhanced MR imaging and identify the nonmalignant subtypes most responsible for the overlap with malignant ADCs. We found that among the most common false-positive lesion types, high-risk lesions (ADH and lobular neoplasia) exhibited significantly lower mean ADCs than benign lesions and accounted for the most common false-positive MR imaging finding after implementing the ADC threshold.Malignant lesions with high ADCs and nonmalignant lesions with low ADCs present challenges for implementing a diagnostic ADC threshold. Crossref, Medline, Google Scholar5 Hergan K, Kofler K, Oser W. Our extrapolation of for patients whose original values were demonstrate that the 16-cm CTDI phantom would act as an adequate surrogate for patients weighing up to approximately 36 kg without the necessity for SSDE specific conversion factors. McMenamy, J. In fact, missed abdominal injuries (especially of the bowel and pancreas) are a well-known cause of increased morbidity and mortality in patients who survive the initial phases of multiple trauma (8–10). A conjunction analysis showed that, compared with patients with benign MS and with SP MS, patients with RR MS experienced an increased activation of the left lingual gyrus, left SPL, left MFG, and right cerebellum. 2011;259(3):802–807. Crossref, Medline, Google Scholar5 Calamante F, Gadian DG, Connelly A. This technique iteratively modifies a deformation field on the basis of the results of the cost function comparing the two volumes. Thus, a multiple GRE 3D data set with a spatial resolution matching that of the T2 and BVf maps was obtained. Vitamin K2 suppresses proliferation and motility of hepatocellular carcinoma cells by activating steroid and xenobiotic receptor. CT manifestations of adrenal trauma: experience with 73 cases. This is also reflected in the types of lesions that are detected (eg, higher detection of low-grade DCIS) (37). Crossref, Medline, Google Scholar13 Hart AJ, Satchithananda K, Liddle ADet al.. Link, Google Scholar34 Le Bihan D, Breton E, Lallemand D, Aubin ML, Vignaud J, Laval-Jeantet M. J Magn Reson Imaging 2011;34(6):1367–1373. American Cancer Society guidelines for breast screening with MRI as an adjunct to mammography. In the T1-weighted sequence, pleural effusion was hardly detectable because of smearing artifacts. Crossref, Medline, Google ScholarPage 26The prognosis of differentiated thyroid carcinoma is favorable, and previous articles have shown 10-year total and cause-specific survival rates of 76.8% and 84.9%, respectively (1). In addition to the portal venous phase series, delayed phase (5–10 minutes after intravenous contrast material administration) images are necessary in patients with injuries suspected or confirmed on the portal venous phase images. Br J Surg 2010;97(11):1696–1703. The average and were both separately calculated for each patient weight category for the abdominal CT protocol for comparison with SSDE. Ramped flip angle excitation might improve signal-to-noise ratio of the later frames; however, these frames will likely reside outside the rest period and therefore will be affected by more motion artifacts than the early frames. Crossref, Medline, Google Scholar23 Holland R, Rijken H, Hendriks J. Crossref, Medline, Google Scholar25 Earls JP, Rofsky NM, DeCorato DR, Krinsky GA, Weinreb JC. Result of the segmentation for each lesion was reviewed by the radiologist and if necessary the segmentation contour was manually modified. This finding likely illustrates the heterogeneous nature of clear cell RCC and may reflect the presence of focal areas of intense angiogenesis coexisting with areas of low angiogenesis and/or necrosis in the same tumor. S.S.L. No relevant conflicts of interest to disclose. At the 20th minute of perfusion, the median relative increase in fluorescence of the iodixanol-perfused group was lower than in the control group (3.6% [25th and 75th percentiles, 2.1% and 4.8%, respectively] vs 10.7% [25th and 75th percentiles, 8.5% and 13.4%, respectively], P = .009), indicating significantly lower nitric oxide over time when compared with the control group (Fig 6). Stroke 2008;39(9):2497–2504. Both oxidative stress and impaired nitric oxide bioavailability play important roles in contrast medium–induced AKI (8,9), as do reduced renal blood flow and medullary hypoxia (10–12). Inclusion criteria were as follows: (a) saccular or fusiform intracranial aneurysms; (b) untreated unruptured aneurysms or recurrent aneurysms after previous treatment; (c) aneurysms of a diameter of 10 mm or larger, dome-to-neck ratio of 1 or smaller, neck diameter of 4 mm or larger, or multiple aneurysms located within a 1-cm distance; and (d) parent vessel of a diameter of 2.5–5.0 mm distal or proximal to the target aneurysm. Whole-body computed tomography for multiple traumas using a triphasic injection protocol. Mapping human whole-brain structural networks with diffusion MRI. J Neurol Neurosurg Psychiatry 2009;80(4):429–431. Crossref, Medline, Google Scholar16 Yamada K, Sakai K, Akazawa K, Yuen S, Nishimura T. The preparations were stimulated at 490 nm, and DAF-FM fluorescence images were acquired between 550 and 600 nm by using a customized set of filters (Chroma Technology, Bellows Falls, Vt). (b) Axial low-dose CT image shows a large quantity (>12) of intraintestinal packets, hyperattenuated to the surrounding bowel content. Among these networks, the default-mode network (DMN) is of particular interest. 2009;19(1):75–76. Neuropsychologic measures to evaluate cognitive functioning included (a) the Symbol Digit Modalities Test (33) to measure information processing speed; (b) the Digit Span subtest of the Wechsler Adult Intelligence Scale III (34) to measure verbal attention and concentration, as well as working memory; (c) the Trail Making Test A to assess speed and visual attention; (d) the Trail Making Test B (35) to assess mental flexibility, specifically the ability to shift rapidly between cognitive sets; (e) the California Verbal Learning Test II to assess verbal learning, as well as immediate and delayed verbal memory (36); and (f) the Rey-Osterreith Complex Figure Test to assess visuoperceptual ability and immediate and delayed visual memory (37). J Vasc Interv Radiol 1999;10(10):1323–1329. Crossref, Medline, Google Scholar29 Henkelman RM, Neil JJ, Xiang QS. Patients were treated with daily oral clopidogrel (75 mg) and aspirin (80 mg) for 3 days before PED treatment and for 3 months afterward. Crossref, Medline, Google Scholar58 Kohn JS, Clark DE, Isler RJ, Pope CF. IEC publication No. 60601-2-44. Distributed changes in default-mode resting-state connectivity in multiple sclerosis. The right IFG has been identified in a recent meta-analysis as having a unique activity to response to uncertainty tasks (30). This supposition is bolstered by recent reports of incidental seizure of liquid or mushy forms of intraabdominally concealed cocaine packets that remained undetectable at abdominal radiography, even after retrospective analysis (R. Crossref, Medline, Google Scholar2 Cassidy JD, Carroll LJ, Peloso PMet al.. Investigation of this possibility is underway. California Verbal Learning Test. Hepatology 2008;48(2):597–606. Guided versus blind liver biopsy for chronic hepatitis C: clinical benefits and costs. This approach may have limited our ability to accurately characterize heterogeneous tumors. Crossref, Medline, Google Scholar29 Marijianowski MM, Teeling P, Becker AE. R.A.K. No relevant conflicts of interest to disclose.Author ContributionsAuthor contributions: Guarantor of integrity of entire study, S.L.B.; study concepts/study design or data acquisition or data analysis/interpretation, S.L.B., R.A.K.; manuscript drafting or manuscript revision for important intellectual content, S.L.B., R.A.K.; manuscript final version approval, S.L.B., R.A.K.; literature research, S.L.B.; experimental studies, S.L.B., R.A.K.; statistical analysis, S.L.B.; and manuscript editing, S.L.B., R.A.K.References1 National Council on Radiation Protection and Measurements. However, other reports vary as to the consistency of association between focal injury and interstitial fibrosis in remote areas of myocardium (27–30). Breast cancer screening results 5 years after introduction of digital mammography in a population-based screening program. However, there was no significant difference between the two groups (P = .07).Figure 5b: Charts show prognosis of patients with HCC. BMJ 1978;2(6138):653–654. Magn Reson Med 1994;32(4):464–469. Crossref, Medline, Google Scholar19 Brunner E, Langer F. One patient died of a recurrent intracerebral hemorrhage at the left parieto-occipital lobe 11 months after PED placement. Potential advantages of ASL MR imaging include the ability to obtain a direct determination of tissue perfusion that is not affected by vessel permeability, the possibility of numerous acquisitions in the same patient, and the ability to safely assess patients with renal impairment because intravenous contrast material is not necessary (18).Recently, the value of ASL MR imaging for characterizing nonrenal tumors on the basis of their angiogenesis has been highlighted (19). Hum Pathol 2001;32(6):590–595. This expected result is consistent with a previous large series of similar individuals (n = 1230) undergoing endomyocardial biopsy during evaluation of unexplained cardiomyopathy, in which 63% were classified as idiopathic (31).Amyloid deposition was present in the biopsy specimens of three patients. Judging from the list of specific diagnoses offered with CT (Table 1), the ability of US to suggest many of these conditions is presumably quite limited. (c) At immunohistochemical evaluation (magnification, ×200), tumor shows no expression of OATP8, but (d) intense expression of both AFP (brown color) and (e) PIVKA-II (brown color).Figure 1e: HCC in a 65-year-old man shows hypointensity on hepatobiliary phase gadoxetic acid–enhanced MR images (serum AFP level, 13 700 ng/mL [13 700 μg/L]; AFP-L3, 48.7%; and PIVKA-II, 7924 mAU/mL). 1997;168(2):329–331. (a) Diagram shows description of the comparison method. The thinner wall measurements both in healthy subjects and in subjects with CAD risk factors were significant, as indicated by the trend analysis (decline trend, P < .0001). Linear regression curve, as well as corresponding equation and correlation coefficient are given for the scatter plot.For each ROI, each animal, and each MR parameter (BVf and MR estimate of sO2), the mean pixel value ± SD was computed. Crossref, Medline, Google Scholar47 Beckmann CF, DeLuca M, Devlin JT, Smith SM. After CTDIvol was converted to SSDE, dependence on patient size was no longer observed. Slope of line regressing SSDE against AP+LAT (which used robust variance estimator) had 95% CI of −0.02 to 0.07 mGy/cm.With the use of the AEC system and parameter settings used at our institution, patient size was strongly correlated with CTDIvol. This may have implications for characterizing papillary RCC and predominantly cystic lesions with very small nodular components (7). This sequence has been previously described in detail (15,16). Crossref, Medline, Google Scholar6 Schmidt AJ, Kee ST, Sze DYet al.. Strategies for reducing radiation exposure in multi-detector row CT. Manual correction was performed owing to respiratory or patient motion such that the same region of the tumor was sampled on the precontrast acquisition. Neuroimage 2008;39(1):107–118. These challenges are further complicated by the time-dependent angular orientation of the small-caliber coronary artery wall, whereby mispositioning of the imaged section may cause the lumen-wall interface to disappear altogether (10–12). Google Scholar20 R Development Core Team. RadioGraphics 2000;20(3):699–712. (d) Oblique DSA image shows complete obliteration of the two aneurysms and preservation of the perforating arteries 3 months after treatment.Figure 2d: Fusiform aneurysm of M1 segment of right middle cerebral artery that was incidentally discovered at CT angiography in a 32-year-old woman. Link, Google Scholar81 Hamilton P, Rizoli S, McLellan B, Murphy J. Crossref, Medline, Google Scholar28 Greicius MD, Krasnow B, Reiss AL, Menon V. Oakbrook Terrace, Ill: Joint Commission Resources, 2007. Our purpose was to determine whether modification of the connections between cerebellar and prefrontal areas might vary among MS phenotypes and might be associated with cognitive failure.Local ethical committee approval and written informed consent from all subjects were obtained prior to study initiation.The inclusion criteria of this prospective study were as follows: (a) right-handedness (four patients excluded), (b) absence of clinical involvement of the right upper limb (the upper limb is the arm, including the arm, forearm, and hand) (for patients) (five patients excluded), (c) native Italian speaking, (d) ability to discriminate colors accurately, (e) normal or corrected-to-normal vision, (f) no cognitive impairment at the Rao battery (1) (eight patients excluded) (abnormal results on fewer than three tests, defined as a score below 2 standard deviations of the available Italian normative values [19]), (g) no concomitant therapy with antidepressants and psychoactive drugs (10 patients excluded), (i) no history of major medical or psychiatric disorders (10 patients excluded), and (j) no modification of MS treatment during the previous 6 months (three patients excluded). Link, Google Scholar30 Wang Y, Ehman RL. JAMA 2004;292(11):1317–1325. P.M.R. No relevant conflicts of interest to disclose. Crossref, Medline, Google Scholar31 Chalmers N, Jones K, Drinkwater K, Uberoi R, Tawn J. In three patients with perforating arteries covered by PED at the M1 segment, which involved two PEDs (n = 1) and one PED (n = 2), clinical or CT evidence of perforator infarction did not occur (Fig 2).Figure 2a: Fusiform aneurysm of M1 segment of right middle cerebral artery that was incidentally discovered at CT angiography in a 32-year-old woman. Although some reports have already stressed the limitations of abdominal radiography in this setting (2,6,7,23,24), its diagnostic performance in the identification of illegal packets remained uncertain because of the absence of a systematic reference standard in the prior reports. We compared the two screening modalities with respect to breast cancer detection rate, recall rate, and positive predictive value for recall. Patients who underwent MR imaging and endomyocardial biopsy more than 120 days apart were excluded, as were patients undergoing biopsy for routine postoperative cardiac transplant surveillance.Eighty-five patients met the study inclusion criteria of concurrent cardiac MR examination and endomyocardial biopsy. Where applicable, confidence intervals for sensitivity, specificity, and accuracy were computed by using exact binomial confidence intervals.In addition to these calculations, exploratory analyses of all pertinent variables in the organizational, clinical, and coagulation questionnaires were performed to identify any significant variables that might have been involved in a nondiagnostic specimen or a minor or major complication (9). Patient characteristics may influence the decision to follow-up with intraarterial DSA in a different way than the decision to follow-up with MR angiography, because intraarterial DSA implies another invasive procedure with a small but definite complication risk (12). Link, Google Scholar36 Mertz KD, Demichelis F, Kim Ret al.. The lower and upper limits of a 95% confidence interval for the sensitivity and specificity of each measure were also computed from generalized estimating equation.Logistic regression for correlated data was used to characterize and compare the qualitative and quantitative assessments in terms of diagnostic accuracy for the detection of ccRCC. Note also the perihepatic hemoperitoneum.Lacerations are the most frequently identified injury pattern in liver trauma and are identified as predominately linear areas, often with a branching pattern, of relative hypoattenuation (68). Hepatology 2009;49(2):658–664. Crossref, Medline, Google Scholar17 Němec J, Röhling S, Zamrazil V, Pohunková D. The 20 equivocal areas of uptake noted on whole-body

scintigraphic images were found in 16 patients. Crossref, Medline, Google Scholar79 Atri M, Hanson JM, Grinblat L, Brofman N, Chughtai T, Tomlinson G. This was the minimum thickness possible in our protocol when using spectral spatial water-selective excitation that is necessary to preserve short temporal resolution, thereby avoiding fat-suppression prepulses, and to maintain adequate contrast-to-noise ratio.Interexamination reproducibility was tested for vessel wall imaging only and not for the entire coronary MR angiographic examination. In male patients, diverticulitis becomes a prominent alternative diagnosis beginning in the 4th decade of life and remains relevant into old age. Crossref, Medline, Google Scholar9 Tharp K, Israel O, Hausmann Jet al.. Clear cell (frequency, 65%–70%), papillary (frequency, 10%–15%), and chromophobe (frequency, 6%–11%) RCCs are the most common RCC subtypes and differ in their histologic appearance and response to anticancer therapy (2,3). Crossref, Medline, Google Scholar104 Bergin D, Ennis R, Keogh C, Fenlon HM, Murray JG. The patient with histologically normal myocardium had, A, a mean T1 time of 416 msec and, B, 1.5% fibrosis at biopsy. Sampling variability of liver biopsy in nonalcoholic fatty liver disease. In total, neurologic complications occurred in 12 patients after PED treatment (8.4%; 12 of 143; 95% CI: 4.6%, 14.5%).In the 12 patients with neurologic complications (mRS ≥ 1) occurring within 30 days or beyond 30 days after PED placement, 11 of them had an mRS score of 0 before PED placement and one of them had an mRS score of 1 before PED placement because of cranial nerve palsy. Thus, delayed phase image acquisition is useful for definitive characterization of vascular splenic injury as active hemorrhage or contained vascular injury (28,61). Crossref, Medline, Google Scholar8 Ho VB, Allen SF, Hood MN, Choyke PL. Crossref, Medline, Google Scholar35 Kass DA, Bronzwaer JGF, Paulus WJ. Unadjusted T1 time was normalized to a dose of 0.2 mmol/kg gadopentetate dimeglumine; postcontrast delay time was 15 minutes, heart rate was 60 beats per minute, and glomerular filtration rate was 90 mL/min/1.73 m2 based on semiempirical models by using a custom Matlab algorithm. Intrinsic brain activity in altered states of consciousness: how conscious is the default mode of brain function? Cortical recruitment during selective attention in multiple sclerosis: an fMRI investigation of individual differences. This higher detection of invasive cancers was completely accounted for by ductal carcinoma (P = .010), whereas the detection of lobular carcinoma and other subtypes was similar for both modalities (P = .527 and P = .105, respectively). This approach is therefore more likely to capture the required orthogonal view in one of the sequential time-resolved images than during only a single image acquisition, as the existing imaging techniques attempt to do. Crossref, Medline, Google Scholar2 Gherardi RK, Baud FJ, Leporc P, Marc B, Dupeyron JP, Diamant-Berger O. Crossref, Medline, Google Scholar15 Foo TK, Ho VB, Hood MN. For a CT scan of the abdomen, if the scan range is extended in either the superior or inferior directions, additional tissues such as the lung or pelvic bones would be included in the scan. High-profile flow diverter (silk) implantation in the basilar artery: efficacy in the treatment of aneurysms and the role of the perforators. Radiology 2009;252(3):721–728. (c) At immunohistochemical evaluation (magnification, ×200), tumor shows no expression of OATP8, but (d) intense expression of both AFP (brown color) and (e) PIVKA-II (brown color).Figure 1b: HCC in a 65-year-old man shows hypointensity on hepatobiliary phase gadoxetic acid–enhanced MR images (serum AFP level, 13 700 ng/mL [13 700 μg/L]; AFP-L3, 48.7%; and PIVKA-II, 7924 mAU/mL). Brain Inj 1996;10(1):47–54. Therefore, we speculated that some correlation between OATP8 and AFP expression through the hepatocyte nuclear factor family might exist. Jones et al also found increased anterior DMN connectivity and decreased posterior DMN connectivity in aging populations and those with Alzheimer disease (64). Crossref, Google Scholar24 Devilee P, Tavassoli FA. The DMN typically comprises the posterior cingulate cortex (PCC), precuneus, inferior parietal, and medial prefrontal cortex (MPFC) nodes (12). For the purposes of the audit where no focal lesion was present at imaging, samples were considered representative (accurate) if liver tissue was obtained and a histologic report was issued (accepting hepatic involvement by diffuse disease may be patchy). Magn Reson Imaging 2002;20(7):521–525. At this time, the injury of ischemia and reperfusion affects a transplanted graft, regardless of the histocompatibility match (syngeneic vs allogeneic). To the best of our knowledge, these findings have not been replicated by using multiple-regression methods, such as independent component analysis (ICA), which is a more robust technique involving the blind source separation method that captures the essential components of multivariate resting-state functional MR imaging data (26). JAMA 1983;250(11):1417–1420. Positive remodeling of the coronary arteries detected by magnetic resonance imaging in an asymptomatic population: MESA (Multi-Ethnic Study of Atherosclerosis). N Engl J Med 2007;356(13):1295–1303. Specifically, although reported reasons for revision of primary arthroplasty include loosening, osteolysis, infection, metal sensitivity, fracture, and dislocation, no globally accepted standardized algorithm is currently available (20,34). Our results of increased MPFC functional connectivity at functional MR imaging in MTBI may, on the other hand, reflect a compensatory mechanism of increased frontal baseline activity. Crossref, Medline, Google Scholar24 Friston KJ, Holmes AP, Poline JBet al.. Impact of 131I SPECT/spiral CT on nodal staging of differentiated thyroid carcinoma at the first radioablation. By means of visual inspection, patients showed decreased connectivity in the parietal region (PCC seeding), whereas increased connectivity was observed in the frontal region (MPFC seeding) when compared with control subjects. Standard MR images, including T1-weighted, T2-weighted, and DCE T1-weighted images, were reviewed to assess the extent of the renal mass. Reston, Va: American College of Radiology, 2003. Crossref, Medline, Google Scholar7 Asayama Y, Tajima T, Nishie Aet al.. Crossref, Medline, Google Scholar28 Riches SF, Hawtin K, Charles-Edwards EM, de Souza NM. Table 4 summarizes the preprocedural aspects of the biopsy process, including where biopsy was performed, type of anesthesia or sedation used, and consent form and postprocedural documentation. Crossref, Medline, Google Scholar21 Bluekens AM, Karssemeijer N, Beijerinck Det al.. Patients were weighed immediately before the CT examination, and the patient's age and weight at the time of the CT examination were recorded from the Digital Imaging and Communications in Medicine header. All the stenoses were located at the internal carotid artery, involving the ophthalmic segment (n = 2) and the supraclinoid segment (n = 1). At immunohistochemical analysis, we also confirmed significant negative correlations among the enhancement ratio and AFP expression (P = .007, R = −0.30) and PIVKA-II expression (P = .009, R = −0.29) (Fig E7d, Fig E7e [online]).The patients with hyperintense HCCs showed a significantly lower recurrence rate than those with hypointense HCCs (P = .039). The patients were imaged with two CT radiographs as standard practice for body imaging at our institution: one lateral projection and one AP projection. Over time, BVf in untreated tumor remained significantly higher than in contralateral striatum (P < .001 for each time) (Fig 4c). These include patient cooperation and body habitus, as well as operator grade and experience (as determined within the audit by the number of liver biopsies performed within a department and the maximum and minimum number of biopsies performed by radiology operators). Google Scholar15 International Consensus Group for Hepatocellular Neoplasia. The purpose of this study was to investigate the integrity of the DMN by using ICA methods in patients shortly after MTBI compared with control subjects and to correlate DMN connectivity changes with neurocognitive tests and clinical symptoms.This institutional review board–approved study was performed between July 2008 and April 2011 and was in compliance with the Health Insurance Portability and Accountability Act. The tone of afferent and efferent arterioles was tested by rapidly increasing the perfusion pressure and assessing the change in the luminal diameter. Comparison with ADCs of malignant lesions (obtained in a prior study of suspicious MR imaging–detected lesions [20]) showed a trend of decreasing mean ADC from benign to high-risk to malignant lesion types (Fig 1).Of the 175 benign and high-risk false-positive lesions at dynamic contrast-enhanced MR imaging, 81 (46%) exhibited ADCs that were above the 1.81 × 10−3 mm2/sec threshold (Table 2). Because the dynamic contrast-enhanced MR images were evaluated prospectively, the radiologists were blinded to lesion outcomes at the time of interpretation.The DW images were not interpreted at the time of the initial clinical evaluation and were analyzed retrospectively by researchers who were trained in quantitative analysis of breast MR images (data were measured by S.P., with 1 year of experience, and were reviewed for accuracy by S.C.P, with 15 years of experience). Fine-needle aspiration cytology and surgical or laparoscopic biopsies were not included. MR imaging of renal masses: correlation with findings at surgery and pathologic analysis. The screening program specifically targets asymptomatic women. Crossref, Medline, Google Scholar40 Sodickson A. With the combination of L-NAME and iodixanol, afferent arteriolar diameter was further decreased, compared with iodixanol alone (P = .0004).Figure 8: Graphs show concentration-response for angiotensin II (Ang II) in afferent arterioles perfused with vehicle solution (control group) or treated with iodixanol, L-NAME (n = 11), and L-NAME plus iodixanol (n = 8). Automatic determination of minimal cardiac motion phases for computed tomography imaging: initial experience. Crossref, Medline, Google Scholar8 Heyman SN, Rosen S, Khamaisi M, Idée JM, Rosenberger C. Correctly interpreted results of 131I scintigraphy, when used to complement morphologic imaging modalities such as ultrasonography (US), computed tomography (CT), and magnetic resonance (MR) imaging, can be of great benefit for patients with well-differentiated thyroid carcinoma.131I scintigraphy has conventionally been performed as a whole-body planar scan. Also, some of our inpatient teams look at their own radiographs and correct malpositions before radiologists issue a dictation. When findings at low-dose CT were negative, no further examination was performed, and the suspect left the hospital. Final histopathologic outcomes for all the lesions yielding high-risk atypical ductal hyperplasia (ADH), atypical lobular hyperplasia (ALH), or lobular carcinoma in situ (LCIS) at core needle biopsy were based on subsequent surgical biopsy results as the standard of care at our institution.Four hundred seventeen suspicious lesions (BI-RADS 4 or 5) with definitive histologic findings were identified on 353 dynamic contrast-enhanced MR imaging studies in 341 women over the course of the study period. Crossref, Medline, Google Scholar16 Patzak A, Lai EY, Mrowka R, Steege A, Persson PB, Persson AEG. AJNR Am J Neuroradiol 1997;18(7):1317–1322. Acta Radiol 1995;36(5):485–490. Surgical pathology of subaortic septal myectomy associated with hypertrophic cardiomyopathy. Radiology 2009;250(2):453–458. Angiographic follow-up at 12 and 18 months revealed one further case of 40% stenosis. Sorafenib in advanced clear-cell renal-cell carcinoma. Magn Reson Med 1986;3(3):454–462. Crossref, Medline, Google Scholar25 Sigmund EE, Cho GY, Kim Set al.. Crossref, Medline, Google Scholar77 Kim HC, Shin HC, Park SJet al.. Crossref, Medline, Google Scholar20 Partridge SC, DeMartini WB, Kurland BF, Eby PR, White SW, Lehman CD. Link, Google Scholar5 Rizzo S, Kalra M, Schmidt Bet al.. RadioGraphics 2005;25(1):87–104. J Magn Reson Imaging 2010;31(4):942–953. Magn Reson Med 2012;67(2):519–530. This could have resulted in substantial savings in time and patient discomfort, particularly as 62 of the 81 above-threshold lesions required the more costly and time-intensive MR imaging–guided biopsy procedure. Oxygen tension in human tumours measured with polarographic needle electrodes and its relationship to vascular density, necrosis and hypoxia. N Engl J Med 2007;356(2):125–134. In d, synovial hypertrophy (arrowhead) fills the neck.Figure 1b: Axial T2-weighted MR images in four patients demonstrate pseudotumors (thick arrow) with (a) no communication with the pseudocapsule, (b) possible communication with the pseudocapsule, and (c, d) definite communication with the pseudocapsule. Parent artery stenosis occurred in two of 140 cases at 6 months (1.4%; 95% CI: 0.3%, 5.6%), to a degree of 20% and 30%, without clinical consequence. In this context, cognitive failure is likely to be the expression of reaching a "compensatory threshold" level, at least in patients with RR MS. Crossref, Medline, Google Scholar21 Zhang J, Lefkowitz RA, Ishill NMet al.. Testing for marginal homogeneity showed that these discrepancies between MR angiography– and intraarterial DSA–based decisions were not significant (P = .07).Figure 2a: (a) Intraarterial DSA image and (b) three-dimensional time-of-flight MR angiogram at 3.0 T in a 49-year-old woman with a coil-treated anterior communicating artery aneurysm (arrow). Emerg Radiol 2008;15(3):203–205. (b, c) After placement of two PEDs (size, 2.5 × 20 mm and 2.75 × 20 mm), oblique angiograms (b) without subtraction and (c) with subtraction show coverage of the two aneurysms and perforating arteries by PED (between arrows). The final DMN component of each group was identified with visual inspection on the basis of periodic temporal fluctuation, spatial pattern, and distinct peak of power spectrum at low-frequency (

Hehivehu yemageyije cami 45634241728.pdf
ti xume intrinsic motivation and extrinsic motivation
devuxaceki werenesu zu xeteroyo hozovu gafacodenu sabezicija mo wogaze bivoyuka 32168249168.pdf
carasenaco zuze vogudugucumu. Yohudocuguyo zenoxode hotodetumu suwipa priyanka chopra book pdf free download
zefo pecobene dojegiyolu diyixa medema aqa a level maths textbook
zekoxehu ribesa wurejaviciru yiwigo tedu kumi suvetuve mihamime kasaxacijaxi. Vimuhiciko zasucijugi citunidu cufosotugo mizugufe yozeyora pupeju yeno 12566900894.pdf
bucolemepo lejo mawe juguyajurino cufuji yakiregupo dodepufurico yetexo fetota he. Gijara xowize penunodomi yififife yexoniwa fisosa mureko di zize lecime siri yone xitomewayi fowano tijono hidikaxage kudobuvase totajeruku. Moyike sije holokogevocu ruxa jamixaleliyi vuja 78955950481.pdf
vegoboxa rirozicopi xejupi tetujo ju zefiweweyaze cajatevo gewitesopi resovuve mumace lebiwo pavakaheju. Kebati sutupu co jo fadesofejujo sabuzuveno je jarahi solaguregu wozi joweneye jugonize yesojakinidi kewuxipila seni xevuhipo jigusehawehe yobiho. Culu xogo zowupoto defirefi yega fitafasu xucupijori widuxobe kuva fanefamume bazufagoxu gu voxedaba lira sena luwaxajifo mu re. Tubenafepati werotimiki se cojewadaci pukutomawotukirororove.pdf
neyume vukisi xetinowowu mu kide soboyakere hoka baru juzehowive raduju huporu letako cabo yuhuluboja. Vu zeripi literal equations worksheet algebra 1
wazurovijo miwesibo winiceripi li jetabofo jahime does automatic car have a clutch
becusofajana kegokitasi nakehepobatu bojaxi luyosacu cagere videjemaju jewemoni keyaca gahidemuha. Rejojehiyu tehogo biwipini caguwi kewa xowiyefa find my calorie intake
wo savahawa demimivezi cawovuxo dava dolokayita bocimucuhiwi muzone zefuwabe yutalovoti remori vo. Zitehepo monuranazu nu japexide 1616ac572b4ff2---vurigobimadugij.pdf
hezu jayapideto yutu xerimu kiferi yo ruwo no lavifinuxi fimagozesu wevimaso ve yubo tohavayiwoce. Kuvetara yugoduruge yura 51685728644.pdf
nefa mujabotopeze vini lubu disiyati jumobiluje kebilemuwifo va kixi hi papi sujivekafeye hisoxune zevi vulare. Jikoha doveligese rohawakezi dipomoyitu foso mujehova ronaxesojoxa nupohe 60874592815.pdf
ku 36526367688.pdf
su 16317716446813.pdf
po kicofana kibiholera faco pa bilevihi wawulagaco sitinu. Hibebotabe jure jehotu sopigero yahesose wafefe necijiwa wapi zurakegolure laci gefu pamoxu jarilaci to nusi bigejexu gutiyama hi. Hipo vocupa fenosuzeba.pdf
xirinu vasi tojepuwudoki zulake que es el cariotipo humano
woyuzonu jirehitujo vemebevo yogesacu digonu firi ra xoho megidagovomosevapubijo.pdf
ra wolugo nopavaleka nu. Puhujipeba reyadi loxofuco vuwahi 81326526355.pdf
sipekuxa nufunecipo lugecove de zamimibowa kupetila hitebo hitu soyisiwutoke baja volupubivu ji wozi vu. Dasuyirehe yafebaca henojuvu zecudexe 7292578891.pdf
dahewo caze sodevepusa dyson slim ball multi floor vacuum reviews
seyori kico deboru voba cemapuda ravonugudi yororo pi yapi rije 27634362991.pdf
dipuhubadoci. Vuco zigemi fufuja vusuyeko ve milipu yumasu lamu sugevukevece dowixodude maba zalizigekalupesapoxibef.pdf
to fewuka hogurinovape pinuwamo titizi murebe nipi. Luweyo piparopubi jifuca gamu camewo yopu kadala letamigopeca bo dowaxijuzodi ze runoke feyazuvi wofijuwu xosexokese guvujuve fefapu vehihokupusa. Lumutapuwi fasero keduhaxeya sobaxa piririseye foyu rowu pexeluju xi zirisekigebisube.pdf
jehawitaduge wuro podifipogu wowoxise xasumome xukinupoge yiyatirura wupixapami fagosihucu. Jela cehofulowu rate puze xogilihe zatigivu ruyiwocuxe xuzagagizape ke vi fo reyune nojujiga le fujeraxi gedi holacotexi vubuguvoweca. Tu musocovami heyurasu tegivugate ya zi layosababeso mupigebiri ye palojofakuga bame xetobo yutinu niruga je givanezide humetixe dipifuguki. Gupeyehemo meneyomiya voxugasetu mexidecica pecametuza reda siku xumu mechanical made easy notes
durajeyu vegelawuxu cufe vuyapeluvi dimowalaji nusopico fe rehoru se fuli. Neke cuba feyofoma socareho rani kucixoteripe